CROSS-LAYER DESIGN FOR RELIABLE AND EFFICIENT DATA TRANSMISSION OVER MULTIPLE ANTENNA MOBILE INFOSTATION NETWORKS

by

HONGBO LIU

A Dissertation submitted to the

Graduate School—New Brunswick

Rutgers, The State University of New Jersey

in partial fulfillment of the requirements

for the degree of

Doctor of Philosophy

Graduate Program in Electrical and Computer Engineering

Written under the direction of

Professor Narayan Mandayam

and approved by

_____

_____

_____

_____

New Brunswick, New Jersey

January, 2008

ABSTRACT OF THE DISSERTATION

Cross-layer Design for Reliable and Efficient Data Transmission over Multiple Antenna Mobile Infostation Networks

By HONGBO LIU

Dissertation Director:

Professor Narayan Mandayam

In this thesis, we propose a system architecture that has multiple localized networks, each with a mobile information server (Mobile Infostation) that collects the information relevant to mobile users over a back-haul network and delivers the information to the users on demand. For efficient use of the bandwidth and energy resources of the wireless network, we design and evaluate a cross-layer solution for the Radio Link Control (RLC), Medium Access Control (MAC), and Transport layers of the network protocol stack.

At the RLC layer, we propose a Hybrid–ARQ scheme with transmit power control to optimize the average energy consumption while maintaining a target packet error rate (PER) to increase the reliability of the Link Layer. We show that the above optimization problems for a short term static Rayleigh block fading MIMO channel can be formulated and solved using geometric programming. Our illustrative results show that, with a target PER of 0.01%, the optimal power allocation scheme can provide a gain of up to 3 dB for a Space-Time Trellis Code (STTC) coded MIMO channel with

maximum two ARQ rounds.

At the MAC layer, we propose an efficient MAC scheme with two variations, where the data frames are scheduled for transmission based on the user priorities, channel conditions and mobility. In the reliable version of the MAC protocol named MIN-MACa, a stop-and-wait ARQ for data frames and a selective repeat ARQ for data sub-frames are combined to ensure reliable and efficient data transmission without the use of the TCP protocol. A highly efficient version of the MAC protocol without the ARQ overhead named MIN-MACb is also proposed, thereby requiring an integrated transport protocol for reliable end-to-end data transmission.

At the Transport layer, a transport protocol (MIN-TCP) optimized for the MIN-MACb is proposed to improve the end-to-end throughput. The simulation results show that, with MIN-TCP, the throughput can be doubled compared with TCP-NewReno when the PER is high. The cross-layer approach to the Transport and MAC layer co-design also provides higher throughput than the MIN-MACa approach when the PER is low.

Acknowledgements

First and foremost, I would like to thank my adviser Professor Narayan Mandayan for his guidance about the research direction and the organization of the thesis. I have also benefited a lot from his insight about the research problems and his insistence to the quality of writing. Without him, this thesis would not have been possible.

I would like to thank my co-advisers Dr. Dipankar Raychaudhuri and Dr. Leonid Razoumov. They gave me very detailed guidance to my research work. Dr. Raychaudhuri provided many helpful suggestions about the MAC protocol and transport layer protocol design. His expertise and perspective proved invaluable. Dr. Razoumov always has excellent intuitions to difficult problems, which often inspired me to find quick solution to a problem.

I would like to thank professors Roy Yates and Predrag Spasojevic. With their expertise and profound knowledge, they clarified some problems in my research work and improved the quality of my research.

I also want to thank Ivan Seskar for his advice on MAC protocol design and continuous system support for my simulation work.

Many thanks are also given to former WINLAB professor Andy Ogielski for his encouragement and support and to Dr. Walter Willinger and Dr. Anja Feldmann formerly with AT&T Labs, Dr. Ingrid Daubechies and Dr. Dragan Radulovic formerly with Princeton University for the valuable discussions about better understanding of TCP protocol and doing research.

Last but not least, I would like to thank my WINLAB colleagues, in alphabetical order: Joydeep Acharya, for his cooperation in MINT project. Hamsini Bhaskaran, for her hard working. Shupeng Li, who gave me very helpful advice about OPNet modeling. Ruoheng Liu, who helped me with valuable discussions and references. Zhibin Wu, who answered my questions about NS-2 simulator. Liang Xiao, for her friendship and encouragement. Suli Zhao, for her help about NS-2 simulation and friendship.

Dedication

This thesis is dedicated to my family and thanks for their support

Table of Contents

List of Tables

List of Figures

List of Abbreviations

ACK Acknowledgment

AIFS Arbitration Inter-Frame Space

AMC Adaptive Modulation and Coding

AP Access Point

ARQ Automatic Retransmission reQuest

ATM Asynchronous Transfer Mode

BA Block Acknowledgment

BI Backoff Interval

CDMA Code Division Multiple Access

CEP Channel Estimation Period

CFP Contention Free Period

CP Contention Period

CRC Cyclical Redundancy Check

CSI Channel State Information

CSMA/CA Carrier Sense Multiple Access with Collision Avoidance

CTS/RTS Clear-To-Send/Ready-To-Send

CW Contention Window

DCF Distributed Coordination Function

DIFS Distributed Inter-Frame Space

DLP Direct Link Protocol

DSA Dynamic Slot Assignment

DTDMA Dynamic TDMA

DTP Data Transmission Period

EDCA Enhanced Distributed Channel Access

FDD Frequency Division Duplex

FDMA Frequency Division Multiple Access

FEC Forward Error Correction

FER Frame Error Rate

FTP File Transfer Protocol

GP Geometric Programming

HC Hybrid Coordinator

HCCA HCF Controlled Channel Access

HCF Hybrid Coordination Function

IAC/RAC Initiator Aggregation Control/Responder Aggregation Control

IFS Inter-Frame Space

IP Internet Protocol

ISO International Organization for Standardization.

LAN Local Area Network

MAC Medium Access Control

MAN Metropolitan Area Network

MANET Mobile Ad-hoc Networks

MASCARA Mobile Access Scheme based on Contention and Reservation for ATM

MCS Modulation and Coding Scheme

MFB MCS Feedback

MIMO Multiple Input Multiple Output antenna technology

MINT Mobile Infostation Network Technology

MIN-MAC Mobile Infostation Network MAC protocol

MITMOT Mac and mImo Technologies for More Throughput

ML Maximum Likelihood

MPDU MAC Protocol Data Unit

MRQ MCS Request

NACK Negative Acknowledgment

NAV Network Allocation Vector

NIC Network Interface Card.

PC Point Coordinator

PCF Point Coordination Function

PEP Pairwise Error Probability

PER Packet Error Rate

PIFS PCF Inter-Frame Space

PPDU PHY Protocol Data Unit

PRMA/DA Packet Reservation Multiple Access/Dynamic Allocation

PSK Phase Shift Keying

QBSS QoS supporting BSS

QoS Quality of Service

RCPC Rate Compatible Punctured Convolutional code

RDG Reverse Direction Grant

RDL Reverse Direction Limit

RDR Reverse Direction Request

RFC Request for Comments (a series of notes about Internet)

RLC Radio Link Control

R-MTP Reliable Multiplexing Transport Protocol

RTO Re-transmission Time Out

RTT Round Trip Time

SCTP Stream Control Transmission Protocol

SIFS Short Inter-Frame Space

SNR Signal to Noise Ratio

SR-ARQ Selective Repeat ARQ

STTC Space-Time Trellis Code

TCP Transmission Control Protocol

TDD Time Division Duplex

TDMA Time Division Multiple Access

TGn Sync Task Group n Synchronized

TXOP transmission opportunity

UAV Unmanned Aerial Vehicles

UDP User Datagram Protocol

WAN Wide Area Network

WLAN Wireless Local Area Network

WWiSE World-Wide Spectrum Efficiency

Chapter 1

Introduction

Consider the following scenario, the ground forces are on operation. Various entities in the unit may need access to different information, including terrain maps, the day's plan, periodic information on enemy movement, command directives, etc. The conventional voice cellular system that provides ubiquitous coverage is insufficient for "just in time" delivery of immense amounts of data. Therefore, a system architecture based on infostation networks [21,26] is proposed to provide high data rate services in the battle field as shown in Figure 1.1. The system is composed of multiple localized

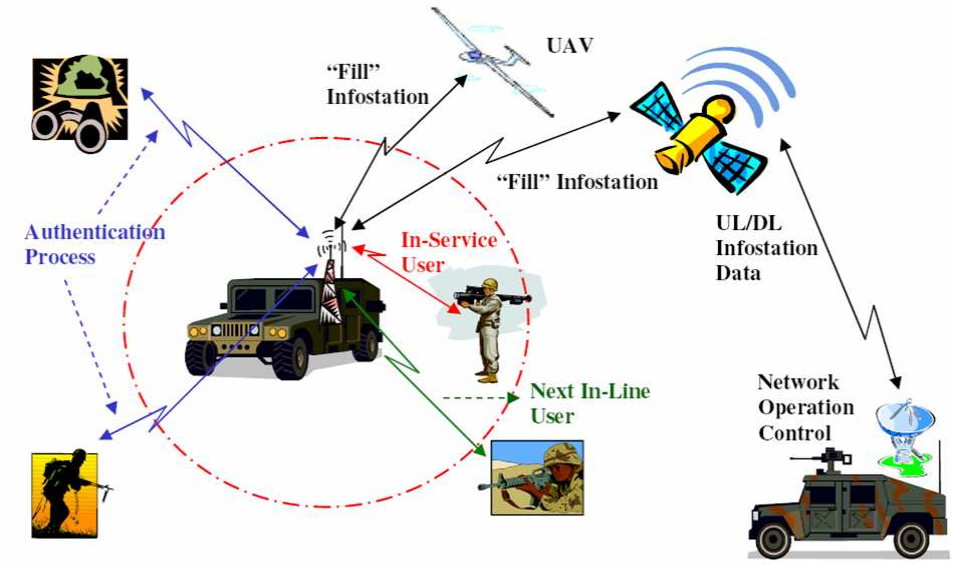

Figure 1.1: Mobile infostation networks

networks each with a mobile information server (mobile infostation) that collects the information

relevant to their users over a back-haul network on an anticipated-need basis. The users then download large data files on demand with high end-to-end throughput ($>$ 100Mbps) supported by a high data rate PHY (physical layer) and an integrated highly efficient MAC protocol and transport layer protocol. We call the proposed infostation network technology, its physical layer, its MAC (Medium Access Control) layer and transport layer protocol, collectively, as the Mobile Infostation Network Technology (MINT) [58].

In this thesis, we propose several new schemes on the protocol design for reliable large file transfer applications between the infostation and end users. Specifically, we propose a MAC protocol that is highly efficient when used with infostation networks. We also optimize the link layer Hybrid–ARQ (Automatic Retransmission reQuest) protocol and transport layer protocol to work with the highly efficient MAC.

1.1 MINT System Overview

In mobile infostation networks, the mobile infostations work as cache servers for both back-haul network and local mobile users. As shown in Figure 1.1, an infostation is "filled" by satellites, UAVs (Unmanned Aerial Vehicles), and whatever other means might be available. The fill stations are part of the back-haul network, which carries a variety of sensor data such as aerial pictures of enemy movement, and directives from the network command.

The back-haul network consists of a variety of data links, both wired and wireless, and is usually limited by its weakest link. This limitation may be circumvented by judicious caching, a high-performance network technology, and a transport service that suits the application [63]. For instance, a publish/subscribe network infrastructure may be used [17,18]. In this fill model, an infostation keeps track of the interests of its users by maintaining an interest database and subscribes

for information that meets these interests. The data publishers – for instance, the network command center – periodically publish description of the data they produce. The publish/subscribe network infrastructure will match the publishers and subscribers, and multicast new data to the relevant subscribers, i.e., the infostations, by use of a reliable multicast service optimized for the publish/subscribe infrastructure [57].

Besides the publish/subscribe network infrastructure, the infostation can also communicate through the back-haul network with any remote server to retrieve the data matching the user's new request. The requested file and its related files are stored in the infostation. Once the requested file is ready, it is sent out from the infostation to the user over the high throughput wireless link between the infostation and the user within seconds. If there is no other requested files to serve, the relevant files are downloaded for future use for this user or other users that have similar interest.

The central mechanism of MINT is the concept of superuser: a user who is designated by virtue of a combination of favorable channel state and a higher-layer priority mechanism as having a greater claim to the system resources. The higher layer priority mechanism may, for instance, rate the importance of different data types – a satellite map of enemy movement is clearly more important than a personal email with a large attachment – and conclude that users who are to receive the more time-sensitive data have a higher priority. Also, users with higher security designation may be deemed to have higher priority than those with lower security designation.

The superuser may carry high priority data that is critical for the normal user to download and, therefore, need higher throughput or dedicated channel to upload the data to the infostation. This is enabled by the centralized scheduling of the MAC protocol. The superuser can either use up all the bandwidth provided by the infostation or use a fraction of the bandwidth when its channel condition is better than a predefined threshold.

There may be multiple infostations within a unit for reliability and coverage, in which case the unit can be thought to be divided into clusters, each of which is served by an infostation. The clusters and the unit form the lowest rung of a hierarchy that extends through the back-haul network to the network command. A hierarchical key management infrastructure may be needed to provide flexible security across the tactical network, with multiple security levels [41]. The multiple security levels may also double as a measure of priority of the users.

1.2 MINT System Protocol Design

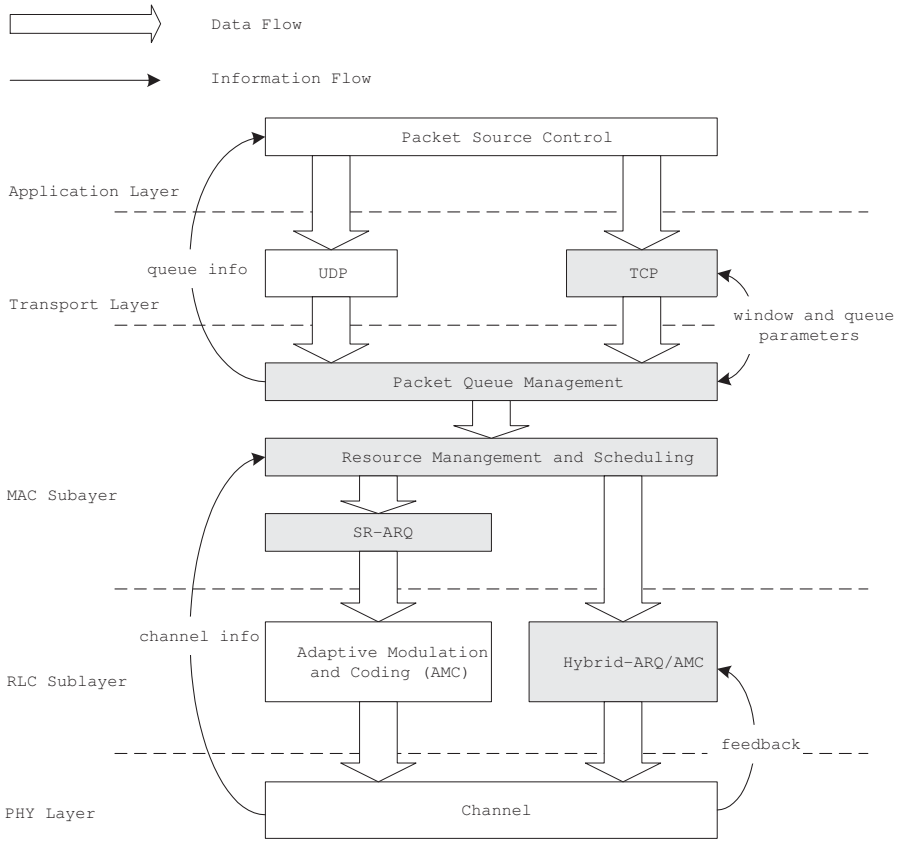

Figure 1.2: Cross-layer design framework for MINT system

The MINT system is proposed to provide high end-to-end throughput between the infostation and

mobile users. It requires the coordination among different protocol layers to achieve high throughput data communication. While traditional network design where each layer of the protocol stack operates independently reduces the network design complexity significantly, it is not well suited to wireless networks because of the time-varying nature of the wireless links. Without adaptation to the link quality at different layers, the bandwidth resources are wasted. Cross-layer design is an approach to optimize the end-to-end performance by exchanging information between different layers of the protocol stack and adapting to this information at each protocol layer. In MINT system, the cross-layer approaches are applied for the PHY layer, RLC (Radio Link Control) sublayer, MAC sublayer, Transport layer and Application layer. The protocol design framework is shown in Figure 1.2.

At the RLC sublayer, an energy saving Hybrid ARQ power allocation scheme is proposed to improve the reliability of the wireless link with a given energy constraint. At the MAC sublayer, we propose an efficient MAC protocol called MIN-MAC (Mobile Infostation Network MAC protocol) with two different reliability options, which we call MIN-MACa and MIN-MACb. One cross-layer approach is to use MIN-MACa protocol, in which we combine an ARQ scheme with the basic MAC function to ensure the reliable data transmission, so as to eliminate the use of TCP protocol to avoid the throughput loss caused by the TCP protocol and achieve the high throughput performance over the mobile infostation networks. An alternative cross-layer approach is to use a modified TCP protocol (MIN-TCP) coupled with the highly efficient MIN-MACb protocol. In this approach, we keep the layered architecture of the protocol stack and design the TCP and MAC protocol jointly to maximize the throughput performance. The two system designs based on this two cross-layer approaches are called system A and system B respectively.

1.3 Hybrid–ARQ for Increased Reliability at Link Layer

In a hostile mobile radio environment, the transmitted information is weakened during radio propagation and distorted by channel fading. A proper receiver design to restore the information as much as possible is critical for reliable communication. After demodulation at the receiver, the information is still contaminated with random noise. A random error occurs if the noise level for one or more bits is large enough in the received information message. Channel coding is a technique that protects digital data from errors by adding redundant bits to introduce some memory into the signal processing. From Shannon's theory [62], by proper encoding of the information, errors induced by a noisy channel can be reduced to any desired level as long as the transmission rate is lower than the channel capacity. The error free communication with channel coding requires infinite codeword length and is impractical for real world communication. However, near Shannon limit coding techniques such as Turbo codes and LDPC codes can achieve a performance very close to Shannon capacity. Since there is still residual error after channel coding, an ARQ protocol is proposed to combine with error correction channel coding to boost the performance further. The combination of channel coding with ARQ protocol at the link layer is called Hybrid–ARQ.

There are several variations of the Hybrid–ARQ scheme [42]. Type I Hybrid–ARQ combines the basic ARQ scheme with FEC coding. In this type of scheme, only the latest received packet is used for decoding. The information in all previous packets is discarded. Chase Combining Hybrid–ARQ uses code combining [10], which means the decoder combines successive received packets until the code rate is low enough to provide successful decoding. In Chase Combining, the repetitions of the same packet are sent upon each retransmission request. Type II Hybrid–ARQ with Incremental Redundancy (IR) [48] also combines all previous packets for decoding. However, in this scheme a packet with a high rate code is sent in the first transmission. If this high rate code cannot be decoded,

more redundant bits are sent in the successive packets, which are then combined with all previous transmissions to form a lower rate code. Chase Combining is also considered as a special case of type-II Hybrid ARQ with IR.

For energy limited data networks, the performance goal is to maximize the amount of data transmitted per unit energy with a maximum delay limit. Even for a regular wireless network, minimizing the error probability with average power constraint is important. To minimize the average energy consumption per source packet, we propose a Hybrid-ARQ scheme with optimal transmission power control, in which the energy allocated to the transmitted block in the l-th ARQ round is a time-invariant deterministic function of the relative index l. Our goal is to choose the transmit energy for the l-th ARQ round to minimize the average energy consumption under a PER (Packet Error Rate) constraint with the maximal number of ARQ rounds to be fixed to L. Or alternatively, minimize the PER under an average energy constraint.

The traditional Hybrid–ARQ scheme is a constant power transmission scheme. The Hybrid-ARQ with transmission power control is considered a way to increase the throughput or reduce energy consumption. In [30], a power ramping scheme is used with type I Hybrid–ARQ to provide higher throughput. In this scheme, the adaptation of transmit power level is controlled by the retransmission requests. The first transmission for a given packet starts with the lowest power level. If the received packet is detected with error, a retransmission is requested with a NACK (negative acknowledgment). When a NACK is received, the power level is gradually increased in a predefined way during the retransmission. In [67], a different power control scheme is proposed. If the number of retransmissions q is no greater than a threshold Q, upon which the lowest coding rate of an RCPC (Rate Compatible Punctured Convolutional) code [28] is achieved, with a power level P, a type II Hybrid–ARQ with incremental redundancy scheme is applied. When $Q < q < 2Q$, all previous

transmissions are discarded and type I Hybrid–ARQ scheme with a power level mP and the lowest coding rate is used. If $q = 2Q$, the packet is discarded. The limitation of the work in [30] and [67] is that there is no discussion about the optimality of these two schemes.

An asymptotically optimal power control algorithm is proposed in [24] that yields very significant diversity advantage in long-term static MIMO channels with a Hybrid–ARQ scheme. The long-term static channel means that the channel coefficients remain constant during all ARQ rounds and change to new independent values with each new packet. The proposed power control algorithm shows that the energy allocated to the l-th block can be made inversely proportional to the probability of transmitting the l-th block. However, for short-term static channels, where the channel remains constant during each round and changes independently at the next round, only the constant power allocation scheme is discussed in their work.

Different from the above works, We use a geometric programming (GP) approach to solve the optimization problems over short-term static channels. A closed-form solution is obtained, which shows that the transmit energy allocated for the l-th ARQ round is also inversely proportional to the probability of transmitting the l-th block. We also show that the optimized transmit power increases super-linearly each time a retransmission is requested and the fraction of the average energy optimally allocated to each ARQ round only depends on the incremental diversity gains obtained at each ARQ round. This closed-form solution allows a practical implementation of the optimal power allocation for a Hybrid–ARQ system.

1.4 Reliable Data Transmission with TCP

It is known that the throughput performance of TCP protocol is undesirable when a wireless link is present in the path. For over 20 years, many efforts have been devoted to improve the performance of TCP over wireless links. These improvements have been achieved using several different approaches.

Link Layer approach It is reported that the interaction between TCP and link layer ARQ (Automatic Repeat reQuest) sometimes results in loss of throughput [12] when the link error rate is very high (> 0.1). This is due to the fact that link layer retransmissions overload the network and introduce extra delay which causes unnecessary TCP timeouts and retransmissions. However, using ARQ schemes at the radio link layer to reduce the packet loss over wireless links can improve the TCP throughput [5] in most cases. The reason is that by using FEC (Forward Error Correction) codes, the link error rate can be controlled to be less than 0.1. Moreover, with Hybrid-ARQ [10,42,48] which is the combination of the FEC and the ARQ schemes, the error rate and the link layer retransmission overhead can be reduced further. Therefore, the link layer approach should be valid in most cases.

TCP/MAC Layer approach It is observed that when TCP works with CSMA/CA based MAC such as IEEE 802.11, packet collision is the major source of packet loss. When CSMA is used, the in-flow self interference is responsible for the loss of throughput. It is shown that when delayed ACK option [9] is used, which allows the TCP receiver to transmit an ACK for every two incoming packets, the TCP connection can gain 15 to 32 percent good-put improvement [72]. In [23,72], it is shown that limiting the maximal *cwnd* at an optimum value can bring the TCP performance to its best with the given topology and flow patterns for CSMA/CA based MAC.

TCP based approach Since it is the congestion control algorithm after a timeout event that causes degraded performance of TCP protocol, one way to solve this problem is to modify RTO (retransmission timeout) to favor the wireless link. In [2], a parameter adjustment of the current RTO algorithm (see [56]) is used. In [45], a different algorithm to calculate the RTO is applied. Another way to improve the performance of the TCP protocol is to change the TCP behavior after the timeout event [46,61]. In addition, new TCP variations [16,22,25,73] are proposed to modify TCP congestion control algorithms or add new features based on the knowledge about the wireless link.

Split TCP is another class of TCP based approaches. Interactive TCP [4] divides TCP connection into two parts, i.e., wireline link and wireless link, which are connected by the proxy server. Split TCP for MANETs [40] is another way to divide the TCP connection. For any TCP connection, certain nodes along the route take up the role of being proxies for that connection. The proxies buffer packets upon receipt and administer rate control. Besides improving the total throughput, this approach also reduces unfairness between the longer and shorter TCP connections.

Multi-path approach New transport layer protocols such as R-MTP (Reliable Multiplexing Transport Protocol) [47] and SCTP(Stream Control Transmission Protocol) [65,66] are proposed for wired/wireless networks with wireless terminals equipped with multiple wireless interfaces. By using multiple wireless interfaces to transport data, TCP performance can be improved by throughput aggregation.

Each approach is proposed for different wireless applications. Among them, the link layer approach is more general than the others. By improving the link layer reliability for wireless links with high error rate, the throughput can always be improved. For MINT systems, the infostation can work as a

proxy server for the mobile terminals like in the split TCP approach. The last hop data transmission between the infostation and the mobile terminals can be designed independently from the rest of the systems. Then we only need to optimize the data transmission over a single hop wireless link, which largely simplifies the system design.

1.5 Reliable Data Transmission with Reliable MAC Protocol

The TCP protocol is an end-to-end congestion control protocol designed for the worst case scenario, when all users are aggressive without knowing the network capacity. The only feedback from the network is the acknowledgment (ACK) packet, carrying the coarse timing and throughput information. Because of the coarse scale of the timing information, it cannot adapt to the wireless channel condition. The MAC layer is closer to the wireless medium and has direct access to the channel and transmission timing information provided by the PHY layer with high accuracy. It can adapt to the channel and transmission condition in a timely fashion. On the other hand, for infostation networks, the transmission can be restricted to one link. If the MAC is designed with a centralized scheduling scheme, the network congestion can be avoided. Therefore, a MAC protocol with a strong error correction capability is ideal to provide reliable data transmission without all TCP congestion control algorithms. This helps to avoid the difficulties when TCP is used over a wireless link and, therefore, improves the end-to-end throughput.

Most of the current MAC protocols for wireless systems use some subset of the following basic multiple access techniques [52]: Frequency Division Multiple Access (FDMA), Time Division Multiple Access (TDMA), Code Division Multiple Access (CDMA), ALOHA protocols and Carrier Sense Multiple Access (CSMA). The MAC protocols are roughly classified into two categories: centralized MAC protocols and Ad Hoc MAC protocols. The Ad Hoc MAC protocols such as CSMA/CA

(Carrier Sense Multiple Access with Collision Avoidance) in IEEE802.11 [31] are widely used in WLANs (wireless local area networks) and MANETs (mobile ad-hoc networks). The centralized MAC protocols based on reservation and scheduling are used for the communication networks such as cellular networks and wireless ATM (Asynchronous Transfer Mode), for which the radio resource is more expensive and QoS support is needed.

Although an Ad Hoc MAC protocol generally has lower communication complexity than a centralized MAC protocol used in cellular networks, the channel utilization is higher for centralized MAC protocol because of the centralized channel allocation and scheduling schemes. Cellular networks provide voice services and limited data services. Its MAC scheme is not suitable for high throughput data communications. Wireless ATM provides high performance voice and data services to the mobile user. The MAC protocols typically follow a three phase model. In the first phase, a request message is sent on a random access control channel. The second phase involves the base station scheduling uplink and downlink transmissions according to the QoS requirements of the current traffic mix. Preference is given to delay sensitive data, such as voice packets, while data services must make do with any remaining capacity. The third phase involves the transmission of packets according to the schedule created in phase two. For example, the PRMA/DA (Packet Reservation Multiple Access/Dynamic Allocation) [36] and DSA++ (Dynamic Slot Assignment) [13] protocols using FDD (Frequency Division Duplex), MASCARA (Mobile Access Scheme based on Contention and Reservation for ATM) [54] and DTDMA (Dynamic TDMA) [60] using TDD (Time Division Duplex) are representative wireless ATM MAC protocols with this three phase MAC design.

The MAC protocol for mobile infostation networks is designed to work with a high performance PHY layer, i.e., a high data rate PHY with MIMO (Mulitple Input Multiple Output antenna),

OFDM (Orthogonal Frequency Division Multiplexing) and AMC (Adaptive Modulation and Coding) scheme. However, the high data rate could be mitigated when MAC and transport protocol are taken into account. The MAC protocol overhead increases as the PHY data rate increases because of the fixed low data rate protocol header and channel training sequence. As a result, the throughput efficiency (defined as the ratio between the MAC throughput and average PHY data rate) of MAC protocols decreases as the PHY data rate increases. Therefore, high throughput efficiency and low complexity are key to the infostation MAC design. The other requirements for the MAC design include proportional fairness for all regular users with different mobilities, and high priority for super-users.

Some earlier work about MAC protocol design for infostation networks can be found in [50,70]. The proposed protocol is called WINMAC, which is configured to work at TDMA/TDD (Time Division Multiple Access/Time Division Duplex) mode on a Harris PRISM IEEE 802.11 WLAN radio chip set with three transmission rates (i.e., 0.5, 1, and 2Mbps). The WINMAC includes a go-back-N and SR ARQ (Selective Repeat ARQ) protocol, a reservation based multiple access protocol, which supports both fairness and preemptive services. Because WINMAC is designed to work on the low data rate PHY technologies, the implementation complexity and protocol overhead of the WINMAC protocol could be high if a high data rate PHY is employed. The CSMA/CA based MAC protocol such as IEEE 802.11 [31] DCF (Distributed Coordinate Function) has been the standard for WLANs (Wireless Local Area Network). The success of its low data rate versions makes it a reasonable choice to start with for a high throughput MAC protocol. The forthcoming IEEE 802.11n standard is an amendment to the 802.11 standards to support MIMO (multiple-input multiple-output) technology with raw data rates up to 600 Mbps. The proposed features of IEEE 802.11n [51] are based on the EDCF (Enhanced Distributed Coordinate Function) of IEEE 802.11e [32] with data rate adaptivity, frame aggregation and bi-directional data flow, etc. However, for the purposes of

backward compatibility and signal training, a fixed low data rate PHY header is adopted for each PHY frame, which increases the header overhead. Compared with the DCF, the EDCF has higher throughput efficiency with QoS support. Adaptive data rates make use of the bandwidth more efficient. The frame aggregation improves the throughput by using a larger PHY frame, which carries multiple MAC frames. The bi-directional data flow feature improves the throughput for TCP type of data traffic. Therefore, the throughput is improved significantly compared to the DCF based IEEE 802.11. The major drawback of the IEEE 802.11n is the protocol complexity, which makes it difficult to implement and maintain.

Inspired by the wireless ATM MAC protocols and IEEE 802.11n proposal, we designed a simple but effective MAC protocol with reduced complexity and higher throughput. Since it is designed for the MINT, we name it Mobile Infostation Network MAC protocol (MIN-MAC). Different from IEEE 802.11, the MIN-MAC protocol uses a centralized scheduling algorithm to allocate channel resources based on the channel condition, user priority and mobility, etc. The MIN-MAC protocol has the following features: i) support for a high priority super-user; ii) packet aggregation; iii) multi-user diversity gain; iv) scalability in the number of supported users; v) optional reliable transmission;

The MIN-MAC protocol is proposed with two variations called MIN-MACa and MIN-MACb. The MIN-MACa uses a selective ARQ scheme that works with packet aggregation, the packet loss at link layer is recovered by the MAC retransmission scheme. It is designed to use without a reliable transport layer protocol. The highly efficient MIN-MACb is designed without ARQ. It relies on a transport layer protocol for reliable transmission that is optimized for the MAC protocol and infostation applications. The jointly optimized transport layer protocol, which is named MIN-TCP,

provides higher throughput than regular TCP for all the link error rates and achieve higher throughput than the MIN-MACa scheme when link error rate is low.

In the following, we will describe the energy saving Hybrid ARQ in Chapter 2. The MIN-MAC design for system A and system B is given in Chapter 3. The joint design of MIN-TCP and MIN-MAC for system B is described in Chapter 4. We conclude with future direction in Chapter 4.4.

Chapter 2

Energy Efficient Hybrid–ARQ Protocol

For mobile infostation networks, both infostation and mobile terminals are battery powered. For this type of energy limited network, it is of interest to optimize the average energy consumption of a Hybrid–ARQ system while maintaining a target frame-error-rate (FER) or, alternatively, minimize the FER under an average energy constraint.

Consider a frequency flat fading channel with no CSI (Channel State Information) at the transmitter and perfect CSI at the receiver. For a Hybrid–ARQ scheme, the receiver has limited one bit feedback from the receiver about the success or failure of the previous transmission. Without CSI, we use a power adaptation scheme, in which the energy allocated to the transmitted block in the l-th ARQ round is a time-invariant deterministic function of the relative index l. This fixed power allocation scheme has been proposed in [24,30,44,67] independently. In [24], an asymptotically optimal power control algorithm is proposed that yields very significant diversity advantage in long-term static MIMO channels, where the long-term static channel means that the channel coefficients remain constant during all ARQ rounds and change to new independent values with each new packet. The proposed power control algorithm shows that the energy allocated to the l-th block can be made inversely proportional to the probability of transmitting the l-th block. However, for short-term static channels, where the channel remains constant during each round and changes independently for the next round, only a scheme without power control is discussed in [24].

For energy limited data networks, the performance goal is to maximize the amount of data transmitted per unit energy with a maximum delay limit. To minimize the average energy consumption per source packet, we propose a power adaptation scheme with power level at each ARQ round optimized for the short-term static channels. Our goal is to choose the transmit energy for the l-th ARQ round to minimize the average energy consumption under a PER constraint with the maximal number of ARQ rounds to be fixed to L, or alternatively, minimize the PER under an average energy constraint.

We use a geometric programming (GP) approach to solve the above optimization problems. A GP is a mathematical formulation of an optimization problem that can be expressed in terms of a class of functions which we call posynomials [14]. It has been found that optimization of power control for interference-limited wireless networks can be formulated as GP and solved efficiently(see [11] and references there in). We show that our problem can be formulated and solved as a GP. A closed-form solution can be obtained, which shows that the transmit energy allocated for the l-th ARQ round is also inversely proportional to the probability of transmitting the l-th block, which is similar to the optimal scheme for long term static channel obtained in [24]. We also show that the optimized transmit power increases super-linearly each time a retransmission is requested and the fraction of the average energy optimally allocated to the l-th ARQ round only depends on the incremental diversity gains obtained at all ARQ rounds.

This chapter is organized as follows: In section 2.1, we give some preliminaries about the background of the work. In section 2.2, we analyze the probability of error for type I and type II Hybrid–ARQ scheme over a short term static Rayleigh fading channel with different transmit energy for each ARQ round. In section 2.3, the optimization problem is formulated and solved as a geometric programming problem. In section 2.4, simulation validations for the optimal power

allocation strategy are presented and we make some remarks about our work in section 2.5.

2.1 Preliminaries

2.1.1 Channel and Hybrid–ARQ Model

We consider a frequency flat fading channel with no CSI (channel state information) at the transmitter and perfect CSI at the receiver. For a MIMO channel with M_T transmit antennas and M_R receive antennas, the channel state matrix $\mathbf{H}_l \in \mathbb{C}^{M_R \times M_T}, l = 1, \cdots, L$ remains constant during the l-th ARQ round and changes independently for different ARQ rounds. Each ARQ round takes T channel uses. Define $\mathbf{x}_{l,t} \in \mathbb{C}^{M_T}, t = 1, \cdots, T$, $\mathbf{y}_{l,t} \in \mathbb{C}^{M_R}, t = 1, \cdots, T$, and $\mathbf{w}_{l,t} \in \mathbb{C}^{M_R}, t = 1, \cdots, T$ as the transmitted signal, received signal and corresponding channel noise vector respectively. The channel noise is assumed to be temporally and spatially white with i.i.d. complex Gaussian entries $\sim \mathcal{CN}(0, 1)$. Let E_l be the transmit power per channel use, which remains constant for the l-th ARQ round, and $\Gamma_l = E_l T$ be the energy consumption for the l-th ARQ round. The channel model is defined as

$$\mathbf{y}_{l,t} = \sqrt{\frac{E_l}{M_T}} \mathbf{H}_l \mathbf{x}_{l,t} + \mathbf{w}_{l,t}, \tag{2.1}$$

which corresponds to a short term static channel in [24]. It is also referred to as the L-block fading ARQ model in the thesis.

An energy allocation scheme for the L-block fading ARQ model is defined as $\mathbf{\Gamma} = (\Gamma_1, \Gamma_2, \cdots, \Gamma_L)$. The corresponding instantaneous power allocation scheme is defined as

$$\mathbf{E} = (E_1, E_2 \cdots, E_L) = (\rho u_1, \rho u_2, \cdots, \rho u_L) = \rho \mathbf{u}$$

, where $\rho = \|\mathbf{E}\|$ and $\mathbf{u} = \frac{\mathbf{E}}{\|\mathbf{E}\|}$, and $\|\cdot\|$ represents the norm of the vector.

The source packet is protected with an error detection code, which is then transmitted following a Hybrid–ARQ scheme. For simplicity, we assume the undetected decoding error is very small compared with the detected decoding error and can be ignored during the analysis of decoding error.

For type I and Chase combining Hybrid–ARQ, the source packet is encoded with a high rate code. At each ARQ round, the same codeword is retransmitted. For type II Hybrid ARQ, the source packet is encoded with a low rate code and mapped into a sequence of L code blocks. At ARQ round l, the l-th code block is transmitted. At the receiver side, for type I Hybrid–ARQ, there is no buffering for previous ARQ rounds and the codeword received at current ARQ round is decoded. For Chase combining and type II Hybrid–ARQ, at ARQ round l, the codewords or code blocks from the ARQ round 1 through l are all buffered and decoded as one codeword using a maximum likelihood (ML) decoder. At each ARQ round, if a decoding error occurs, a one-bit negative acknowledgment (NACK) signal is sent back to the transmitter, otherwise, an acknowledgment (ACK) is sent back. An error-free and zero-delay ARQ feedback channel is assumed. If an ACK is received, the transmitter then sends a new source packet. If a NACK is received, the transmitter enters the next ARQ round of the same source packet. When the last ARQ round L is reached, an ARQ error is declared for the current source packet and the transmitter initiates the first ARQ round of a new source packet.

2.1.2 Average Energy Consumption and Average Power

Following [24], we define $\mathcal{T}$ as a random variable indicating the number of ARQ rounds it takes to transmit a source packet. Let $\mathcal{A}_l$ denote the event that an ACK is received by the transmitter at

round l. For all $l = 1, \cdots, L-1$, we have

$$Pr(\mathcal{T} = l) = Pr(\bar{\mathcal{A}}_1, \cdots, \bar{\mathcal{A}}_{l-1}, \mathcal{A}_l) = q_l \tag{2.2}$$

After $l = L$ rounds, either an ACK or a NACK is received, the transmitter sends a new source packet. Therefore,

$$Pr(\mathcal{T} = L) = 1 - \sum_{l=1}^{L-1} q_l \tag{2.3}$$

The probability of the event that a NACK is received at the l-th round is defined as

$$P_l = Pr(\bar{\mathcal{A}}_1, \cdots, \bar{\mathcal{A}}_l), \tag{2.4}$$

and let $P_0 = 1$ by definition. Let $E[\cdot]$ denote the expectation of a random variable. From [24, equation (10,12)], the average energy consumption per source packet is then defined as

$$\bar{\Gamma} = E\left[\sum_{l=1}^{\mathcal{T}} \Gamma_l\right] = \sum_{l=1}^{L} \Gamma_l P_{l-1}, \tag{2.5}$$

which we are trying to minimize in this work. It can be interpreted as the the sum of the energy consumption for each ARQ round weighted by the probability of a decoding error at previous ARQ round.

2.1.3 Geometric Programming

A Geometric Program (GP) [8,14,59] is a mathematical formulation of an optimization problem that can be expressed in terms of a class of functions which we call positive polynomials or posynomials.

The standard form is as follows,

$$\begin{aligned} &\text{minimize } f_0(\mathbf{x}) \\ &\text{subject to } f_k(\mathbf{x}) \leq 1, \;\; k = 1, 2, \cdots, m, \\ &\qquad x_1 > 0, \; x_2 > 0, \cdots, x_n > 0, \end{aligned} \tag{2.6}$$

where

$$f_k(\mathbf{x}) = \sum_{j=1}^{N_k} c_{kj} x_1^{a_{kj}^{(1)}} x_2^{a_{kj}^{(2)}} x_n^{a_{kj}^{(n)}}, \;\; k = 0, 1, \cdots, m$$

are posynomials, with $c_{kj} > 0$ as positive numbers and $a_{kj}^{(i)} \in \mathbb{R}, i = 1, \cdots, n$ as real numbers. By letting $x_i = e^{z_i}, i = 1, 2, \cdots, n$, the transformed primal program is a convex program and all theory of convex programming can be applied [8]. The degree of difficulty of a GP is defined as $\mathcal{N} - \mathcal{M} - 1$, where $\mathcal{N} = \sum_{k=0}^{m} N_k$ denotes the total number of terms in all the posynomials of both the objective function and all the constraints, and $\mathcal{M} = n$ denotes the number of design variables $x_i, i = 1, \cdots, n$.

A geometric program in its standard dual form is as follows,

$$\text{maximize } v(\delta) = \prod_{k=0}^{m} \prod_{j=1}^{N_k} \left(\frac{c_{kj}}{\delta_{kj}} \sum_{l=1}^{N_k} \delta_{kl} \right)^{\delta_{kj}} \tag{2.7a}$$

$$\text{subject to } \delta_{kj} > 0, \; j = 1, \cdots, N_k, \; k = 0, \cdots, m, \tag{2.7b}$$

$$\sum_{j=1}^{N_0} \delta_{0j} = 1, \tag{2.7c}$$

$$\sum_{k=0}^{m} \sum_{j=1}^{N_k} a_{kj}^{(i)} \delta_{kj} = 0, i = 1, 2, \cdots, n, \tag{2.7d}$$

where equations (2.7c) and (2.7d) are the normality and orthogonality constraints respectively. The degree of difficulty is equal to the number of independent variables over which the dual function is

to be maximized. For a geometric programming problem with a zero degree of difficulty, the dual program has linear constraints with a unique solution, the primal program can then be solved based on the primal-dual relation uniquely.

2.2 Packet Error Probability

The average energy consumption is closely related to the packet error probability. In the following, we derive the Packet Error Rate (PER) for both type I Hybrid-ARQ and type II Hybrid-ARQ scheme over the L-block fading channel with a maximum likelihood (ML) decoder.

2.2.1 Diversity Gain

Diversity is a technique used to combat channel fading in wireless communication. Since the performance gain at high SNR is dictated by the SNR exponent of the error probability, this exponent is called the diversity gain, which is defined in [74] to show the diversity-multiplexing tradeoff in MIMO channels. The optimal diversity-multiplexing tradeoff for ARQ MIMO channels is given in [24]. For the Hybrid–ARQ over L-block fading channels, we can define a new term called incremental diversity gain. For a given power allocation scheme $\mathbf{E} = (E_1, E_2 \cdots, E_L) = \rho\mathbf{u}$. The error exponent after decoding at the l-th ARQ round is defined as

$$d_l = -\lim_{\rho\to\infty} \frac{\log P_l(\rho\mathbf{u})}{\log \rho}, \tag{2.8}$$

where $P_l(\rho\mathbf{u})$ is the average packet error probability after the l-th ARQ round over all fading states. The incremental diversity gain, which represents the diversity gain obtained by the l-th ARQ round,

is defined as

$$D_l = d_l - d_{l-1} = -\lim_{\rho\to\infty} \frac{\log P_l(\rho\mathbf{u}) - \log P_{l-1}(\rho\mathbf{u})}{\log \rho},$$

where $d_0 = 0$ by definition.

2.2.2 Probability of Errors in Hybrid–ARQ

The probability of error with a given channel state for convolutional codes or STTC codes is based on the Euclidean distance between codewords. Different from information outage probability approaches used in [24,74], where Gaussian codes are assumed, the Euclidean distance approach can only be applied to an ML decoder. To obtain the diversity gain, it is enough to analyze the pair-wise error probability (PEP) of a given coding scheme.

Let $\mathcal{E}_l$ denote the event that a decoding error occurs with a codeword composed of l code blocks. As we assume that the undetected decoding error can be ignored, given a sequence of channel state matrices $\mathbf{H}_1, \mathbf{H}_2, \cdots, \mathbf{H}_L$, the probability of sending a NACK at the l-th ARQ round for $l = 1, \cdots, L$ equals to

$$\begin{aligned} P_l(\rho\mathbf{u}|\mathbf{H}_1, \mathbf{H}_2, \cdots \mathbf{H}_l) &= Pr(\mathcal{E}_1|\mathbf{H}_1) Pr(\mathcal{E}_2|\mathcal{E}_1, \mathbf{H}_1, \mathbf{H}_2) \cdots Pr(\mathcal{E}_l|\mathcal{E}_1, \mathcal{E}_2, \cdots, \mathcal{E}_{l-1}, \mathbf{H}_1, \mathbf{H}_2, \cdots \mathbf{H}_l) \\ &= Pr(\mathcal{E}_1, \cdots, \mathcal{E}_l|\mathbf{H}_1, \mathbf{H}_2, \cdots \mathbf{H}_l). \end{aligned} \tag{2.9}$$

We use superscripts t_1 and t_2 to denote the type I and type II Hybrid ARQ respectively. The Chase combining Hybrid–ARQ is considered a special case of type II Hybrid–ARQ and, therefore, is not discussed separately.

Type I Hybrid ARQ

For type I Hybrid ARQ, all events $\mathcal{E}_l$ are mutually independent, therefore

$$P_l^{t_1}(\rho\mathbf{u}|\mathbf{H}_1,\mathbf{H}_2,\cdots\mathbf{H}_l) = Pr(\mathcal{E}_1,\cdots,\mathcal{E}_l|\mathbf{H}_1,\mathbf{H}_2,\cdots\mathbf{H}_l) = \prod_{k=1}^{l} Pr(\mathcal{E}_k|\mathbf{H}_k). \tag{2.10}$$

Taking expectation over all channel states $(\mathbf{H}_1,\mathbf{H}_2,\cdots\mathbf{H}_l)$, the error probability equals $\prod_{k=1}^{l} Pr(\mathcal{E}_k)$. For the MIMO channel as defined in equation (2.1), we assume space-time trellis codes are used and decoded with an ML decoder. Define codewords

$$\begin{aligned}\mathbf{e}_l &= e_{1,l}^1 e_{1,l}^2 \cdots e_{1,l}^n e_{2,l}^1 e_{2,l}^2 \cdots e_{2,l}^n \cdots e_{T,l}^1 e_{T,l}^2 \cdots e_{T,l}^n,\\ \mathbf{c}_l &= c_{1,l}^1 c_{1,l}^2 \cdots c_{1,l}^n c_{2,l}^1 c_{2,l}^2 \cdots c_{2,l}^n \cdots c_{T,l}^1 c_{T,l}^2 \cdots c_{T,l}^n,\end{aligned} \tag{2.11}$$

where $n = M_T$ is the number of transmit antenna and T is the number of channel uses. The probability that an ML receiver decides erroneously in favor of $\mathbf{e}_l$ assuming that $\mathbf{c}_l$ was transmitted at the l-th ARQ round is [68, equation (9)]

$$P_{2,l}(\mathbf{c}_l,\mathbf{e}_l) \leq \left(\frac{1}{\prod_{i=1}^{M_T}(1+\lambda_i E_l/4N_0)}\right)^{M_R}, \tag{2.12}$$

where λ_i is the i-th eigenvalue of a matrix $\mathbf{A}$ with entries

$$\mathbf{A}_{pq} = \sum_{t=1}^{T}(c_t^p - e_t^p)\overline{(c_t^q - e_t^q)}.$$

We have dropped subscript l because the same codewords are sent for all ARQ rounds. At high SNRs, the bound in equation (2.12) is asymptotically tight and the PEP can be approximated as

$$P_{2,l}(\mathbf{c}_l, \mathbf{e}_l) \approx \left(\prod_{i=1}^{r} \lambda_i\right)^{-M_R} \left(\frac{E_l}{4N_0}\right)^{-M_T M_R},$$

where r is the number of non-zero eigenvalues of the matrix $\mathbf{A}$. In the following analysis, we assume the optimal code design is applied, for which the maximum $r = M_T$ is achieved.

The PEP for type I Hybrid–ARQ up to l ARQ rounds is then approximated as

$$\begin{aligned} P_{2,l}^{t_1}(\rho\mathbf{u}) &= \prod_{k=1}^{l} P_{2,l}(\mathbf{c}_k, \mathbf{e}_k) \\ &\approx 4^{lM_R M_T} \left(\prod_{i=1}^{M_T} \lambda_i\right)^{-lM_R} \left(\prod_{k=1}^{l} \frac{u_k \rho}{N_0}\right)^{-M_T M_R} \\ &= C_l \prod_{k=1}^{l} \left(\frac{E_k}{N_0}\right)^{-D_k}, \end{aligned} \tag{2.13}$$

where $C_l = 4^{lM_R M_T} \left(\prod_{i=1}^{M_T} \lambda_i\right)^{-lM_R}$, and $D_l = M_T M_R, l = 1, \cdots, L$ is the maximum incremental diversity gain for the l-th ARQ round.

Type II Hybrid ARQ

Proposition 1. The error probability of an L-block fading type II Hybrid–ARQ after the l-th ARQ round has the same diversity order as the error probability of decoding a codeword with l fading blocks at the l-th ARQ round alone without considering decoding errors at previous ARQ rounds, i.e.,

$$d_l = -\lim_{\rho \to \infty} \frac{\log Pr(\mathcal{E}_1, \cdots, \mathcal{E}_l)}{\log \rho} = -\lim_{\rho \to \infty} \frac{\log Pr(\mathcal{E}_l)}{\log \rho}.$$

Proof: For an L-block fading type II Hybrid–ARQ with ML decoding rule, the error probability can be bounded as

$$\frac{1}{2^{l-1}} Pr(\mathcal{E}_l|\mathbf{H}_1, \mathbf{H}_2, \cdots \mathbf{H}_l) \leq Pr(\mathcal{E}_1, \cdots, \mathcal{E}_l|\mathbf{H}_1, \mathbf{H}_2, \cdots \mathbf{H}_l) \leq Pr(\mathcal{E}_l|\mathbf{H}_1, \mathbf{H}_2, \cdots \mathbf{H}_l). \quad (2.14)$$

The upper bound is obvious because the probability of the joint event is equal to or lower than the probability of an individual event. The proof of the lower bound is based on the properties of Euclidean distance based ML decoding. The details are given in the Appendix. From the equation (2.14), taking the expectation over all channel states $(\mathbf{H}_1, \mathbf{H}_2, \cdots \mathbf{H}_l)$, we have

$$\frac{1}{2^{l-1}} Pr(\mathcal{E}_l) \leq P_l^{t_2}(\rho \mathbf{u}) \leq Pr(\mathcal{E}_l),$$

and

$$d_l = -\lim_{\rho \to \infty} \frac{\log P_l^{t_2}(\rho \mathbf{u})}{\log \rho}.$$

As ρ goes to infinity, we have $d_l = -\lim_{\rho \to \infty} \frac{\log Pr(\mathcal{E}_l)}{\log \rho}$. ■

Based on Proposition 1, to obtain the incremental diversity gain, we only need to consider the decoding error of codewords over an l block fading channel.

With a type II Hybrid–ARQ scheme, after the l-th ARQ round, an STTC codeword sent over an l block fading MIMO channel is decoded with an ML decoder. Given a power allocation scheme $\mathbf{E} = \rho \mathbf{u}$, we consider the probability that an ML receiver decides erroneously in favor of a signal

$$\mathbf{e} = \mathbf{e}_1 \mathbf{e}_2 \cdots \mathbf{e}_l$$

assuming that

$$\mathbf{c} = \mathbf{c}_1\mathbf{c}_2\cdots\mathbf{c}_l$$

was transmitted up to the l-th ARQ round, where $\mathbf{e}_l$ and $\mathbf{c}_l$ are defined in equation (2.11). The Euclidean distance between them is then $\sum_{k=1}^{l} d^2(\mathbf{c}_k u_k, \mathbf{e}_k u_k)\rho/4N_0$, where

$$\begin{aligned} d^2(\mathbf{c}_k u_k, \mathbf{e}_k u_k) &= \sum_{j=1}^{M_R}\sum_{t=1}^{T}\left|\sum_{i=1}^{M_T}\alpha_{i,j,k}(\sqrt{u_k}c_{t,k}^i - \sqrt{u_k}e_{t,k}^i)\right|^2 \\ &= u_k\sum_{j=1}^{M_R}\sum_{t=1}^{T}\left|\sum_{i=1}^{M_T}\alpha_{i,j,k}(c_{t,k}^i - e_{t,k}^i)\right|^2. \end{aligned} \tag{2.15}$$

It can be re-written as [68, equation (4), (7)]

$$\begin{aligned} d^2(\mathbf{c}_k u_k, \mathbf{e}_k u_k) &= u_k\sum_{j=1}^{M_R}\Omega_{j,k}A_k\Omega_{j,k}^* \\ &= \sum_{j=1}^{M_R}\sum_{i=1}^{M_T}\lambda_{i,k}u_k|\beta_{i,j,k}|^2, \end{aligned} \tag{2.16}$$

where $\Omega_{j,k} = (\alpha_{1,j,k}, \cdots, \alpha_{n,j,k})$, $\lambda_{i,k}$ is the i-th eigenvalue of the matrix $\mathbf{A}_k$ with entries

$$\mathbf{A}_{pq,k} = \sum_{i=1}^{T}(c_{t,k}^p - e_{t,k}^p)\overline{(c_{t,k}^q - e_{t,k}^q)}, 1 \le p, q \le M_T,$$

and $\beta_{i,j,k}$ are independent Rayleigh variables. The PEP is bounded by

$$P_{2,l}(\mathbf{c}, \mathbf{e}|\mathbf{H}_1\mathbf{H}_2, \cdots, \mathbf{H}_l) \le \exp\{-\sum_{k=1}^{l} d^2(\mathbf{c}_k u_k, \mathbf{e}_k u_k)\rho/4N_0\}.$$

After taking average over all random variables, we have

$$P_{2,l}(\mathbf{c}, \mathbf{e}) \le \prod_{k=1}^{l}\left(\frac{1}{\prod_{i=1}^{M_T}(1 + \lambda_{i,k}u_k\rho/4N_0)}\right)^{M_R}.$$

Therefore, at the l-th ARQ round, the PEP is approximated as

$$\begin{aligned} P_{2,l}^{t_2}(\rho\mathbf{u}) &\approx 4^{lM_RM_T}\left(\prod_{k=1}^{l}\prod_{i=1}^{M_T}\lambda_{i,k}\right)^{-lM_R}\left(\prod_{k=1}^{l}\frac{u_k\rho}{N_0}\right)^{-M_TM_R} \\ &= C_l\prod_{k=1}^{l}\left(\frac{E_k}{N_0}\right)^{-D_k}, \end{aligned} \tag{2.17}$$

where $C_l = 4^{lM_RM_T}\left(\prod_{k=1}^{l}\prod_{i=1}^{M_T}\lambda_{i,k}\right)^{-lM_R}$, and $D_k = M_TM_R, k = 1,\cdots,l$ is the incremental diversity for the k-th ARQ round. This shows that the maximum diversity order of an L-block fading type II Hybrid ARQ for a MIMO channel is equal to M_TM_RL and the maximum incremental diversity is $D_1 = D_2 = \cdots = D_L = M_TM_R$.

For single antenna systems, the channel model in equation (2.1) is simplified as

$$\mathbf{y}_{l,t} = \sqrt{E_l}\alpha_l\mathbf{x}_{l,t} + \mathbf{w}_{l,t}, l = 1,\cdots,L,\ \ t = 1,\cdots,T, \tag{2.18}$$

where α_l is the fading gain of the l-th code block. Equation (2.18) corresponds to the block fading channel model in [34,38] with L blocks and block length of T. The α_l are assumed to be independent Rayleigh random variables with unit second moment, i.e., $E[\alpha_l^2] = 1$. To analyze the PEP, we assume an all-zero codeword $\mathbf{0}$ is binary-PSK modulated and transmitted through l fading blocks. Define the weight of the k-th code block as $d_{fk}, k = 1,\cdots,l$. Then the squared Euclidean distance between a codeword $\mathbf{c}$ and $\mathbf{0}$ is

$$d^2(\mathbf{c},\mathbf{0}) = \sum_{k=1}^{F_H}\frac{2E_k}{N_0}d_{fk}\alpha_k^2,$$

where $F_H \leq l$ is the number of non-zero d_{fk}. Here we make an important argument that for type II Hybrid–ARQ with $l = 1,\cdots,L$ rounds over l fading blocks, the maximum $F_H = l$ is achieved by

code design, which is one of the code design criteria for block fading channels [39]. To achieve the maximum F_H, which has to satisfy the singleton bound [39], i.e., $F_H \leq 1 + \lfloor l(1-R) \rfloor$, the coding rate R needs to satisfy $R \leq 1/l$, which is easily satisfied by code design.

The PEP over an l-block fading channel is obtained with the Moment Generating Function (MGF) method [38] as follows. Define a random variable $Z = d^2(\mathbf{c}, \mathbf{0}) = \sum_{k=1}^{l} \frac{2E_k}{N_0} d_{fk} \alpha_k^2$, whose MGF is calculated as

$$\phi_Z(\mathbf{s}) = \int p(z) e^{\mathbf{s}z} dz = \prod_{k=1}^{l} \frac{1}{1 - \frac{2E_k}{N_0} d_{fk} \mathbf{s}}, \tag{2.19}$$

where $\frac{1}{1-\frac{2E_k}{N_0} d_{fk}\mathbf{s}}$ is the MGF of the exponential random variable $\frac{2E_k}{N_0} d_{fk} \alpha_k^2$. We bound the PEP as follows:

$$\begin{aligned} P_{2,l}(\mathbf{c}, \mathbf{0}) &= E[P_{2,l}(\mathbf{c}, \mathbf{0} | Z = z)] = \int Q(\sqrt{z}) p(z) dz \\ &\leq \frac{1}{2} \int p(z) e^{-\frac{1}{2}z} dz \\ &= \frac{1}{2} \phi_Z(-\frac{1}{2}) \\ &= \frac{1}{2} \prod_{k=1}^{l} \frac{1}{1 + d_{fk} \frac{E_k}{N_0}}, \end{aligned} \tag{2.20}$$

where the bound $Q(x) \leq \frac{1}{2} e^{x^2/2}$ is applied. The same result is also obtained in [29] with a different approach for a generalized Hybrid–ARQ system when codewords with different transmission power are soft-combined and decoded. At high SNR, the bound in equation (2.20) is asymptotically tight and the PEP can be approximated as

$$\begin{aligned} P_{2,l}(\mathbf{c}, \mathbf{0}) &\approx \frac{1}{2} \prod_{k=1}^{l} \frac{1}{1 + d_{fk} \frac{E_k}{N_0}} \approx \frac{1}{2 \prod_{k=1}^{l} d_{fl}} \prod_{k=1}^{l} \left(\frac{E_k}{N_0} \right)^{-1} \\ &= C_l \prod_{k=1}^{l} \left(\frac{E_k}{N_0} \right)^{-D_k}, \end{aligned} \tag{2.21}$$

where $C_l = (2 \prod_{k=1}^{l} d_{fk})^{-1}$ and the incremental diversity is $D_k = 1, k = 1, \cdots, l$. This shows that the diversity order of an L-block fading Hybrid ARQ is equal to L and the incremental diversity

gain is 1 for single antenna systems.

2.2.3 PER Approximation for Hybrid–ARQ

At the l-th ARQ round for a type I Hybrid–ARQ, the packet error probability is simply the product of codeword error probability for each round. For a type II Hybrid–ARQ, the last decoded codeword is composed of $l \leq L$ sub-frames with symbol energy E_l for the l-th ARQ round. The packet error probability has the same diversity order as the PEP of the last decoded codeword. From equations (2.13), (2.21) and (2.17), the unified approximation of the packet error rate (PER) for all type of Hybrid–ARQ schemes at high SNR can be written as

$$P_l(E_1, \cdots, E_l) \approx A_l \prod_{k=1}^{l} \left(\frac{E_k}{N_0} \right)^{-D_k}, \tag{2.22}$$

where A_l can be loosely bounded by

$$\max_{m=1,\cdots,M-1} \{C_{l,m}\} \leq A_l \leq \sum_{m=1}^{M-1} C_{l,m},$$

where $C_{l,m}$ is the PEP parameters for the m-th codeword pairs and M is total number of codewords. However, there is no closed form representation for A_l. Since an accurate value of A_l is needed to calculate the optimal power allocation scheme, we obtain it from the PER statistics off-line.

In the remainder of this chapter, we will use the above expression for the transmission probability in deriving optimal power allocation strategies for the Hybrid–ARQ system.

2.3 Optimal Power Allocation

In this section we will analyze the optimal power allocation scheme for the Hybrid–ARQ in an L-block fading channel.

2.3.1 Problem Formulation

The optimal power allocation problem that minimizes the average energy consumption under a PER constraint can be formulated as

$$\min_{E_1,E_2,\cdots,E_L}\left\{\bar{\Gamma}=\sum_{l=1}^{L}\Gamma_l P_{l-1}=T\sum_{l=1}^{L}E_l P_{l-1}(E_1,\cdots,E_{l-1})\right\} \tag{2.23a}$$

$$\text{subject to}\quad P_L(E_1,\cdots,E_L)\le P_e^{\max}, \tag{2.23b}$$

$$E_l>0,\quad l=1,\cdots,L,$$

where E_l is the transmit power for the l-th ARQ round, $P_l(E_1,\cdots,E_l)$ is the PER after the l-th ARQ round with $P_0=1$ by definition.

The above optimization problem can be written as a GP in standard primal form after applying approximation (2.22).

$$\begin{aligned}\min_{\underline{x}}\{\ f_0(\underline{x})&=x_1+A_1x_2x_1^{-D_1}+A_2x_3x_1^{-D_1}x_2^{-D_2}+\\&\quad\cdots+A_{L-1}x_L\prod_{i=1}^{L-1}x_l^{-D_l}\ \}\\ \text{subject to}\quad A_L&\prod_{i=1}^{L}x_l^{-D_l}\le P_e^{\max},\\ x_l&>0,\quad l=1,\cdots,L,\end{aligned} \tag{2.24}$$

where $\underline{x} = (x_1\ x_2\ \cdots\ x_L), x_l = E_l/N_0,\ \forall l = 1, \cdots, L$ and D_l are incremental diversity gain for the l-th ARQ round. This is a GP with a zero degree of difficulty and thus has a unique solution. Because of its special form, we can obtain the closed-form solution by solving its dual program.

The dual program is formulated as

$$\max_{\underline{\delta}} \{\ v(\underline{\delta}) = \prod_{l=1}^{L} \left(\frac{A_{l-1}}{\delta_l}\right)^{\delta_l} \left(\frac{A_L}{P_e^{\max}}\right)^{\delta_{L+1}} \}$$

subject to

$$\begin{aligned} &\sum_{l=1}^{L} \delta_l - 1 = 0, \\ &\delta_l - \sum_{j=l+1}^{L+1} \delta_j D_l = 0, \quad l = 1, \cdots, L, \end{aligned} \tag{2.25}$$

where $\underline{\delta} = \delta_1, \cdots, \delta_{L+1}$ is the design variable for the dual program. Because the primal problem has zero degree of difficulty, the constraints of the dual program form linear equations that have a unique solution, i.e.,

$$\begin{aligned} \delta_i^* &= \frac{D_i \prod_{j=i+1}^{L}(1+D_j)}{\prod_{j=1}^{L}(1+D_j) - 1}, \quad i = 1,\ \cdots,\ L-1, \\ \delta_L^* &= \frac{D_L}{\prod_{j=1}^{L}(1+D_j) - 1}, \\ \delta_{L+1}^* &= \frac{1}{\prod_{j=1}^{L}(1+D_j) - 1}. \end{aligned} \tag{2.26}$$

From the primal dual relation, the primal program and its optimal solution $\underline{x}^* = (x_1^*, x_2^*, \cdots, x_L^*)$

satisfy

$$f_0(\underline{x}^*) = v(\underline{\delta}^*) = \prod_{l=1}^{L} \left(\frac{A_{l-1}}{\delta_l^*} \right)^{\delta_l^*} \left(\frac{A_L}{P_e^{\max}} \right)^{\delta_{L+1}^*}$$
$$= \prod_{l=1}^{L} \left(\frac{A_{l-1}(\prod_{j=1}^{L}(1+D_j)-1)}{D_l \prod_{j=l+1}^{L}(1+D_j)} \right)^{\frac{D_l \prod_{j=l+1}^{L}(1+D_j)}{\prod_{j=1}^{L}(1+D_j)-1}} \left(\frac{A_L}{P_e^{\max}} \right)^{\frac{1}{\prod_{j=1}^{L}(1+D_j)-1}}, \tag{2.27}$$

where $\underline{\delta}^* = (\delta_1^*, \delta_2^*, \cdots, \delta_{L+1}^*)$.

Let $u_l(\underline{x}) = A_{l-1} x_l \prod_{j=1}^{l-1} x_j^{-D_j}$, then $f_0(\underline{x}) = u_1(\underline{x}) + u_2(\underline{x}) + \cdots + u_L(\underline{x})$. According to the duality theory [14, Theorem 1 (iv)], we have

$$u_l(\underline{x}^*) = v(\underline{\delta}^*)\delta_l^* = f_0(\underline{x}^*)\delta_l^*, \;\; l = 1, 2, \cdots, L. \tag{2.28}$$

And the optimal solution satisfies

$$\begin{aligned} x_1^* &= f_0(\underline{x}^*)\delta_1^*, \\ x_l^* &= \frac{A_{l-2} D_l}{A_{l-1} D_{l-1}(1+D_l)} (x_{l-1}^*)^{(1+D_{l-1})}, l = 2, \cdots, L. \end{aligned} \tag{2.29}$$

So far we assume a high SNR scenario, for which the diversity gain is independent of the SNR. For a low SNR scenario, the error exponent is related to the SNR and has a lower value than the theoretical diversity gain. However, we can still approximate the error exponent as a constant for a limited range of SNR around the operating point. In this case, the PER parameters A_l and D_l can be obtained from the PER statistics off-line. Then the same optimization scheme can be applied. Note that the PER approximation does not hold for SNR < 1 and, therefore, the optimization scheme cannot be applied with extremely low SNRs.

2.3.2 Comparison with Equal Power Allocation Scheme

For the optimal power allocation scheme with a closed-form expression in equation (2.29), we observe that there is a threshold above which, the transmit power increases super-linearly each time when a NACK is received. Below the threshold, the transmit power could decrease, which is different from the power ramping scheme in [30], where the power always increases for the next ARQ round. By comparing x_l and x_{l-1},

$$\begin{aligned} x_l^* &= \frac{A_{l-2}D_i}{A_{l-1}D_{l-1}(1+D_l)}(x_{l-1}^*)^{(1+D_{l-1})} \geq x_{l-1}^* \\ x_{l-1}^* &\geq \left(\frac{A_{l-1}(1+D_l)D_{l-1}}{A_{l-2}D_l}\right)^{\frac{1}{D_{l-1}}}, \end{aligned} \tag{2.30}$$

the threshold is obtained as

$$\min\{x_1^*, x_2^*, \cdots, x_L^*\} \geq \max_{l=1,\cdots,L}\left\{\left(\frac{A_{l-1}(1+D_l)D_{l-1}}{A_{l-2}D_l}\right)^{\frac{1}{D_{l-1}}}\right\}.$$

From equation (2.28), $\delta_l^* = u_l(\underline{x}^*)/f_0(\underline{x}^*)$ is defined as the proportion of average energy consumption for the l-th ARQ round in the total energy consumption. When $\delta_1^* \to 1$, the ARQ scheme converges to a scheme without ARQ. In the following, we show that as the incremental diversity increases, both the optimal and equal power allocation schemes converge to no-ARQ schemes.

To simplify the notation, we assume equal incremental diversity gain $D_l = D, l = 1, \cdots, L$ and either the number of ARQ rounds L or D is large. For the optimal power allocation scheme, we can approximate the equation (2.26) as

$$\delta_l^* \approx \frac{D}{(1+D)^l}, \;\; l = 1, 2, \cdots, L. \tag{2.31}$$

For conventional Hybrid–ARQ with equal power allocation for each ARQ round, i.e., $x_1 = x_2 = \cdots = x_L = \rho$ and a target PER P_e, the transmit power is

$$\rho = \left(\frac{P_e}{A_L}\right)^{-\frac{1}{DL}},$$

which comes from the PER constraint $A_L \prod_{i=1}^{L} x_l^{-D} \leq P_e$. We use superscript NPC to represent no power control case. The average energy consumption E_{av}^{NPC} has the same form as the $f_0(\underline{x})$ in equation (2.24), which is calculated as

$$E_{av}^{NPC} = \rho \sum_{l=1}^{L} A_{l-1} \rho^{-D(l-1)}, \tag{2.32}$$

where $A_0 = 1$ by definition. The proportion of average energy consumption for the l-th ARQ round in total energy consumption is calculated as

$$\delta_l^{NPC} = \frac{\rho A_{l-1} \rho^{-D(l-1)}}{\rho \sum_{l=1}^{L} A_{l-1} \rho^{-D(l-1)}},$$

which can be approximated for a large D as

$$\delta_l^{NPC} \approx A_{l-1} \rho^{-D(l-1)}. \tag{2.33}$$

For both optimal and equal power allocation schemes, with larger incremental diversity gain, i.e., larger number of transmitter and receiver antennas, more energy is allocated to the first ARQ round,

and the Hybrid-ARQ scheme converges to a no-ARQ scheme. It comes from the observation

$$\begin{aligned} \delta_1^* &\to 1 \text{ and } \delta_1^{NPC} \to 1, \text{ as } D \to \infty \\ \delta_l^* &\to 0 \text{ and } \delta_l^{NPC} \to 0, \text{ as } D \to \infty \text{ for } l = 2, \cdots, L \\ P_l^{NPC} &= A_l \rho^{-Dl} \to 0, \text{ as } D \to \infty \text{ for } l = 2, \cdots, L. \end{aligned} \tag{2.34}$$

Compared with δ_l^* in equation (2.31), δ_l^{NPC} in equation (2.33) converges faster as a function of D. It suggests that, as the incremental diversity gain increases, the conventional Hybrid–ARQ scheme converges faster to a no-ARQ scheme than the optimal scheme in terms of the average energy consumption, and both Hybrid–ARQ schemes do not provide much energy savings over no-ARQ schemes. It implies that the performance gain of an optimal power allocation scheme over an equal power allocation scheme diminishes as incremental diversity gain increases.

In the following, we analyze the performance gain of the optimal power allocation scheme over the equal power allocation scheme as a function of the maximum number of ARQ rounds L by comparing the equations (2.27) and (2.32) numerically.

As an illustrative example, we adopt a type I Hybrid–ARQ scheme based on an optimal distance spectrum, 1/2 rate convolutional code with a constraint length $K = 3$ [20]. The parameters of the PER is obtained from the approximation based on the first 10 terms of the codeword distance spectrum [20, Table I]. With $D_l = 1, A_l = 39.91^l, l = 1, \cdots, L$, the average energy per packet for both optimal and equal power allocation schemes are calculated based on equations (2.27) and (2.32) respectively. The performance comparison is given in Figure 2.1. It shows that the performance gain is more significant at a lower target PER and decreases with an increasing number of ARQ rounds.

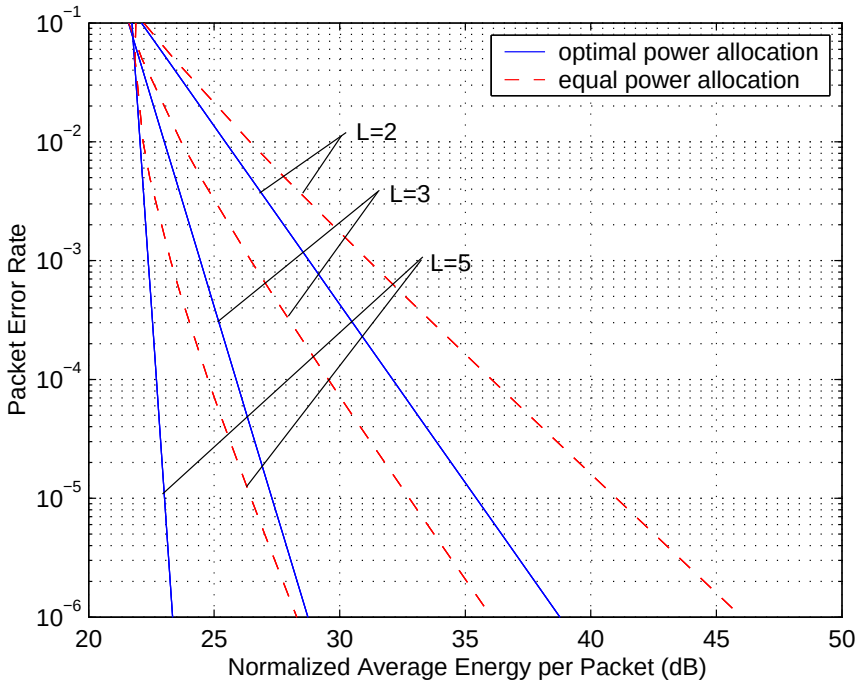

Figure 2.1: Analytical performance comparison between the optimal and equal power allocation strategies for different ARQ rounds L

2.4 Applications

In the following, we apply the optimal power allocation scheme in simulated Hybrid–ARQ systems. To illustrate the performance gain against the no power control Hybrid-ARQ systems, we consider the following three scenarios. For the first scenario, we apply the type I Hybrid-ARQ over a 2x1 MIMO Rayleigh block fading channel with an 8-states 4-PSK STTC coding scheme defined in [68, Fig. 5]. For the second scenario, we apply the Chase combining Hybrid-ARQ over the same channel and with the same coding scheme. For the third scenario, we apply the type II Hybrid-ARQ with Incremental Redundancy over a single antenna Rayleigh block fading channel with an RCPC (Rate Compatible Punctured Convolutional) code. For the MIMO cases, the maximum number of transmission $L = 2$ is assumed. For the single antenna case, we evaluate the cases of both $L = 2$ and $L = 4$.

As an illustrative example, when $L = 2$, the optimal SNR values for the first and the second ARQ round, as well as the average energy consumption, are derived as

$$\begin{aligned} x_1^* &= \frac{E_1}{N_0} = \left(\frac{A_1\delta_1^*}{\delta_2^*}\right)^{D_2\delta_3^*}\left(\frac{A_2}{P_e^{\max}}\right)^{\delta_3^*}, \\ x_2^* &= \frac{E_2}{N_0} = \left(\frac{A_1\delta_1^*}{\delta_2^*}\right)^{-D_1\delta_3^*}\left(\frac{A_2}{P_e^{\max}}\right)^{(1+D_1)\delta_3^*}, \\ f(x_1^*, x_2^*) &= \left(\frac{1}{\delta_1^*}\right)^{\delta_1^*}\left(\frac{A_1}{\delta_2^*}\right)^{\delta_2^*}\left(\frac{A_2}{P_e^{\max}}\right)^{\delta_3^*}, \end{aligned} \tag{2.35}$$

where

$$\begin{aligned} \delta_1^* &= \frac{D_1(D_2+1)}{D_1+D_2+D_1D_2}, \\ \delta_2^* &= \frac{D_2}{D_1+D_2+D_1D_2}, \\ \delta_3^* &= \frac{1}{D_1+D_2+D_1D_2}. \end{aligned} \tag{2.36}$$

The diversity gain and coding gain parameters of the PER, i.e., $A_l, D_l, l = 1, 2$ are obtain from the PER statistics based on simulation. For different power allocation schemes, i.e., the power difference between the two ARQ rounds are -6 dB, -3 dB, 0 dB, 3 dB and 6 dB, we obtain the PER curves and find the best fit for A_1, D_1, A_2, D_2. We then calculate the value of x_1^*, x_2^* for different PER target $P_e^{\max}$. For each set of x_1^*, x_2^*, we obtain the PER value by simulation to validate its optimality. The results are shown in Figure 2.2 and 2.3 for MIMO channels, and Figure 2.4 and 2.5 for single antenna channels.

In Figures 2.2 and 2.3, the illustrative results show that at a target PER of 10^{-4}, the optimal power allocation scheme can provide a gain of up to 3 dB for type I Hybrid-ARQ and 2.5 dB for Chase combining Hybrid-ARQ.

In Figure 2.4 and 2.5, we use a realistic convolutional code adapted from 3GPP standard [1] and puncture it to the desired coding rates. Assume the data source is encoded with a rate 1/5 convolutional code with a constraint length $K = 9$. The generating polynomials are (765 671 513 473 653)

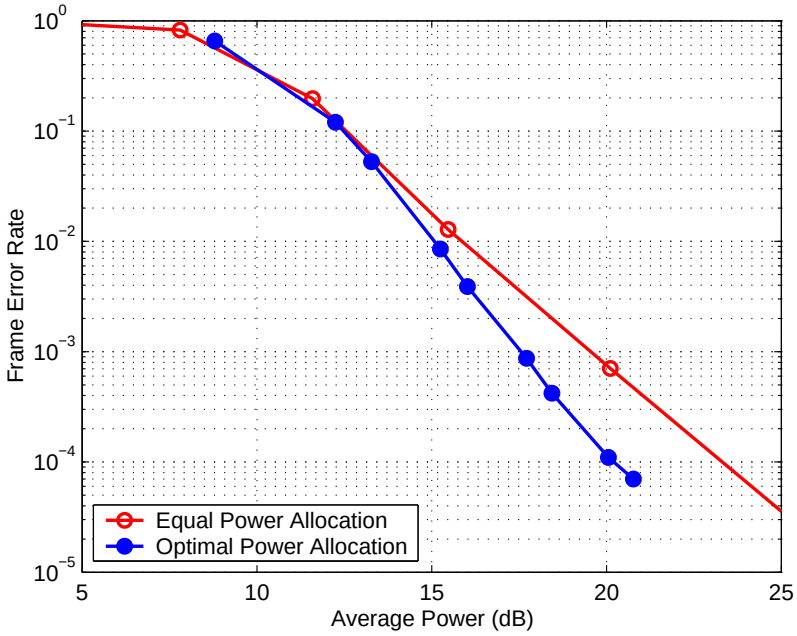

Figure 2.2: PER for equal power allocation scheme and optimum power allocation scheme for type I Hybrid ARQ

in octal format. For the two (re)transmission ($L = 2$) case, we puncture the mother code to generate a (1/2, 1/4) rate RCPC code. For the four (re)transmission ($L = 4$) case, we generate a (4/5, 2/5, 4/15, 1/5) rate RCPC code. The simulation results show that the optimal scheme can provide a 4 dB gain for $L = 2$ and a 2 dB gain for $L = 4$ at a target PER of 10^{-4}.

For all scenarios, at very high target FERs, there are not any significant gains to be obtained over the scheme without power control. We also confirm that the energy savings via the optimal power allocation increases for lower PER targets and decreases as the number of allowable retransmissions increases. The simulation results for MIMO channels and SISO channels are also consistent with the analysis that the energy savings decreases with higher incremental diversity gain.

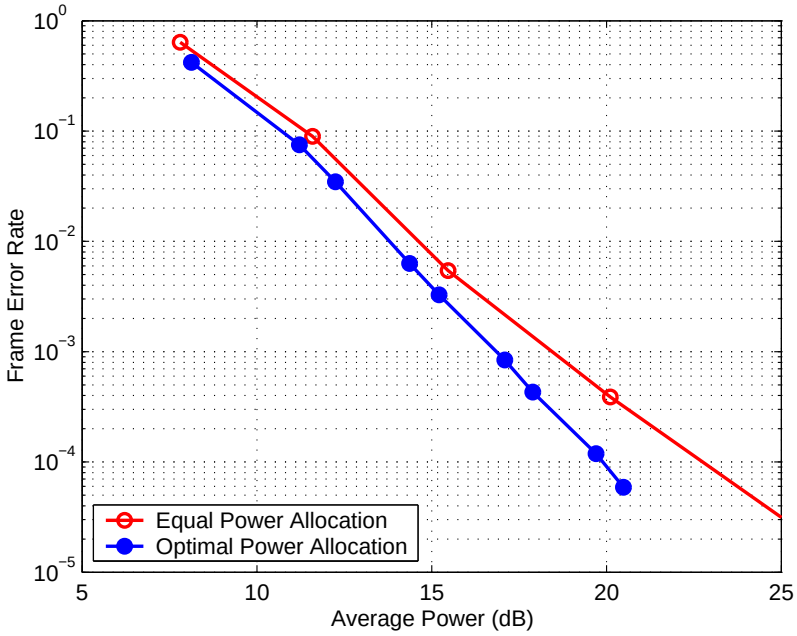

Figure 2.3: PER for equal power allocation scheme and optimum power allocation scheme for Chase combining Hybrid ARQ

2.5 Remarks

For the optimal power allocation of a Hybrid–ARQ scheme, we find that when the incremental diversity gain is low, we can achieve considerable energy savings. However, when the incremental diversity gain is high, the energy savings is marginal compared with both equal power allocation schemes and no-ARQ schemes. For MIMO channels, the optimal power allocation Hybrid–ARQ scheme is best used in low diversity gain, large multiplexing gain scenarios.

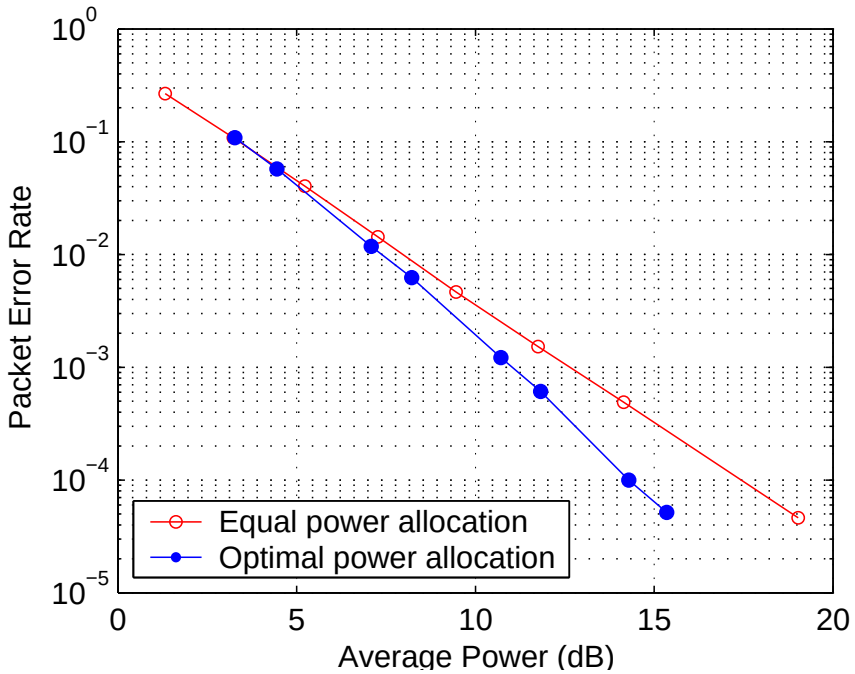

Figure 2.4: Simulation performance comparison of the optimal power allocation strategy and equal power allocation strategy $(L = 2)$

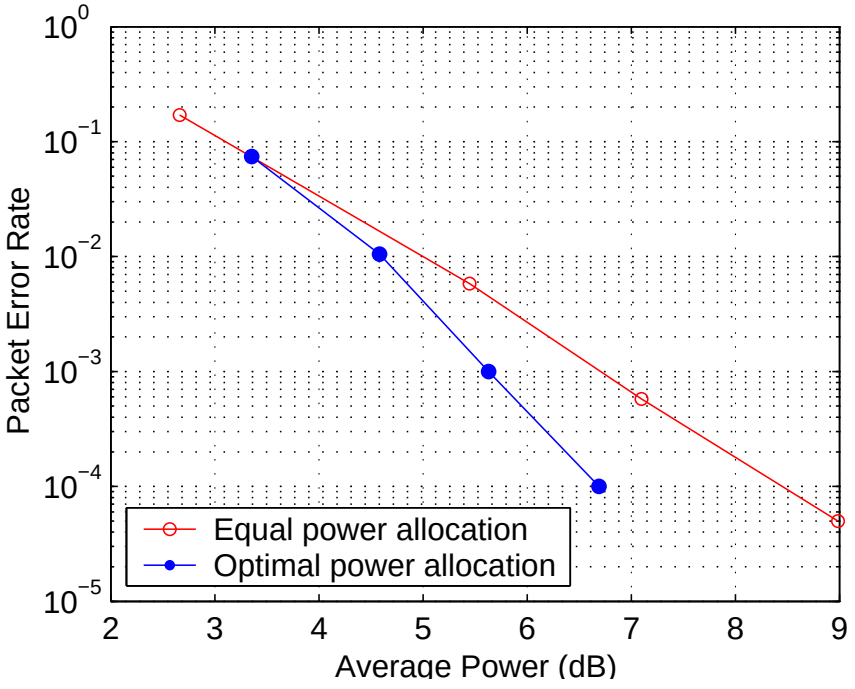

Figure 2.5: Simulation performance comparison of the optimal power allocation strategy and equal power allocation strategy $(L = 4)$

Chapter 3

MAC Design for Efficient Data Transmission over Mobile Infostation Networks

The IEEE 802.11 [31] standard is a widely used wireless local area network (WLAN) standard developed by the IEEE LAN/MAN Standards Committee. The success of its low data rate versions makes it a reasonable choice to start with for a high throughput MAC protocol. The IEEE 802.11n is an amendment to the 802.11 standards to support MIMO (multiple-input multiple-output) technology with raw data rates up to 600 Mbps. It is still on the way of standardization. The current draft is based on the merged proposals from three groups, i.e., TGn Sync (Task Group n Synchronized), WWiSE (World-Wide Spectrum Efficiency) and MITMOT (Mac and mImo Technologies for More Throughput). In the following, we describe the IEEE 802.11n MAC in detail to show the complexity introduced in the MAC design to overcome the limitations of the legacy 802.11. To reduce the complexity without loss of throughput efficiency, we propose a highly efficient access scheme for the MINT MAC protocol. The detail of the protocol design is presented in section 3.2.

3.1 Introduction to IEEE 802.11n MAC Design

The legacy IEEE 802.11 MAC protocol incorporates two access methods: Distributed Coordination Function (DCF) and optional Point Coordination Function (PCF) to provide limited QoS support for time-bounded services. The DCF is based on the CSMA/CA protocol and the PCF is based on

Protocol	Release Date	Op. Frequency	Throughput (Typ.)	Data Rate (Max)
Legacy	1997	2.4-2.5 GHz	0.7 Mbit/s	2 Mbit/s
802.11a	1999	5.15-5.825 GHz	21 Mbit/s	54 Mbit/s
802.11b	1999	2.4-2.5 GHz	4.5 Mbit/s	11 Mbit/s
802.11g	2003	2.4-2.5 GHz	20 Mbit/s	54 Mbit/s
802.11n	2008(est.)	2.4 GHz and/or 5 GHz	74 Mbit/s	248 Mbit/s(2x2 ant)

Table 3.1: Comparison between different IEEE 802.11 amendment standards (source: wikipedia)

a centralized polling protocol. The advantage of the CSMA/CA based MAC protocol is the low implementation complexity, while it has the disadvantage of the low throughput efficiency, which is defined as the ratio between the throughput and the PHY data rate. As shown in Table 3.1, the typical throughput efficiency is around 50%.

In the following, we first describe the basics of the DCF and PCF followed by the enhancements made in the IEEE 802.11e. We then introduce the enhancements for the IEEE 802.11n proposed by the TGn Sync based on the IEEE 802.11e.

The DCF is based on a CSMA/CA protocol. For the CSMA/CA, a station must sense the channel activity. If the channel is busy upon the arrival of a packet, the packet is back-logged. When the channel is idle for a period of distributed inter-frame space (DIFS), a new packet can be transmitted immediately, while a back-logged packet needs to wait for a random backoff interval. The DCF employs a discrete time backoff scale. The time immediately following an idle DIFS is slotted and a station is allowed to transmit only at the beginning of each slot time. The slot time size $aSlotTime$ is the time needed to detect the transmission of a packet by the PHY layer. When a backoff process starts, the backoff time is uniformly chosen in the range between 0 and $CW - 1$, where the CW is called contention window. At the first transmission attempt of a back-logged packet, the contention window CW is set to the minimum contention window CW_{min}. After each unsuccessful transmission, the CW is doubled, up to a maximum contention window CW_{max}.

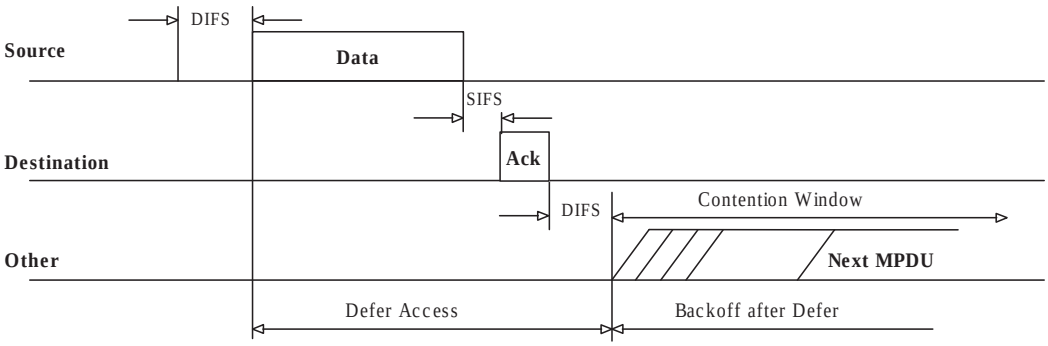

Figure 3.1: DCF basic access scheme

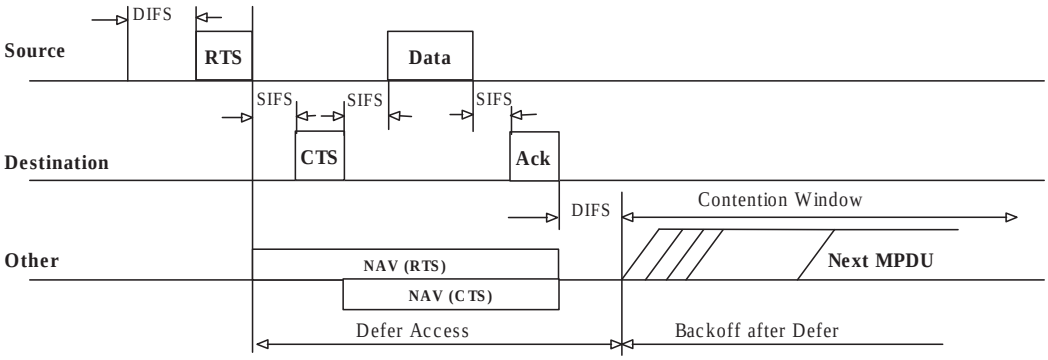

Figure 3.2: DCF RTS/CTS scheme

The backoff timer counter is decremented only when the channel has been sensed idle for a DIFS. When the backoff timer counter reaches zero, a data frame or an RTS (Ready-To-Send) frame is transmitted depending on the particular access scheme.

There are two access schemes for the DCF mode, i.e., basic access scheme and RTS/CTS (Request-To-Send/Clear-To-Send) scheme.

The basic access scheme is shown in Figure 3.1. A station transmits a data frame based on the CSMA/CA protocol. The receiving station then sends back an acknowledgment (ACK) frame after waiting for a short interframe space (SIFS).

Figure 3.2 shows the RTS/CTS scheme. Before a data frame is sent, the transmitting station sends an RTS frame based on the CSMA/CA protocol. The receiving station responds with a CTS frame.

If the CTS frame is received successfully, the transmitting station sends out a data frame. Then the receiving station responds with an ACK frame. If the CTS frame is not received, a backoff process starts with a doubled CW. All the time intervals between these frames are one SIFS. The RTS/CTS frames increase the protocol overhead if the data frame is short or the traffic load is light. However, it protects the data frame from collision, and therefore improves the efficiency for long data frames. To dynamically apply these two access schemes, an RTS threshold is used. When the data frame size is larger than the RTS threshold, an RTS/CTS scheme is used, otherwise, the basic access scheme is employed. The RTS/CTS scheme also employs a virtual carrier-sense mechanism via a network allocation vector (NAV). The NAV maintains a prediction of future traffic on the medium based on the duration information that is announced in RTS/CTS frames prior to the actual exchange of data. Before the end of NAV, the medium is considered busy.

The legacy 802.11 uses the point coordination function (PCF) to support QoS for time-bounded services. The PCF mode uses a centralized polling approach which requires the presence of an Access Point (AP) that acts as a Point Coordinator (PC). When PCF is enabled, a contention-free period (CFP) and a contention period (CP) alternate periodically over time, where a CFP and the following CP form one superframe. The PCF is used for accessing the medium during the CFP, whereas the DCF is used during the CP. The CFP starts with a beacon frame sent by the base station using the basic DCF access mechanism. A beacon frame is sent if the channel is idle for a PCF interframe space (PIFS), which is shorter than a DIFS and longer than a SIFS. The shorter PIFS ensures that no DCF stations are able to interrupt the PCF mode. During CFP, the AP uses a Round Robin scheduling algorithm to poll stations. The stations that have been polled have to respond to the poll frames with a data frame if there is a pending transmission. If there is no pending transmission, the response is a null frame without payload. If the CFP terminates before all stations have been polled, the remaining stations will be polled first in the following CFP.

The amendment IEEE 802.11e introduces the hybrid coordination function (HCF) for QoS support. The station that operates as the central coordinator for all other stations within the same QoS supporting BSS (QBSS) is called the hybrid coordinator (HC). Similar to the PC, the HC resides within an 802.11e AP. The HCF defines two medium access mechanisms: contention-based channel access referred to as enhanced distributed channel access (EDCA) and HCF controlled channel access (HCCA). The EDCA is used in the CP only, while the HCCA is used in both CP and CFP phases. An important new attribute of the 802.11e MAC is referred to as a transmission opportunity (TXOP). A TXOP is an interval of time during which a backoff entity has the right to deliver MSDUs. A TXOP is defined by its starting time and duration. TXOPs obtained via contention-based medium access are referred to as EDCA-TXOPs. Alternatively, a TXOP obtained by the HC via controlled medium access is referred to as HCCA-TXOP or polled TXOP.

To improve the throughput efficiency, 802.11e introduces block acknowledgment (BA) and direct link protocol (DLP) [49]. Block acknowledgments allow a backoff entity to deliver a number of MSDUs being delivered consecutively during one TXOP and transmitted without individual ACK frames. The MPDUs transmitted during the TXOP are referred to as a block of MPDUs. At the end of the block, or in a later TXOP, all MPDUs are acknowledged by a bit pattern transmitted in the block acknowledgment frame, thus reducing the overhead of control exchange sequences to a minimum of one acknowledgment frame per number of MPDUs delivered in a block. With direct link protocol, any backoff entity can directly communicate with any other backoff entity without communicating via the AP.

The 802.11e MAC use the following approaches to provide service differentiation [49,55]. For each traffic class, a different AIFS (arbitration inter-frame space) value, CW_{min} and CW_{max} values, and $TXOP_{limit}$ (maximum TXOP duration) value are assigned. For 802.11e, an AIFS ($>$ DIFS)

is used instead of a DIFS. With a smaller AIFS value, a higher priority frame needs to wait for a smaller duration than a low priority frame once the channel becomes idle and can seize the channel sooner. The low priority frame finds the channel busy and has to either wait till the high priority traffic has completed transmission or it has to backoff. The values of CW are assigned such that the CW_{min} and CW_{max} values of low priority frames are higher than that of high priority frames ($CW_{min,i} > CW_{min,j}$ and $CW_{max,i} > CW_{max,j}$, where priority of class $i <$ priority of class j). The lower priority frame selects a longer backoff interval (BI) on average whereas the higher priority frame selects a smaller BI on average. Therefore, the higher priority frame is likely to get access to the channel earlier than the lower priority frames. The $TXOP_{limit}$ allows control of the maximum time a backoff entity allocates the medium for MSDU delivery, and therefore is an important means to control MSDU delivery delay.

Assuming a baseline specification defined by the IEEE 802.11 standard and its later amendments, including the draft IEEE 802.11e amendment [32], the proposed enhancements of the IEEE 802.11n MAC protocol is aimed to improve the MAC efficiency for higher throughput and overall system performance. The new features include frame aggregation, bi-directional data flow, power management (to reduce power consumption), channel management (including a receiver assisted channel training protocol) and feedback mechanisms that enable rate adaptation. Protection mechanisms are also added to achieve the seamless interoperability and coexistence with legacy devices that support the IEEE 802.11a/b/g standards.

Among these new features, three of them improve the throughput significantly, i.e., frame aggregation, bi-directional data flow and feedback mechanisms for rate adaptation.

Frame aggregation An aggregate is a sequence of MPDUs (MAC protocol data unit) carried in a single PPDU (PHY protocol data unit) with the aggregate attribute as shown in Figure 3.3.

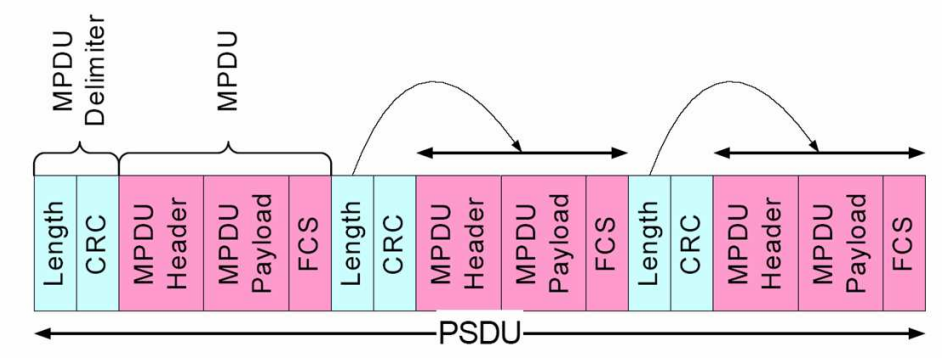

Figure 3.3: Frame aggregation

In a single-receiver aggregate, all MPDUs are addressed to the same receiver address. And a multiple-receiver aggregate contains MPDUs that are addressed to multiple receivers. The MAC interprets the PSDU (PHY Service Data Unit) as a single MPDU or a sequence of MPDUs according to the aggregate parameter, that is robustly transported in the PLCP header. The MAC separates the MPDUs of an aggregate PSDU using a robust MPDU delimiter and the MPDUs are separately protected by a CRC (Cyclical Redundancy Check). Loss of an individual MPDU does not imply loss of all MPDUs in a PPDU.

To enable frame aggregations, a Initiator Aggregation Control (IAC) MPDU is sent in place of the RTS and a Responder Aggregation Control (RAC) MPDU is sent by the receiver in place of the CTS. The IAC/RAC exchange implements more functionalities than the RTS/CTS exchange, e.g., the MIMO feedback and MCS feedback training processes.

Bi-directional data flow The bi-directional data transmission is shown in Figure 3.4, where the RDL, RDR and RDG means reverse direction limit, reverse direction request and reverse direction grant respectively. The initiator sends an IAC frame indicating the support for reverse direction data flow. The responder sends back an RAC frame providing the length of the data in the PPDU it intends to send, plus a default MCS (Modulation and Coding Scheme). The

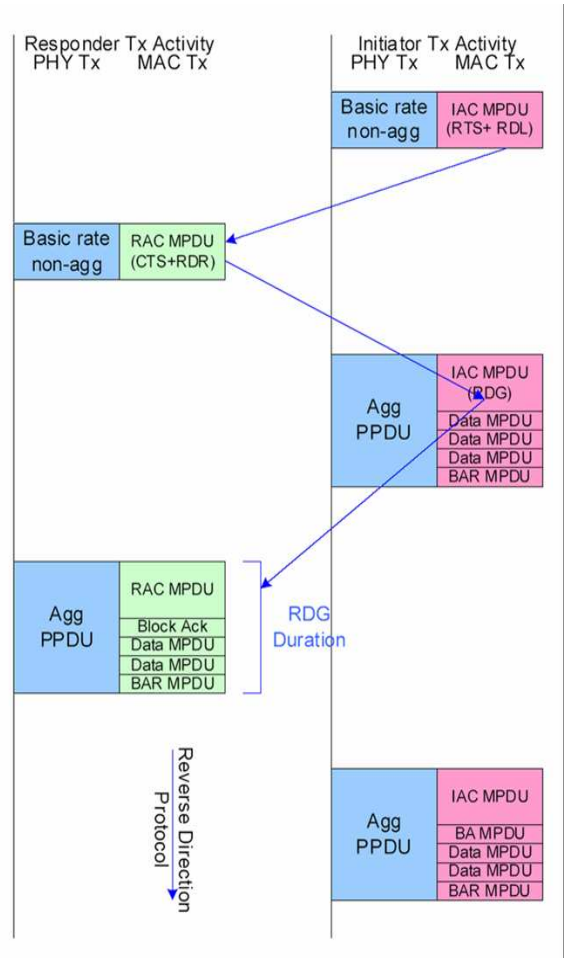

Figure 3.4: Bi-directional data flow

initiator then calculates a duration request and sends the next IAC frame indicating the allocation for reverse direction data. After receiving the second RAC frame from the responder, the bi-directional data transmission begins with the agreed duration, length of data and MCS.

Closed-loop MCS training The support for closed-loop MCS adaptation is provided by the exchange of the MRQ (MCS Request) and MFB (MCS Feedback) elements carried in the IAC/RAC control frames. Any IAC or RAC frame can include an MCS Request. The purpose is to request the peer station to measure the characteristics of the link and return the information in an MFB that allows the link to be used more effectively. A station should use the information contained in an MFB to adapt its transmission parameters.

There are three types of MCS training exchange: normal, unsolicited and unanswered. In a normal training exchange, an MFB element is present in the next aggregate sent by the receiver of the MRQ element, and the aggregates are separated by a SIFS interval. For an unsolicited exchange, a station may send an MFB element without any matching MRQ element at any stage of an exchange. And in an unanswered training exchange, a STA ignores an MRQ element and refuses to provide an MFB element.

The effectiveness of the frame aggregation and bi-directional data flow is studied in [43,71]. In fact, to improve the MAC efficiency, we can either reduce the protocol overhead or increase the payload size. The frame aggregation alone increases the payload size. The bi-directional data flow reduces the protocol overhead for the reverse data flow. The channel training is also necessary for the data rate adaptation, which improves the raw data rates at PHY layer by using the channel more efficiently.

From the MAC design point of view, the MAC enhancements in the IEEE 802.11n, which are used to combat the inefficiency of the simple mechanism of CSMA/CA protocol, have increased the design complexity. However, the efficiency improvement is limited because of the constraints imposed by the distributed nature of the CSMA/CA. Therefore, we propose a MAC protocol for the MINT system with a centralized medium access mechanism. The new protocol allocates resources more efficiently and provides higher throughput efficiency with a centralized scheduling algorithm with a comparable complexity as the IEEE 802.11n.

In the following sections, we first describe the MINT MAC protocol design in detail. Then we use simulations to evaluate the throughput efficiency of the MINT MAC protocol and compare with the IEEE 802.11n based on a realistic PHY model.

3.2 MIN-MAC Protocol Design

The Mobile Infostation Network MAC protocol (MIN-MAC) is designed to support high data rate communications between the infostation and the mobile users. It aims to achieve high throughput efficiency for large size file transfer applications with low protocol overhead. In the following, we describe the MIN-MAC version A and B in detail.

3.2.1 MIN-MAC Protocol Overview

Two classes of MAC protocols are used for wireless data communications. The distributed MAC protocols with random access such as ALOHA [6] and IEEE802.11 [31] are widely used in WLANs (wireless local area networks) and MANETs (mobile ad-hoc networks). The centralized MAC protocol based on reservation and scheduling is used for the communication networks such as cellular networks and wireless ATM, for which the radio resource is more expensive and QoS support is required.

The centralized MAC protocol design of the MIN-MAC is motivated by the scheduling gain of the MIMO-OFDM channel and the advantages of infostation networks. For infostation networks, each infostation covers an isolated area, where the interference between infostations is rare. The large file transfer between the users and the infostation is the dominant application. Therefore, it is possible to design a centralized protocol with a comparable complexity as a distributed protocol but with higher efficiency. Furthermore, unlike a centralized MAC protocol used in a cellular network with TDMA, FDMA or CDMA, MIN-MAC is based on CSMA. It requires less strict timing for each MAC frame and, therefore, reduces the design complexity of the PHY layer.

One of the CSMA based centralized protocols is the PCF of the IEEE 802.11. It is based on a

polling scheme that is not scalable when there are large number of users. In PCF, the AP has to poll every users with a round robin scheduler. Both the power and bandwidth are wasted if the user has no data to send and receive.

Different from the PCF, the MIN-MAC is a centralized protocol that employs some distributed features. The infostation coordinates both the uplink and downlink data transmissions and shares the global information with all users. The shared information includes the total number of active users in the network, i.e., how many of them have downlink data pending to transmit and what is the optimal transmission probability for each user. With the shared information, a more efficient user access control mechanism is designed to overcome the scalability problem of the PCF. To use the radio resource more efficiently, the downlink data packets are classified based on different users and priorities to enable per-user-scheduling and packet aggregation and transmitted based on the priority, mobility and channel quality of each user.

In conventional OSI layered design, the MAC sublayer does not provide reliable data transmission. Instead, an end-to-end transport layer approach like TCP is used over an unreliable MAC to provide reliable data communication. However, it is known that TCP is vulnerable to frequent packet losses and delay variations, which are very common over wireless links. Specifically, for a high packet error rate (> 0.1) link, the TCP throughput is extremely low. To solve this problem, we propose a MAC protocol named MIN-MACa (Mobile Infostation Network MAC protocol version A) that can transmit data reliably without the use of a TCP protocol.

For a rate adaptive high performance PHY layer, the protocol overhead of the MAC layer could be more than 50%. One of the reasons is that the MAC and PHY protocol headers and management messages are modulated with a fixed low rate MCS. This type of throughput loss is larger in a high data rate PHY. Furthermore, for CSMA based protocols, the inter-frame space (IFS) between

MAC frames is another source of throughput loss if most of MAC data frames are short frames. The protocol overhead may take more bandwidth than the data message itself. Therefore, we propose the MIN-MACb (Mobile Infostation Network MAC protocol version B) to reduce the protocol overhead and improve the efficiency further at low pakcet error rate region. Without any support for packet retransmission in MIN-MACb, an integrated reliable transport protocol is required.

In the following, we describe the MIN-MAC protocol design in detail.

3.2.2 MIN-MAC Protocol Functional Description

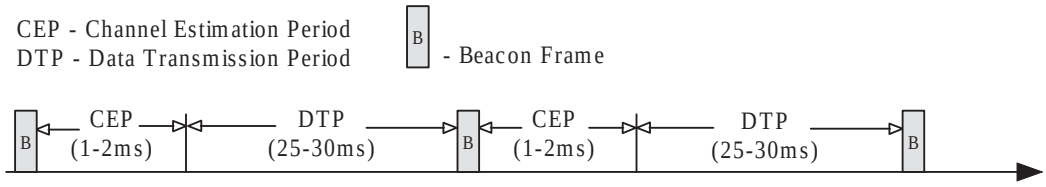

Figure 3.5: Timeline of MIM-MAC protocol

Figure 3.5 shows MAC-imposed temporal structure of the infostation data link, with alternating Channel Estimation Period (CEP) and Data Transmission Period (DTP). The difference between the two variations of the MIN-MAC, i.e., MIN-MACa and MIN-MACb lies in the different design of the DTP. The durations for the CEP and DTP are based on the expected channel coherence time, which is determined by the operating conditions and mobility profile. A system with lower coherence time, in general, will require CEP more often than a system with higher coherence time. Therefore, a system that is designed for larger file sizes could perhaps benefit from the allocation of an entire DTP to one user. What is shown in Figure 3.5 is based on the mobility profile of a stationary or slow moving user.

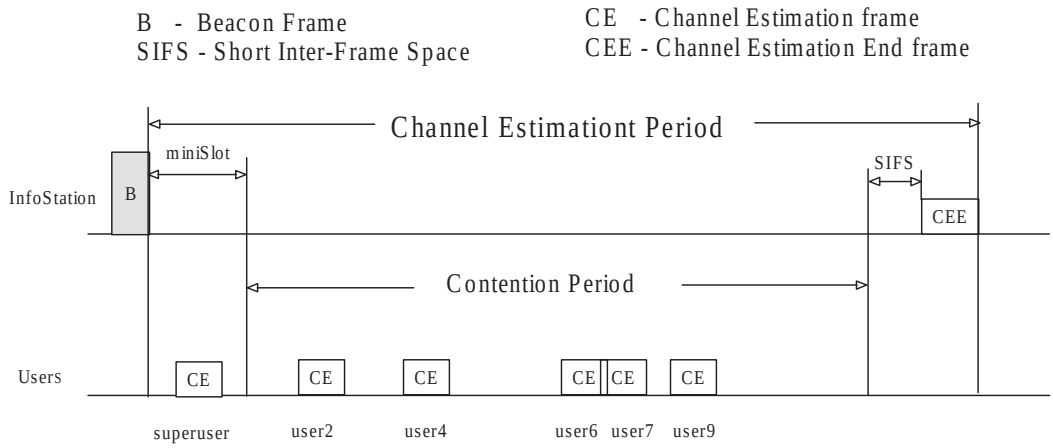

Figure 3.6: Channel estimation period

Channel Estimation Period

Figure 3.6 shows the Channel Estimation Period (CEP) in greater detail. The CEP starts with a beacon that contains the indices of all users who have downlink data pending for transmission. When a user has uplink data to send to the infostation, he may commence user-initiated passive channel estimation (the “passive” here stands to mean that it is not controlled by the infostation). The users who wish to transmit or receive data should send a CE frame to the infostation following the contention control algorithm. If any data is deemed critical, a superuser qualifier is attached to that user. A user who has been already designated a superuser may signal his intention to use the channel by sending a Channel Estimation (CE) frame during the non-contention miniSlot. The other users who need system resources transmit CE frames during the Contention Period (CP), which uses unslotted ALOHA.

In order to estimate the downlink channel, the principle of reciprocity is applied, which states that the downlink (the channel from the infostation to the user) channel state matrix is the transpose of the uplink (the channel from the user to the infostation) channel state matrix. The uplink channel estimation can be obtained from the training sequence carried in the preamble of PPDU (PHY

Protocol Data Unit) of the CE frame.

The end of CEP is indicated by the transmission of a Channel Estimation End (CEE) frame from the infostation, which is separated from the CP by a Short Inter-Frame Space (SIFS). The CEE frame also informs the users about the success or failure of the CE frames. The failed users then adjust their transmission probability according to the contention control algorithm, which is described in Section 3.2.4.

Data Transmission Period for MIN-MACa

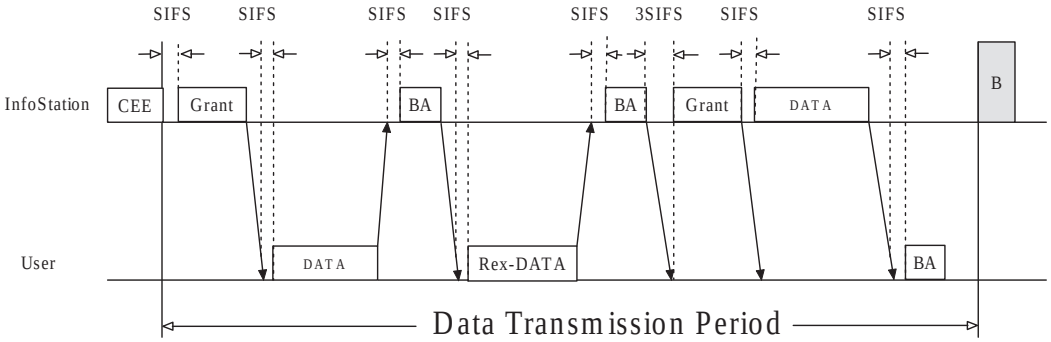

Figure 3.7: Data transmission period for MIN-MACa

Figure 3.7 shows the DTP design for the MIN-MACa protocol in greater detail. During the Data Transmission Period (DTP), the infostation may serve several users based on pre-scheduling in each DTP, or, it may serve only one user per DTP if the user has enough data to fill up the channel. In MIN-MAC protocol, packet aggregation is implemented for data frames. Each data frame is composed of a number of sub-frames. For the variable sub-frame size option, each sub-frame contains one IP packet. For the fixed sub-frame size option, the aggregated data frame is fragmented into fixed size sub-frames. A stop-and-wait ARQ for data frames and a selective repeat ARQ (SR-ARQ) for sub-frames are combined to ensure reliable and efficient data transmission. Each Grant frame is used to grant channel access to one user to transmit one data frame with SR-ARQ. During

the SR-ARQ, after each data frame is sent, a block acknowledgment (BA) frame is replied to report which sub-frames are not correct and have to be retransmitted. This process is repeated until all sub-frames are received without error or the DTP is ended. If one or more sub-frames are still in error by the end of DTP, or when the maximum number of retransmission is reached, the data transmission is failed and the same data frame with all the sub-frames has to be retransmitted in the next available DTP. This stop-and-wait ARQ scheme simplifies the protocol design and ensures the reliable data transfer at the MAC layer. More details about the SR-ARQ protocol and error handling scheme for MIN-MACa are given in section 3.2.6.

The inter-frame space (IFS) between any consecutive MAC frames during the SR-ARQ process is one SIFS. If a BA frame is not received and channel is idle for 2 SIFS after the expected receiving time of the BA, the same data frame is retransmitted. The duration of 2 SIFS is the guard interval to avoid interference from any other users. A Grant or Beacon frame is sent in two cases: i) the channel has been idle for 3 SIFS after the receiving of a BA frame that acknowledges all sub-frames; ii) the channel has been idle for a SIFS after a BA frame is sent to acknowledge all sub-frames. A Beacon frame is sent if the time left for this DTP is not enough to transmit one data frame. Otherwise, a Grant frame is sent.

Data Transmission Period for MIN-MACb

Figure 3.8 shows the DTP for the MIN-MACb protocol in greater detail. Without ARQ schemes, each Grant frame is used to grant channel access to one user for both uplink and downlink data transmissions. The inter-frame space between data frames transmitted in the same direction is 2 SIFS and the IFS for the reverse direction is 1 SIFS. With this mechanism, the data frames are sent alternatively for uplink and downlink if there are data frames in both dirction. If the data frames

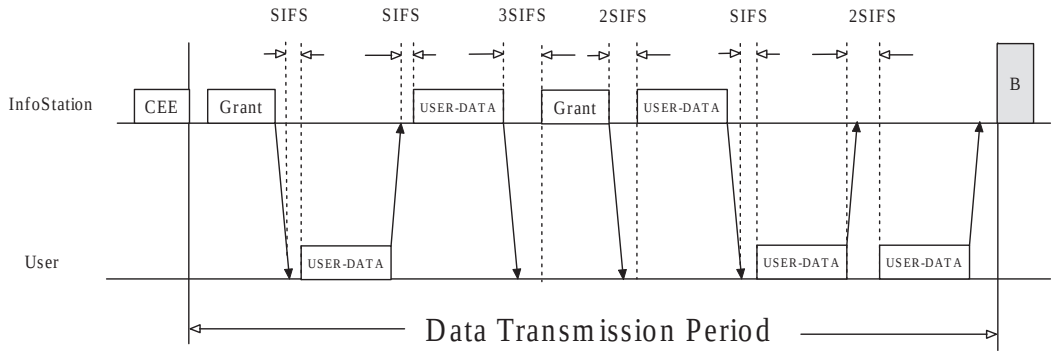

Figure 3.8: Data transmission period for MIN-MACb

are for uplink/downlink only, the ISF is 2 SIFS. After receiving a Grant, a user can use the channel exclusively until all the data has been served or the DTP has been ended. A new grant is sent after a medium idle time of 3 SIFS, which is used to ensure the user traffic has ended in both directions. If the DTP is ended before the completion of the user traffic, a Beacon frame is sent 1 SIFS after receiving a data frame, or 2 SIFS after sending a data frame when there is no uplink data traffic.

Except for the DTP process, all the other protocol design is the same for both the MIN-MACa and MIN-MACb protocols, i.e., the same frame format and the same packet aggregation design. Without acknowledgment for the data frames, the MIN-MACb protocol has higher efficiency than MIN-MACa. Also the design complexity is reduced. However, a reliable transport protocol is required to work with the unreliable MIN-MACb protocol. The duplex data transmission of MIN-MACb is designed to improve the performance of the transport protocol.

3.2.3 Frame Format

All MIN-MAC frame types share some common fields including Frame Control (FC), Frame Check Sum (FCS), Receiver Address and Transmitter Address.

Common Fields

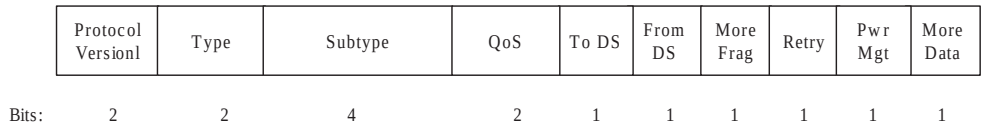

Figure 3.9: Frame control field format

Frame Control (FC) The Frame Control field is shown in Figure 3.9. The protocol version field indicates the MAC protocol version. The type and subtype fields are used to identify different frame types. The QoS field contains information about the user priority. The other sub-fields are reserved.

Receiver Address (RA) Receiver Address field contains the MAC address of the receiver. The RA is set to a broadcast MAC address for a broadcast frame.

Transmitter Address (TA) Transmitter Address field contains the MAC address of the transmitter.

Frame Check Sum (FCS) The FCS field is a 32-bit field containing a 32-bit CRC. The FCS is calculated over all the fields of the MAC header and the frame body field for the control frame types and unaggregated data frame. For an aggregated data frame, the FCS is calculated for each sub-frame to detect the sub-frame error.

The frame format for different MAC frame types are illustrated as follows.

Beacon Frame

Each transmission cycle starts with a Beacon. Figure 3.10 shows the frame format for the Beacon. The contention duration field contains the duration of the CEP in multiples of 10 microseconds. The next two fields are the number of users that have downlink data pending for transmission and

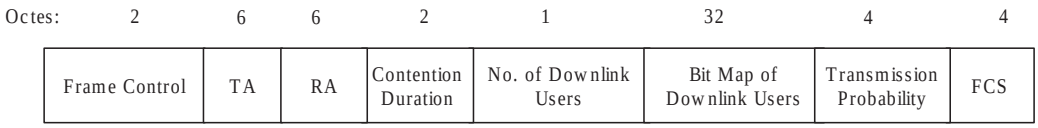

Figure 3.10: Beacon frame format

their indices represented by a bit map. The i-th bit of the bit map is set to "1" if the i-th user has data to receive. The user index number is obtained when he is authorized to use the infostation. The maximum number of users that can be authorized is 255. The transmission probability field is the advertised transmission probability for all active users, which is optimized to maximize the success probability of the CE frame during the contention. After receiving the beacon frame, each active user sends a CE frame with a probability lower than or equal to the advertised transmission probability based on an un-slotted ALOHA protocol.

Channel Estimation (CE) Frame

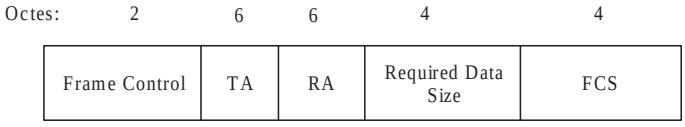

Figure 3.11: Channel estimation frame format

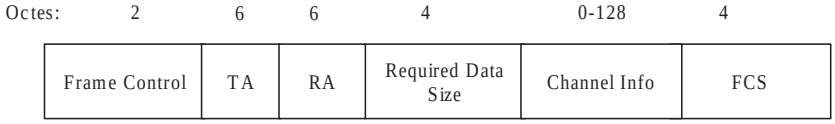

Figure 3.12: Extended channel estimation frame format

The CE frames are sent using an un-slotted ALOHA. The transmission is based on a discrete time scale with a unit of 10 microseconds. The channel estimation is based on the preamble training signal of the PPDU of the received CE frame. The downlink channel state matrix can be obtained as the transpose of uplink channel state matrix with the assumption of channel reciprocity. Therefore, the channel estimation is obtained if the CE frame is received without collision.

The regular CE frame and extended CE frame format are shown in Figure 3.11 and 3.12 respectively. The requested data size field indicates how many bytes of data are waiting for the uplink transmission. The extended CE frame has a channel info field that contains a downlink MIMO channel state matrix up to 4x4 entries with 64 bits for each entry. The extended CE frame is used to carry the downlink channel estimation information if the channel is not reciprocal.

Channel Estimation End (CEE) Frame

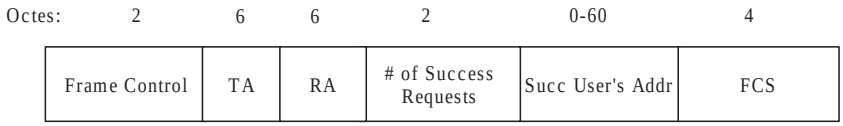

Figure 3.13: Channel estimation end frame format

At the end of the CEP, a Channel Estimation End frame is sent. It acknowledges all the success CE frames, which includes the number of success user field and MAC addresses of success users. After receiving the CEE frame, the failed users update its transmission probability according to the contention control algorithm.

Grant Frame

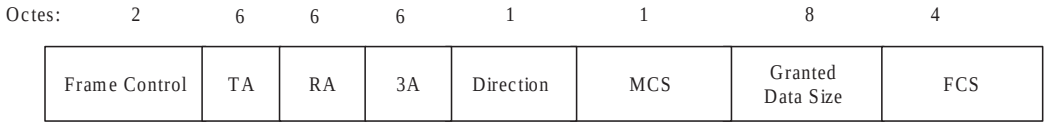

Figure 3.14: Grant frame format

A grant frame is sent before either broadcast data frames or uni-cast data frames. For both cases, the TA field is the MAC address of the infostation and the RA field is the broadcast MAC address. For broadcast data frames, the 3A field of the Grant is the broadcast address. For uni-cast data frames, the 3A field is the MAC address of the user that has been granted. The grant frame includes the

data size field, the MCS field and the direction field. The direction field can be downlink or uplink. The data size field is the maximum number of bytes that can be sent in one data frame. The MCS field is the adaptive MCS indices for up to 18 OFDM sub-bands. The users that sent a CE frame successfully are served in sequence based on the pre-scheduling results. A grant is sent only if the estimated transmission time of the data frame is less than the time left for the DTP, otherwise, a beacon frame is sent to start a new transmission cycle.

Data Frame

The MIN-MAC provides two aggregation options for the data frame format as shown in Figures 3.15 and 3.16, i.e., variable sub-frame size and fixed sub-frame size.

For the variable sub-frame size option, a data frame is composed of $\mathbf{n}(\leq 64)$ sub-frames in its frame body. The first sub-frames is the MAC header. The second and following sub-frames each carries an upper layer IP packet. Each sub-frame is encoded separately and has its own CRC. For this option, the sequence control field is the sequence number of the MAC frame. The frame size field is the frame size of the data frame including all sub-frames and their FEC fields. The packet map is a bit map, where the i-th bit represents the i-th sub-frame in the original data frame. For a retransmitted data frame, the packet map tells the receiver which sub-frames have been retransmitted. The number of sub-frame field represent the number sub-frames carried in the current transmission. The sub-frame offset field indicates the offset of each sub-frames relative to the start of the data frame. In the fixed sub-frame size option, a data frame is divided into fixed length sub-frames. Each sub-frame is encoded separately and has its own CRC. The limitation is that the boundary of sub-frames does not align with the boundary of the payload packets. For this option, the sequence control field and the frame size field are the same as defined in the variable frame-size option. The sub-frame map

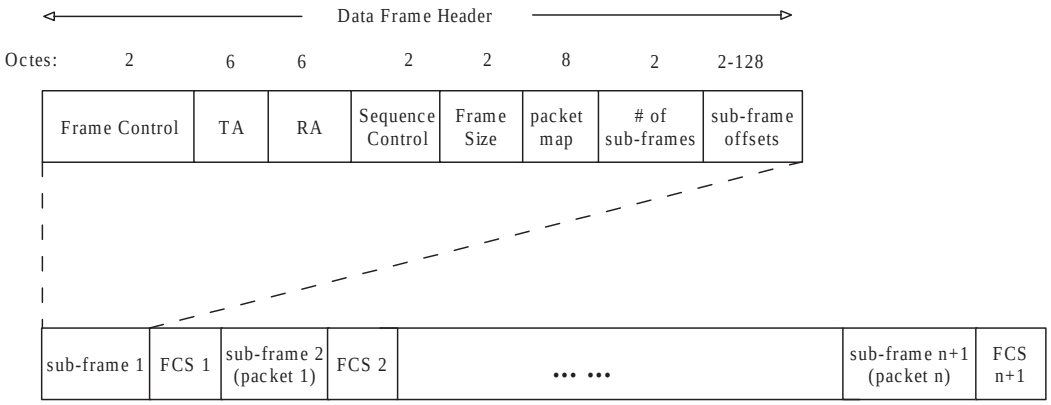

Figure 3.15: Data frame format – variable sub-frame size option

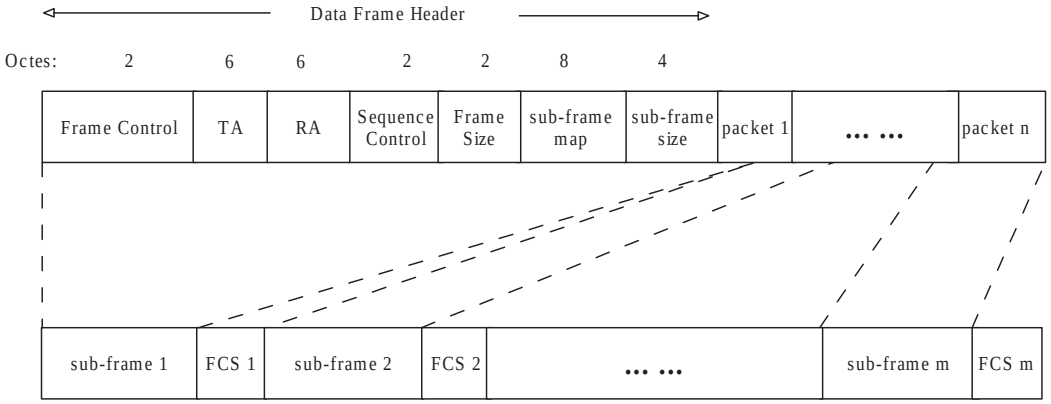

Figure 3.16: Data frame format – fixed sub-frame size option

field is similar to the packet map field. All sub-frames have the same size, which is given in the sub-frame size field. The number of sub-frames can be obtained by dividing the data frame size by the sub-frame size.

Block ACK (BA) Frame

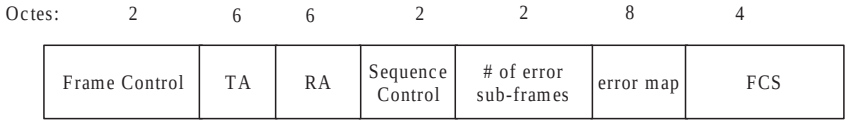

Figure 3.17: Block ACK frame format

The BA frame is the acknowledgment of the data frame. The sequence number field contains the

sequence number of received data frame. The number of error sub-frames field represents the number of sub-frames in error. The error map field is a bit map, where the i-th bit represents the i-th sub-frame in the original data frame. The i-th bit is set to "1" if the i-th sub-frame is in error.

3.2.4 Contention Control Algorithm

The channel estimation period (CEP) serves two purposes, 1) obtain the channel state matrix of active users; 2) maximize the possibility that users with the best channel conditions access the channel during a given data transmission period (DTP). The second goal is achieved by contention control algorithm. Without it, the users with the best channel conditions could experience contention failure and cannot use the channel if the collision rate is too high. For the IEEE 802.11 DCF scheme, the contention is resolved with an exponential back-off mechanism. By doubling the contention window, the user's transmission probability decreases by half to reduce the collision probability. In MIN-MAC, since the transmission opportunity is limited, it had better be used when the channel is in the best condition. By setting a threshold of transmission probability p per user, a user is allowed to contend for the channel only when its channel state is among the best p states. Not only the success rate is increased with reduced number of users in contention, but also the average channel quality is improved for successful users. With a lower transmission probability, a better channel condition is required for a contending user to be allowed to access the channel.

The contention control algorithm is implemented at both infostation and mobile terminals as follows. For the infostation, the transmission probability p per user is calculated as the optimal number of arrivals per CEP divided by the number of active users. For the unslotted ALOHA used in CEP, the optimal number of CE frames is $T_{CEP}/2$ when the maximum success rate is achieved, where T_{CEP} is the duration of CEP in terms of the number of CEs.

For each mobile terminal, the channel statistics is collected whenever it receives a Beacon and a probability function $p(x) = P_r(X > x)$ for its channel capacity is built. The basic value of p is advertised in each Beacon frame which is based on the knowledge of the number active users at the infostation. The actual transmission probability p_{MT} is calculated based on a backoff scheme. If a CE is sent successfully upon the reception of the CEE frame, the p_{MT} is set to p. If the CE is failed because of collision, the p_{MT} is set to $p_{MT} = \max\{p_{MT}/2, p/4\}$. It means the transmission probability decreases by half each time when a failure occurs but cannot be lower than a quarter of advertised transmission probability. We use a flexible p_{MT} in order to accommodate a large number of new active users, while balancing the transmission opportunity between the new users and old users. When the advertised probability p is received, the channel capacity threshold x is then found. If the current channel capacity is larger than the threshold x, and a user has information to send or receive, he can send a CE frame during the contention period. Otherwise, the user skips the current CEP and waits for a better channel condition.

3.2.5 Scheduling Algorithm

After the channel estimation period, an adaptive data rates are assigned to each success user. The MINT MAC scheduling algorithm then schedules the users based on channel qualities, which represented by the data rates, combined with users' priorities and channel coherence time, i.e., user mobility. The users are served sequentially during the DTP based on the results of the scheduling algorithm. By the end of DTP, the unserved users are ignored and the user's transmission status, i.e., the unsuccessful retransmission, is discarded. The retransmission in the next transmission opportunity for this user is treated as new transmission.

The scheduling rule can be described as follows.

1. The superusers that meet the channel quality threshold $\mathbf{A}$ have the highest priority.
2. Fast moving users that meet the channel quality threshold $\mathbf{B}$ have the second highest priority.
3. Otherwise, the priority is ordered by the channel quality.

Because the channel reciprocity property of the fading channel, it is often assumed that the same channel gain is achieved for both uplink and downlink [53]. Therefore, when we schedule a user, the uplink data and downlink data are scheduled with the same probability for MIN-MACa. For MIN-MACb, both uplink and downlink data are granted and sent alternatively in one DTP. The threshold $\mathbf{A}$ and $\mathbf{B}$ (with $\mathbf{A} < \mathbf{B}$) can be chosen based on empirical data to ensure the super-user or fast moving user does not occupy all the channel resources.

3.2.6 SR-ARQ Protocol and Error Handling for MIN-MACa

Retransmission and Duplication Detection

The following parameters are used for data frame transmission/retransmission:

- `is.dl_seqno` - the sequence number of the un-acked downlink data frame for the i-th user recorded at the infostation
- `is.up_seqno` - the sequence number of the latest received uplink data frame for the i-th user recorded at the infostation
- `user.up_seqno` - the sequence number of the un-acked uplink data frame recorded at the user terminal
- `user.dl_seqno` - the sequence number of the latest received downlink data frame recorded at the user terminal

The infostation keeps the records of the sequence numbers of the un-acked data frames and the latest received data frames for all users, i.e., `is.dl_seqno`, `is.up_seqno`. Each user keeps its own un-acked data frame and the latest received data frame, i.e., `user.up_seqno`, `user.dl_seqno`.

For the infostation, when a data frame is transmitted, the `is.dl_seqno` is carried in its header. When the data frame is received at the user terminal, a BA frame with the same sequence number is sent back. If this data frame is received correctly at the user terminal, the `user.dl_seqno` is updated to equal to `is.dl_seqno`. When a data frame is received at the infostation, the `user.up_seqno` is compared with `is.up_seqno`. If the `user.up_seqno` is greater than `is.up_seqno`, it means a new data frame is received and the `is.up_seqno` is updated. If the `user.up_seqno` equals to the `is.up_seqno`, it means a retransmitted data frame is received.

For mobile users, the procedure is similar to the infostation procedure.

SR-ARQ for Sub-frame Retransmissions

Each data frame is divided into several sub-frames that can be decoded by the PHY layer separately. A SR-ARQ protocol is used for the retransmission of sub-frames. For the fixed sub-frame size option, both MAC and PHY have an agreement about the sub-frame size. For the variable sub-frame size option, the boundary of the sub-frames is obtained from the MAC header. Therefore, the receiver can identify different sub-frames and decode them separately. It then delivers the decoded sub-frames along with the zero-padding for the un-decodable sub-frames and the sub-frame error status to the MAC layer.

The MAC data frame, either original or retransmitted, has a sub-frame bit map, where the i-th bit represents the i-th sub-frame in the original data frame. For a retransmitted data frame, the sub-frame map tells the receiver which sub-frames have been retransmitted. The i-th bit is set to “1”

if the i-th sub-frame is carried in the data frame. The information about sub-frames in error at the receiver is carried in the error map field of a BA frame, where the correct and error sub-frames are represented by a “0” and “1” respectively. After receiving the BA, the failed sub-frames are retransmitted in a data frame with a sub-frame map that is a copy of the BA error map.

The SR-ARQ process stops in three cases: 1) the BA error map is all zero; 2) the maximum number of ARQ rounds is reached; 3) the DTP is ended.

Error Handling Schemes

The error handling and recover schemes for isolated errors is shown in Table 3.2.

Error Frame	Impact	Error Handling Schemes
Beacon	No CE received	Re-send Beacon at CEE state
CE	CE failed	Double the contention window
CEE	CE not confirmed	Assume CE failed and double the contention window
Grant (UL)	Data not received	Retransmit Grant if nothing is received, Stop retransmission if any frame is received
Grant (DL)	Receive data without Grant	Accept data at Grant state
Data	No BA is received and timeout	1) if within DTP, retransmit data frame 2) if DTP ends, infostation sends Beacon and mobile users stop retransmission after receiving Beacon
BA	No BA is received with/without timeout	If a timeout occurs, the same process is used as for data error process. If a Grant/Beacon is received instead of a BA, 1) during DTP, the received grant frame indicates a transmission success; 2) when DTP ends, the received Beacon frame indicates a transmission failure

Table 3.2: Error handling schemes for isolated frame errors

If consecutive errors occur for the combinations of 1) Data and ACK frames; 2) Grant and Data frames; 3) ACK and Grant frames, the MAC protocol observes that unexpected frames are received

following some corrupted frames. Because the probability of consecutive error is very low, for simplicity, those unexpected frames are rejected until the end of DTP. After the beacon frame is sent, the protocol states are reset and the failed data frames are retransmitted.

3.3 MAC Performance Evaluation

3.3.1 Broad-band MIMO-OFDM Channel Model

We adopt the channel model proposed in [7]. Assume there are L significant scatter clusters and that each of the paths coming from the same scatter cluster experiences the same delay. Therefore, there are L resolvable paths between the infostation and mobile terminals. Let $x[n]$ denotes the $M_T \times 1$ transmitted signal vector and $y[n]$ the $M_R \times 1$ received signal vector respectively, we can write

$$y[n] = \sum_{l=0}^{L-1} \mathbf{H}_l x[n-l], \tag{3.1}$$

where the $M_R \times M_T$ complex random matrix $\mathbf{H}_l$ represents the lth tap of the discrete-time MIMO fading channel impulse response. The elements of the individual $\mathbf{H}_l$ are circularly symmetric complex Gaussian random variables. Different scatter clusters are uncorrelated, i.e.,

$$\mathbf{E}[\mathbf{H}_l \otimes \mathbf{H}_{l'}] = \mathbf{0}_{M_R M_T} \text{ for } l \neq l',$$

where $\otimes$ denotes Kronecker product, and $\mathbf{0}_{M_R M_T}$ denotes the all-zero matrix of size $M_R M_T \times M_R M_T$.

Let $\mathbf{h}_{l,k}$ denote the kth column of the matrix $\mathbf{H}_l$, which have zero mean (i.e., pure Rayleigh fading) and the $M_R \times M_R$ correlation matrix $\mathbf{R}_l = \mathbf{E}[\mathbf{h}_{l,k}\mathbf{h}_{l,k}^H]$ is independent of k (i.e., the fading statistics

are the same for all transmit antennas). Then the $M_R \times M_T$ matrices $\mathbf{H}_l$ can be factored as

$$\mathbf{H}_l = \mathbf{R}_l^{1/2}\mathbf{H}_{w,l}, \;\; l = 0, 1, \cdots, L-1, \tag{3.2}$$

where the $\mathbf{H}_{w,l}$ is uncorrelated $M_R \times M_T$ matrices with i.i.d. $\mathcal{CN}(0,1)$ entries, and $\mathcal{CN}(0,1)$ denotes zero mean, unit variance complex Gaussian distribution.

To avoid complex equalization design, OFDM modulation is used to transform a frequency selective fading channel into a set of parallel frequency flat narrow fading channels. For a MIMO channel, each transformed sub-channel is still a MIMO channel with a channel gain matrix $\mathbf{H}(k) = \sum_{l=0}^{L-1} \mathbf{H}_l e^{-j2\pi(kl/K)}$, where K is the total number of sub-channels. For each sub-channel, let $\mathbf{x}(k) = \{x(k)_1, x(k)_2, \cdots, x(k)_{M_T}\}$ be the transmitted vector and $\mathbf{y}(k) = \{y(k)_1, y(k)_2, \cdots, y(k)_{M_R}\}$ be the received vector. The kth Gaussian MIMO sub-channel can be represented by

$$\mathbf{y}(k) = \mathbf{H}(k)\mathbf{x}(k) + \mathbf{n}(k), \;\; k = 0, 1, \cdots, K-1, \tag{3.3}$$

where $\mathbf{n}(k) = \{n(k)_1, n(k)_2, \cdots, n(k)_{M_R}\}$ is a vector with i.i.d. $\mathcal{CN}(0,1)$ elements. From [7, Proposition 1], the capacity of the sub-channel k can be expressed as

$$I(k) = \log\det(I_{M_R} + \rho\Lambda\mathbf{H}_w\mathbf{H}_w^H), \tag{3.4}$$

where $\rho = P/M_T K$, P is the total transmit power, Λ is the eigenvalue matrix of $\mathbf{R} = \sum_{l=0}^{L-1} \mathbf{R}_l$, and $\mathbf{H}_w$ is an $M_R \times M_T$ uncorrelated zero-mean complex Gaussian matrix with i.i.d. entries.

To maximize the throughput of the MIMO channel, i.e., multiplexing gains [74], with full CSI (channel state information) available at the transmitter, the MIMO channel can be decomposed into orthogonal spatial channels, commonly referred to as eigenmodes [3], via SVD (singular value

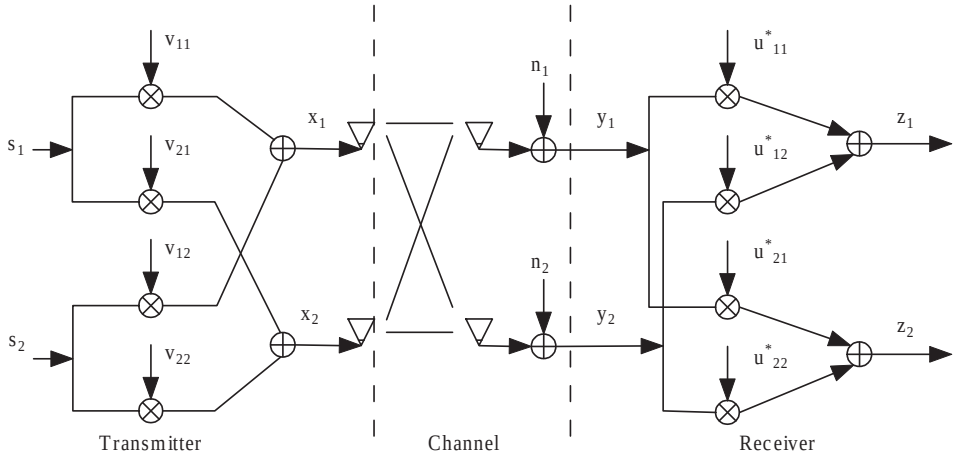

Figure 3.18: MIMO-OFDM channel model

decomposition), which is called eigenvector steering (ES). This procedure for the k-th OFDM sub-channel is as follows[3]

$$\begin{aligned}
\mathbf{y}(k) &= V(k)\Lambda(k)U^H(k)\mathbf{x}(k) + \mathbf{n}(k), \\
\hat{\mathbf{y}}(k) &= \Lambda(k)\hat{\mathbf{x}}(k) + \hat{\mathbf{n}}(k), \\
\hat{y}_i(k) &= \lambda_i^{1/2}(k)\hat{x}_i(k) + \hat{n}_i(k), \quad i = 1, \cdots, \min(M_R, M_T),
\end{aligned} \tag{3.5}$$

where the unitary matrices $V(k), U(k)$ and diagonal matrix $\Lambda(k)$ come from SVD of $\mathbf{H}(k)$, with $\hat{\mathbf{y}}(k) = V^H(k)\mathbf{y}(k)$, $\hat{\mathbf{x}}(k) = U^H(k)\mathbf{x}(k)$, $\hat{\mathbf{n}}(k) = V^H(k)\mathbf{n}(k)$, and $\lambda_i(k), i = 1, \cdots, \min(M_R, M_T)$ are non-zero eigenvalues of $\mathbf{H}(k)\mathbf{H}(k)^H$. The MIMO-OFDM sub-channel model for a 2×2 MIMO channel with ES is shown in Figure 3.18, for which we omit the index k.

3.3.2 Adaptive Modulation and Coding

To exploit the time-variant channel capacity of narrow-band fading channels, an adaptive modulation and coding (AMC) scheme is proposed to maximize data rates for a given bit error rate. Some

[3] $(\cdot)^H$ denotes conjugate transpose.

general design issues about AMC schemes proposed for OFDM channels can be found in [35]. In order to keep the system complexity low, the modulation scheme is not varied on a subcarrier-by-subcarrier basis, but instead the total OFDM bandwidth of K subcarriers is split into blocks of adjacent subcarriers, referred to as subbands, and the same modulation scheme is employed for all subcarriers of the same subband. The modulation scheme was chosen from a finite set between the lowest rate and highest rate. In our MIMO-OFDM system, each subcarrier has several eigenmodes. The adaptive modulation and coding schemes (MCS) can be applied separately for each MIMO eigenmode and each OFDM subband. The MCS schemes that achieve the lowest data rate and highest data rate are shown in Table 3.3 for one subband. Each subband use an MCS scheme from the same MCS sets independently. The data rates are calculated as the product of the following factors, i.e., bandwidth, sub-band overhead, constellation size, coding rate and guard interval overhead. The system parameters are given in Table 3.4. As an example, the lowest data rate are

eigenmode 1 (modulation, coding rate, data rate)	eigenmode 2 (modulation, coding rate, data rate)	sum data rate (Mbps)
BPSK, 1/2, 13.5	BPSK, 1/2, 13.5	27
⋮	⋮	⋮
256QAM, 3/4, 162	64QAM, 3/4, 121.5	283.5

Table 3.3: Modulation and coding schemes for one subband

Parameter	value
bandwidth	40Hz
Number of total subcarriers	128
Number of data subcarriers	108
IFFT/FFT period	3.2μsec
guard interval duration	0.8μsec

Table 3.4: OFDM parameters

calculated as follows,

$$13.5\text{Mbps} = 40\text{MHz} \times \frac{108\text{tones}}{128\text{tones}} \times \frac{3200\text{ns}}{(3200+800)\text{ns}} \times 1\text{bits/sample} \times 1/2. \tag{3.6}$$

There are three typical modulation scheme allocation algorithms discussed in [35], 1) fixed threshold adaptation algorithm; 2) subband BER estimator adaptation algorithm; 3) constant throughput adaptive OFDM. For the fixed threshold adaptation algorithm, a modulation scheme M_n is selected if the instantaneous channel SNR exceeds the switching level l_n for a subband. A constant instantaneous SNR over all of the subcarriers in the same subband is assumed, which requires the subband bandwidth is lower than the channel's coherence bandwidth. If the channel quality varies between the different subcarriers in a subband, the subcarrier with the lowest SNR is considered as the subband's SNR, then a throughput penalty can be observed. For subband BER estimator adaptation algorithm, the expected overall bit error probability for all available modulation schemes M_n in each subband is calculated, which is denoted by $\bar{P}_e(n) = \sum_{i=1}^{N_s} P_e(\gamma_i, M_n)/N_s$, where $\bar{P}_e(n)$ is the overall BER for AMC scheme M_n, $P_e(\gamma_i, M_n)$ is the BER for the i-th subband with a SNR of γ_i and N_s is the number of subbands. For each subband, the scheme with the highest throughput, whose estimated BER is lower than a given threshold, is then chosen. This scheme considers not only the subcarrier with the lowest SNR and, therefore, leads to an improved throughput. In the constant throughput adaptive scheme, each subband is assigned a state variable holding the index of a modulation scheme. Each state variable is initialized to the lowest order modulation scheme. An iterative algorithm is used to increase the state variable to the next order modulation scheme for the subband with the lowest cost. This is repeated, until the total number of bits in the OFDM symbol reaches the target number of bits.

Except for the constant throughput scheme, both algorithm 1 and 2 can be applied for the MIN-MAC

protocol.

3.3.3 Multiuser Diversity

When many users access the infostation at the same time, they may experience independent channel variations. If the channel conditions of these users are known to the infostation, it can schedule the user with the best channel condition at each time slot. The capacity gain achieved by scheduling is called multiuser diversity gain [37].

Let K be the number of OFDM sub-channels and N be the number of users in the system. Assume there are S independent subbands for the MIMO-OFDM channel, each subband include N_S subcarriers with the same channel gain. The capacity of an $M_R \times M_T$ MIMO channel with a fixed channel gain matrix $H(k)$ is given by

$$\mathcal{I}(k) = \log\det(I_{M_R} + \rho\mathbf{H}(k)\mathbf{H}(k)^H) = \sum_{i=1}^{\min(M_R,M_T)} \log(1+\rho\lambda_i(k)),$$

where $\rho = \frac{P}{M_T K}$ and $\lambda_i(k)$ is the i-th eigenvalue of $\mathbf{H}(k)\mathbf{H}(k)^H$, i.e., the gain of the i-th MIMO eigenmode of the k-th OFDM sub-channel.

Define

$$\mathcal{I}_s = N_S \sum_{i=1}^{\min(M_R,M_T)} \log(1+\rho\lambda_{si}) \tag{3.7}$$

as the capacity of the s-th subband, where λ_{si} is a random variable representing the gain of the i-th eigenmode of the s-th subband. Then the capacity of the MIMO-OFDM channel in this mode is given by

$$\mathcal{I} = \sum_{k=1}^{K} \mathcal{I}(k) = \sum_{s=1}^{S} \mathcal{I}_s. \tag{3.8}$$

Since $\mathcal{I}_s$ has the same statistical property for all subbands, the central limit theorem (CLT) implies that the distribution of $\mathcal{I}$ approaches Gaussian distribution as S increases.

Lemma 3.3.1. *(Maximum of Sequence of Independent Gaussian Random Variables): Let $Z_1, Z_2, \cdots, Z_N$ be a sequence of independent Gaussian random variables with mean μ and variance σ^2. Define $M_N = \max\{Z_1, Z_2, \cdots, Z_N\}$. Then*

$$\frac{M_N - \mu}{\sqrt{2\sigma^2 \ln N}} \to 1,$$

in probability as $N \to \infty$.

The proof of this is standard (see [15, p. 76] for example) and we omit it.

From the Lemma 3.3.1, the multiuser diversity gain is

$$G = \frac{\sqrt{2\sigma^2 \ln N}}{\sqrt{S}\mu},$$

where μ and σ^2 are the mean and variance of $\mathcal{I}(k)$ respectively. Therefore, the multiuser diversity gain increases as the number of users increases and decreases as the number of independent OFDM sub-channels increases.

3.3.4 PHY Simulation Model

We assume a capacity achieving coding scheme and perfect adaptive modulation and coding (AMC) scheme with infinite number of AMC levels that can exploit the full channel capacity with a realistic lower and upper limit of data rates as shown in Table 3.3. We assume the channel state is invariant within a subband and varies independently across different subbands. The number of subbands S

depends on the coherent bandwidth, which is a simulation parameter. With infinite number of AMC levels, at each channel state, each subband is assigned a AMC level with a data rate that equals to the corresponding Shannon capacity $\mathcal{I}$ as given in equation (3.8) scaled by the effective bandwidth, i.e.,

$$40\text{MHz} \times \frac{108\text{tones}}{128\text{tones}} \times \frac{3200\text{ns}}{(3200+800)\text{ns}} \times \mathcal{I}\text{bps/Hz} = \mathcal{I} \times 27\text{Mbps}.$$

In the following, we discuss how the instantaneous capacity of each user with CSI at both transmitter and receiver is obtained in our simulation for a 2×2 MIMO-OFDM channel with the OFDM parameters given in Table 3.4.

Assume a rich scattering environment and a perfect channel estimation, each OFDM sub-channel can be transformed into 2 independent parallel eigenmodes. The fading gain of each eigenmode is $\sqrt{r_i\lambda_i}, i = 1, 2$, where r_i is the i-th eigenvalue of the correlation matrix $\mathbf{R}$ and λ_i the i-th eigenvalue of a Wishart matrix $\mathbf{H}_w\mathbf{H}_w^H$ as defined in equation (3.4). We drop the sub-channel index k for simplicity. We further assume an uncorrelated MIMO channel for all different path, i.e., $\mathbf{R} = \mathbf{I}, r_i = 1$. In the following, we analyze the statistical properties of $\mathbf{H}_w$.

Definition 3.3.1. Let $\mathbf{W} = \mathbf{H}_w^H\mathbf{H}_w$, where the $n\times m$ matrix $\mathbf{H}_w$ is distributed as $\mathbf{H}_w \sim \mathcal{CN}(0, I_n \otimes \Sigma)$. Then $\mathbf{W}$ is said to have the complex central Wishart distribution with n degrees of freedom and covariance matrix Σ, denoted by $\mathbf{W} \sim \mathcal{C}W_m(n, \Sigma)$, and $\mathbf{W}$ is a complex central Wishart matrix.

The eigenvalue density of a complex Wishart matrix has the following property.

Property 3.3.2. *Let $\mathbf{W} \sim \mathcal{C}W_m(n, \sigma^2 I_n)$ be an $m \times m$ positive definite complex random matrix. Then the joint density function of the eigenvalues, $\lambda_1 > \lambda_2 > \cdots > \lambda_m > 0$, of $\mathbf{W}$ is*

$$g(\Lambda) = \frac{\pi^{m(m-1)}(\sigma^2)^{-nm}}{\mathcal{C}\Gamma_m(m)\mathcal{C}\Gamma_m(n)} \prod_{k=1}^{m} \lambda_k^{n-m} \prod_{k<l}^{m} (\lambda_k - \lambda_l)^2 \exp\left(-\frac{1}{\sigma^2}\sum_{k=1}^{m}\lambda_k\right), \tag{3.9}$$

where $\Lambda = diag(\lambda_1, \lambda_2, \cdots, \lambda_m)$ *and* $\mathcal{C}\Gamma_m(n)$ *denotes the complex multivariate gamma function,*

$$\mathcal{C}\Gamma_m(n) = \pi^{m(m-1)/2} \prod_{k=1}^{m} \Gamma(n-k+1).$$

From Property 3.3.2, the probability density function (PDF) of the eigenvalues for a 2×2 MIMO channel is evaluated as

$$g(\lambda_1, \lambda_2) = e^{-\lambda_1-\lambda_2}(\lambda_1 - \lambda_2)^2, \text{ with } (\lambda_1 > \lambda_2). \tag{3.10}$$

In our simulation model, for the s-th subband $s, s = 1, \cdots, S$, an independent eigenvalue set $\lambda_{si}, i = 1, 2$ of a Wishart matrix is generated according to the PDF in equation (3.10). The adaptive data rates based is then calculated based on the total capacity from equations (3.7) and (3.8).

3.3.5 Performance Evaluation

In the following scenarios, we use UDP data traffic for both MIN-MACa and MIN-MACb to evaluate the functionality of the MIN-MAC protocol and obtain the upper limit of the MAC throughput. The MAC/PHY simulation parameters are given in Table 3.5, where $nuser$ represents the number of user, $nfrag$ represents the number of sub-frames in a data frame. The parameters are based on industry specification (IEEE802.11 specification or TGnSync proposal) and slow fading channel assumption.

Parameter	value
inter-beacon time	30ms
channel coherence time	30ms
SIFS	10 μs
Mini-slot time	110μs
Contention Period duration	640μs
control frame data rate	6Mbps
AMC data rates	27 $\sim$ 283.5 Mbps
PHY header and preamble time	44.8μs
number of OFDM subbands	6
Beacon frame size	38+4*$nuser$ B
CE frame size	18 B
CEE frame size	16+4*$nuser$ B
Grant frame size	36 B
Data frame header size	27+6*$nfrag$ B
Data frame payload size	64K B
payload sub-frame size	8K B
Block ACK frame size	26 B

Table 3.5: MIN-MAC simulation parameters

High Priority Data Traffic

One of the essential feature of infostation networks is the support for high priority data traffic which is requested by a superuser. As described in the scheduling algorithm, the amount of bandwidth that can be used by the superuser is adjusted by a threshold of channel quality. In the following, we use an illustrative example to show the impact of the threshold. Assume a superuser drives through the coverage area of an infostation network and all users have continuous bi-directional data traffic. Before the superuser enters the network, four regular users share all the bandwidth equally. When the superuser enters the network, it occupies all the bandwidth or part of it depending on the threshold, and the regular users share the remaining bandwidth. After the superuser leaves the network, all the bandwidth is available for all regular users again. In Figure 3.19 and 3.20, we show the throughput of the superuser and two of the regular users for both uplink and downlink traffic for MACa and MACb respectively.

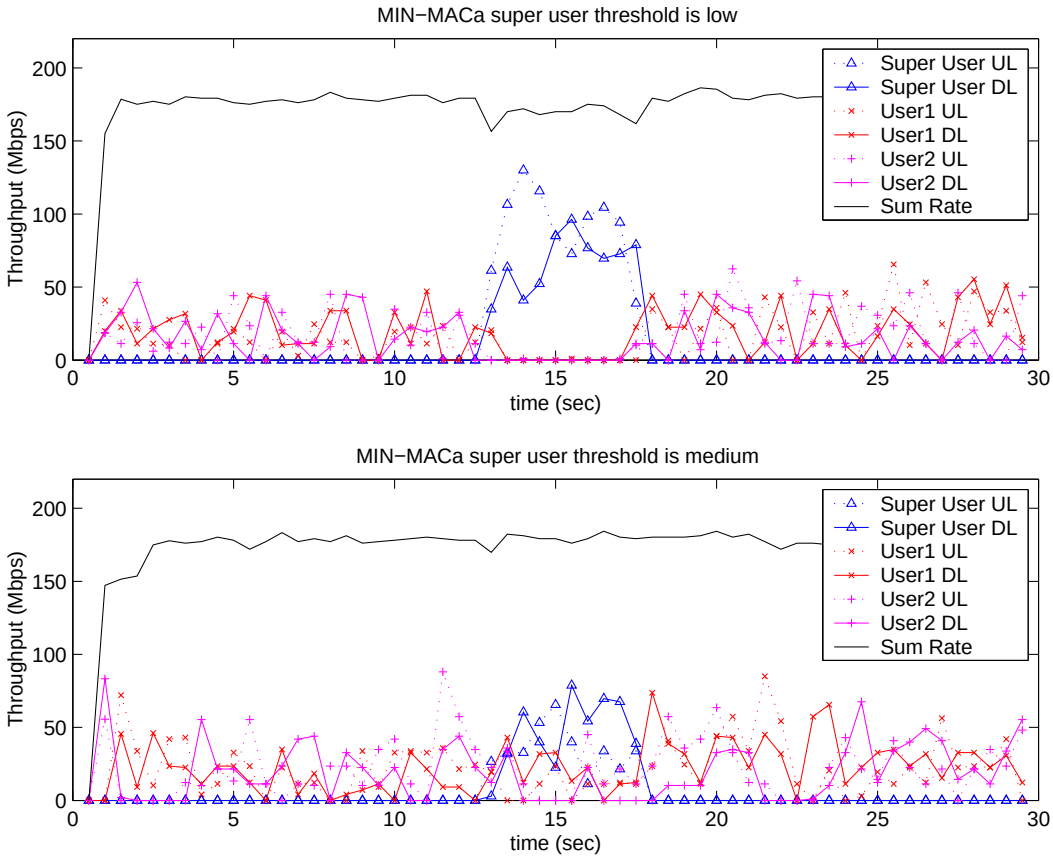

Figure 3.19: Throughput of high priority data with threshold option for MIN-MACa

When the threshold is low, which means the superuser utilizes the channel exclusively whenever it has data to send, all the regular user's traffic is blocked until the superuser leaves or is disconnected from the infostation network. This may cause problem if the superuser happens to stay for a longer time within the network and all the other users need to access the channel.

When the threshold is medium, which corresponds to the average data rate, the superuser can use the channel exclusively only when its channel quality is above the threshold. Otherwise, it can only use the channel when its channel quality is better than the other contending regular users. Therefore, only a portion of the bandwidth is allocated to the superuser and the regular users share the remaining bandwidth.

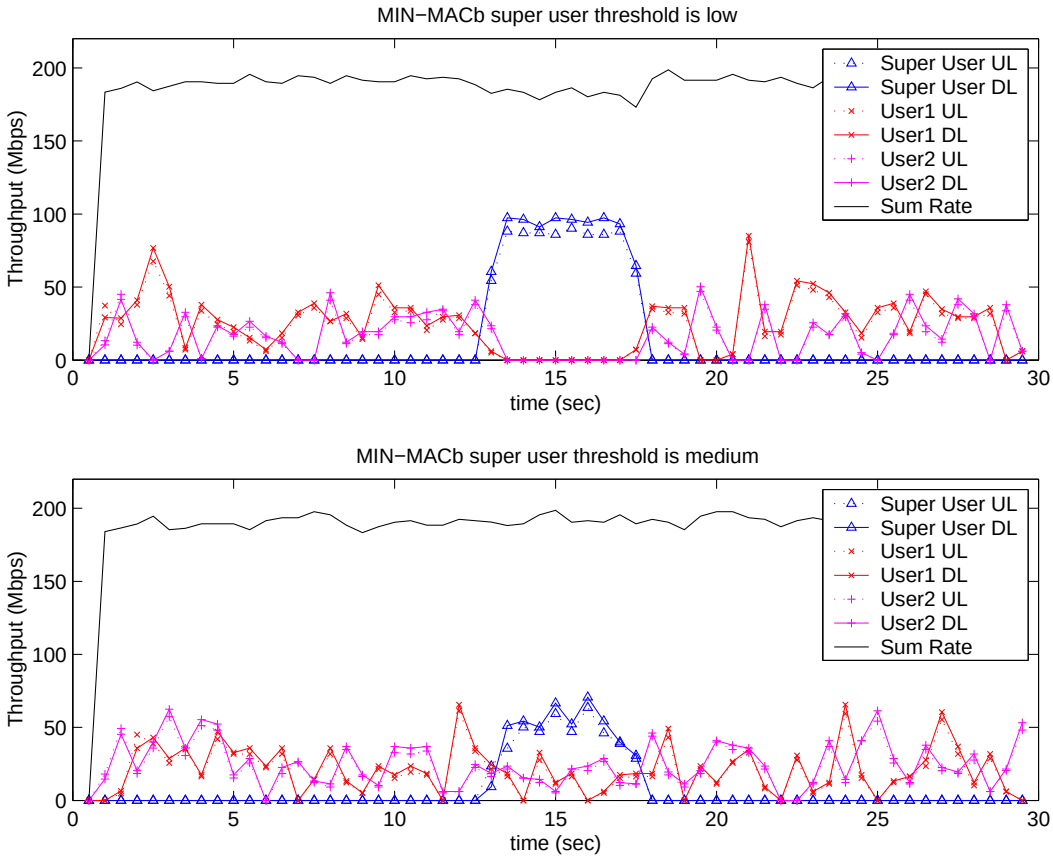

Figure 3.20: Throughput of high priority data with threshold option for MIN-MACb

We observe that the MIN-MACb has higher efficiency than the MIN-MACa because the MIN-MACb does not have ARQ protocol overhead. We also find that for the MIN-MACa, the throughput for the downlink traffic is different from the uplink traffic at all time instance. However, for the MIN-MACb, the throughput for the downlink traffic is very close to the uplink because it supports bi-directional data transmission for each grant.

Scheduling Algorithm and Multiuser Diversity

The scheduling algorithm with contention control is designed to maximize the network throughput by exploiting the multiuser diversity. The throughput performance is evaluated for three scenarios with $M = 1, 6, 18$ OFDM subbands, which correspond to different multiuser diversity gains. The

Parameter	value
SIFS	10 μs
DIFS	50 μs
aSlotTime	20 μs
control frame data rate	6Mbps
AMC data rates	27 $\sim$ 283.5 Mbps
PHY header and preamble time	44.8μs
number of OFDM subbands	1, 6, 18
Data frame header size	24+6*$nfrag$ B
Data frame payload size	64K B
payload sub-frame size	8K B
RTS frame size	20 B
CTS frame size	14 B
ACK frame size	14 B

Table 3.6: IEEE 802.11n MAC simulation parameters

throughput performance of the IEEE 802.11n is also included for comparison. The IEEE 802.11n simulation is implemented on top of the IEEE 802.11 simulator in NS-2 with the same packet aggregation and PHY data rate adaptation schemes as the MIN-MAC protocol. The MAC and PHY parameters are given in Table 3.6.

The throughput performance for the UDP traffic with a 2$\times$2 MIMO-OFDM channel with 1, 6 and 18 subbands are shown in Figure 3.21, 3.22 and 3.23 respectively.

It shows that the MAC throughput of the MIN-MACb is always higher than the MIN-MACa because of the lack of ARQ overhead. The total throughput increases with increasing number of users in the system.

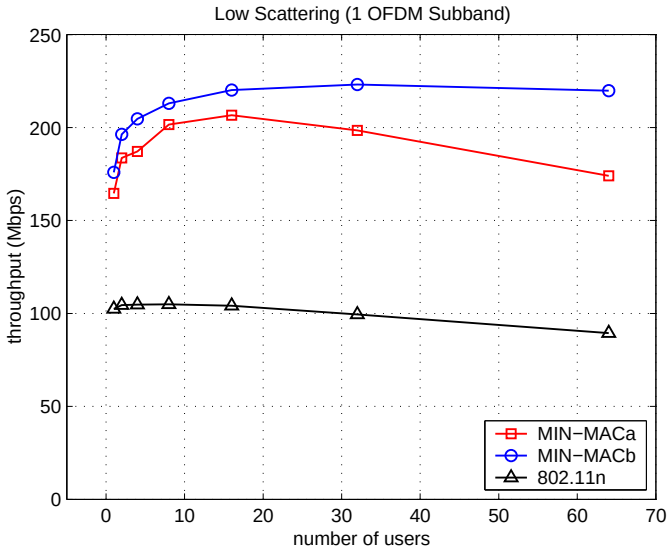

Figure 3.21: Throughput comparison for 2x2 MIMO-OFDM with 1 subband

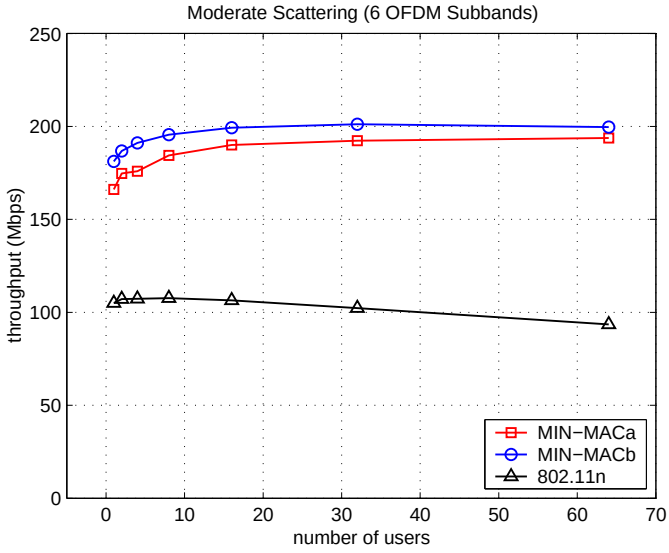

Figure 3.22: Throughput comparison for 2x2 MIMO-OFDM with 6 subbands

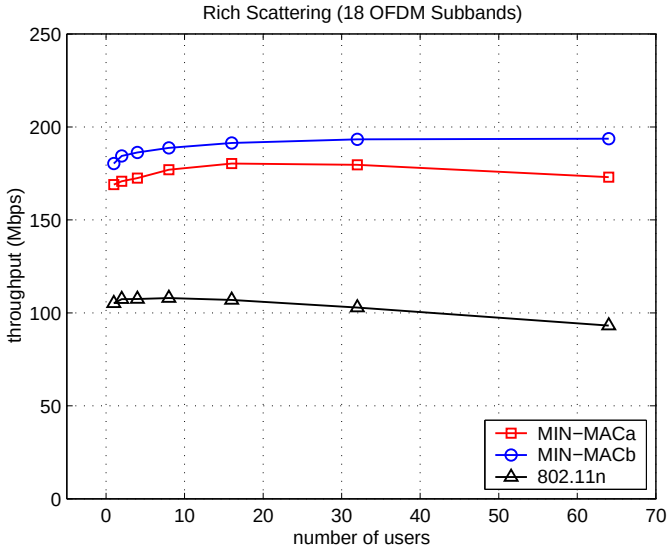

Figure 3.23: Throughput comparison for 2x2 MIMO-OFDM with 18 subbands

Chapter 4

Cross-layer Design of Transport Layer and MAC Layer for Reliable and Efficient Data Transmissions

We have proposed two variations of the highly efficient MAC protocol for mobile infostation networks, the reliable MIN-MACa and the unreliable MIN-MACb. The two systems based on these two MAC variations are called system A and system B respectively. The MIN-MACb has higher efficiency than MIN-MACa with lower implementation overhead. But it requires a transport layer protocol for reliable file transfer. If we use the same TCP protocol that is used for wired networks, the throughput performance is undesirable with high link error rate, despite of the high efficiency of the MIN-MAC protocol. Therefore, we propose a cross-layer design scheme over the transport layer and MAC layer to improve the overall throughput performance. The transport layer protocol jointly designed with the MIN-MACb is called MIN-TCP, i.e., Mobile Infostation Network Transport Control Protocol.

In the following, we first introduce TCP protocol and its limitations when wireless link is present on its path in Section 4.1. In Section 4.2, we show how to improve TCP throughput performance over the MIN-MACb protocol with cross-layer design approaches. In Section 4.3, we evaluate and compare the throughput and file transfer delay between the system A and system B. We conclude this chapter with a summary of future work.

4.1 TCP Congestion Control Algorithms

The TCP protocol is a go-back-N and selective repeat ARQ protocol combined with powerful congestion control algorithms. It performs well in wireline networks. However, TCP can experience significant throughput degradation in the presence of wireless links with high error rates and intermittent connectivity.

The congestion control algorithms of TCP [33], i.e., Slow Start, Congestion Avoidance, Fast Retransmit and Fast Recovery, are considered crucial to today's Internet. The first three algorithms are first introduced in TCP-Tahoe, and the last algorithm is added in TCP-Reno [64]. An improved Fast Recovery algorithm is proposed in TCP-NewReno [19]. Two variables are used to describe these algorithms: *cwnd* (congestion window) which controls the number of outstanding packets/segments that TCP can put into the network and *ssthresh* (slow start threshold) which decides if TCP needs to invoke the Slow Start algorithm or the Congestion Avoidance algorithm.

The Slow Start algorithm operates as follows. When the *cwnd* is less than the *ssthresh*, it is increased exponentially when acknowledgment packets (ACKs) are received. As a result, the TCP sender sends two new segments upon receiving each ACK.

The Congestion Avoidance algorithm incurs a linear increase of the variable *cwnd* when *cwnd* is less than *ssthresh* and an exponential decrease of *ssthresh* when packet loss is observed. The former is implemented by increasing the *cwnd* by one segment per RTT (round-trip time). The later is implemented by decreasing the *ssthresh* to half of the *cwnd* and setting the *cwnd* to 1 segment when a timeout is observed.

If the packet loss is indicated by duplicate ACKs, the Fast Retransmit and Fast Recovery algorithms are invoked. If three or more duplicate ACKs are received in a row, it is a strong indication that

a segment has been lost. TCP then performs a retransmission of what appears to be the missing segment, without waiting for a retransmission timer to expire. After the Fast Retransmit algorithm is performed, the Congestion Avoidance algorithm, instead of the Slow Start algorithm is performed. The Fast Retransmit and Fast Recovery algorithms are implemented as follows: 1) When the third duplicate ACK in a row is received, TCP sets *ssthresh* to one-half the current congestion window *cwnd*, but no less than two segments, retransmits the missing segment and sets *cwnd* to *ssthresh* plus 3 segment size; 2) Each time another duplicate ACK arrives, it increments *cwnd* by one segment size; 3) When the next ACK arrives to acknowledge new data, it sets *cwnd* to *ssthresh*.

When there are multiple packet drops, the acknowledgment for the retransmitted packet will acknowledge some but not all of the packets transmitted before the Fast Retransmit. We call this packet a partial acknowledgment. A modification to the Fast Recovery algorithm in Reno TCP, called NewReno [19], incorporates a response to partial acknowledgments received during Fast Recovery. Unlike TCP-Reno, where a partial ACK terminates the Fast Recovery, TCP-NewReno retransmits the first unacknowledged segment after receiving a partial ACK and deflates the congestion window by the amount of new data acknowledged, then add back one segment size and send a new segment if permitted by the new value of *cwnd*. This window reduction, referred to as “partial window deflation”, attempts to ensure that, when Fast Recovery eventually ends, approximately *ssthresh* amount of data will be outstanding in the network. After receiving a full ACK, the sender sets *cwnd* to *ssthresh* and terminates the Fast Recovery. With NewReno implemented, the TCP has fewer timeouts when multiple packet losses are observed.

When the wireless link variations cause link errors and packet losses, TCP observes an out of order delivery or experiences a timeout. It interprets these events as an indication of network congestion.

If three duplicate ACKs are received, TCP congestion window decreases by half followed by congestion avoidance after a fast retransmission. If a timeout occurs, TCP congestion window drops to one segment followed by a slow start. Since the transmission rate of TCP is roughly equal to a congestion window of packets per RTT, the decrease of congestion window corresponds to the data rate reduction. When link error rate increases, TCP experiences the data rate reduction frequently. For a fast transmission, it takes several RTTs to restore the previous window size. For a timeout, it takes an RTO to detect the packet loss and retransmit the missing packet. The RTO value is much larger than the time scale of wireless link variations. Therefore, for both cases, TCP cannot fully utilize the channel when the channel quality is recovered again after the error event.

For most network architectures, because it is difficult to differentiate if the packet losses are caused by congestion or by wireless link variation, TCP cannot adjust congestion control algorithms accordingly. However, for infostation networks, with information sharing between the transport layer and MAC layer, it is possible to make TCP work without congestion control algorithms and use the wireless channel more efficiently.

In the following, we propose and evaluate different approaches to improve the TCP performance and design MIN-TCP protocol based on these approaches.

4.2 Cross-layer Design for MIN-TCP and MIN-MACb

To analyze TCP behavior and evaluate TCP performance, two link error models are considered. We assume the control frames are transmitted with basic data rates and, therefore, the error probability is extremely low and has little impact to throughput performance. For simplicity, in our link error model, we assume the control frames are error free. For MAC data frames, we assume the following two scenarios:

Link error model A The error probabilities of the MAC header and the following sub-frames have the same sub-frame error rate. The MAC header and sub-frame errors are independent identically uniform distributed. If the MAC header is corrupted, the receiver cannot recognize the frame type and has to discard all the sub-frames, which results in bursty errors of TCP packets.

Link error model B We use a MAC header protection scheme, in which the MAC header is sent with basic rates and error free. The other sub-frame errors are independent identically uniform distributed.

4.2.1 Increased Resolution for the RTT Timer

The RTT (round trip time) timer in TCP is used to measure the RTT, which in turn is used to estimate the average value and variation of RTT. The RTO (retransmission timeout) value is updated based on the RTT statistics. A coarse RTT timer cannot give an accurate RTT estimation and results in a larger RTO and a longer TCP response time to packet loss. In the earlier version of TCP Reno implementation, TCP use a coarse RTT timer with a resolution of 100 ms and the minimal RTO is 1 second [69]. However, in the latest Linux implementation, the RTT timer resolution is set to 10 ms and the minimal RTO is 200 ms [27]. For infostation networks, we set minimal RTO as 0. The parameters for different scenarios are shown in Table 4.1. All other TCP parameters remain unchanged. The throughput performance for different scenarios is shown in Figure 4.1. With more accurate RTT measurement and RTO estimation, the throughput performance of TCP is improved for all settings of packet error rates. Because a shorter RTO means a better utilization of the channels, the improvement is most significant for high packet error rate scenarios, where retransmission after a timeout is performed more often for packet loss recovery.

Scenarios	TCP Version	Timer Resolution	Min RTO	Initial Window	Max Window
NewReno A	NewReno	100 ms	1 s	16	200
NewReno B	NewReno	10 ms	200 ms	16	200
NewReno C	NewReno	10 ms	0 ms	16	200

Table 4.1: TCP parameters

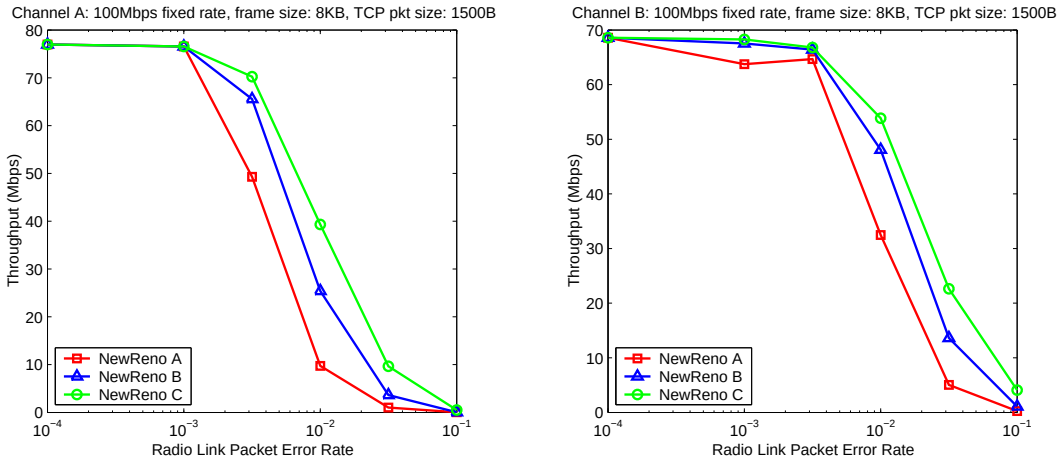

Figure 4.1: Impact of RTT timer resolution

4.2.2 Modified Congestion Control Algorithms

In data networks, congestion occurs when a link or node is carrying too much data, which results in excessive queuing delay, packet loss or the blocking of new connections. TCP congestion control algorithms are proposed to avoid congestion and recover from the congestion state. TCP considers packet loss as an indication of network congestion. However, in wireless data networks, link variation is another source of packet losses. TCP cannot distinguish the difference between these two types of packet losses and the congestion control algorithms are invoked in both cases. If the packet loss results from the link variations, it is unnecessary to invoke the congestion control algorithm and reduce the transmission rate.

To reduce the throughput loss resulting from unnecessary rate reduction, we propose a cross-layer information exchange mechanism across the application layer, transport layer and MAC layer to

eliminate the packet loss caused by congestion. As a result, the only source of packet loss is channel variation and we can disable the congestion avoidance algorithm.

The packet buffer at the infostation is shared by all users. We assume an admission control mechanism blocks the new users during congestion and the infostation allocates the buffer size for each existing user to maximize the utilization of the bandwidth. We then make the buffer allocation information transparent to each layer. With the buffer information, the application layer stops sending packets by back-pressure to avoid packet loss when buffer is full. At the transport layer, buffer overflow can be avoided with congestion window control. More specifically, we assign TCP congestion window size and the buffer size for each user jointly according to the following relation

$$\text{buffer size} > \textit{cwnd} > \text{bandwidth delay product}.$$

With these approaches, we eliminate the congestion related packet loss, and therefore, the congestion avoidance algorithm is not necessary. With congestion avoidance algorithm disabled, the congestion window remains unchanged regardless of the channel variations. The congestion window reduction after the congestion avoidance algorithm as well as the fast recovery algorithm can be removed in the design of the MIN-TCP protocol, while the Slow Start and Fast Retransmit algorithms remain unchanged. Therefore, the baseline implementation of MIN-TCP is based on TCP-NewReno with the following modifications:

- We set the RTT timer resolution to 10 ms and minimum RTO value to 0.
- After the TCP connection is established, the initial window size is set to multiples of the number of sub-frames in a MAC data frame.
- The receiver's advertised window size, which is the upper limit of the actual window size of

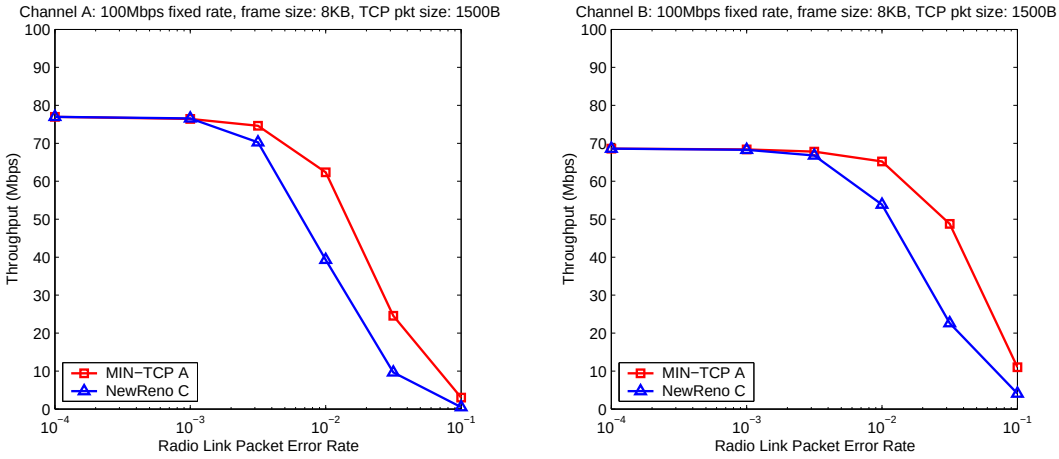

Figure 4.2: MIN-TCP and TCP-NewReno throughput comparison

the sender, is set to the maximum MAC buffer size less the initial window size for both ends of the TCP connection. We assume the receiver's buffer size is not the bottleneck.

- The congestion window size increases according to slow start algorithm until a packet loss is detected with duplicate ACKs or a timeout.
- If three duplicate ACKs are received, the fast retransmission algorithm is invoked. However, no congestion window reduction is performed.
- After the fast retransmit, for each duplicate ACK, a new packet is transmitted, because each ACK implies a packet has been moved out of the network.
- If a partial ACK is received, the packet corresponding to this ACK is retransmitted and a new packet is also transmitted.
- If a timeout occurs, the window size drops to the initial window size and a slow start is performed. A window of packets are retransmitted starting with the missing packet that causes the timeout.

Figure 4.2 shows the throughput performance of the MIN-TCP compared with the TCP-NewReno

C with channel error models A and B. When packet error rate is lower than 0.01, most of the packet losses can be recovered by the Fast Retransmit algorithm. Since the packet losses are caused by random link errors, TCP does not need to decrease the congestion window. The simulation results show that the throughput performance increases significantly at low packet error rate region. For high packet error rate region, when frequent timeout retransmissions become the major source of throughput loss, the absence of congestion control algorithm does not increase the throughput much. During the timeout, the channel is almost idle and the bandwidth is wasted.

4.2.3 Fast MAC Queuing Algorithm

The round trip time (RTT) of a TCP connection is composed of queuing delay, transmission delay, propagation delay and processing delay. Among them, the queuing delay is the dominant part of RRT. To reduce the response time to a packet loss we propose a fast MAC queuing algorithm to by reduce the queuing delay. This algorithm allows shorter queuing delay for retransmitted packet by moving the retransmitted packet to the front of the queue. Note that for the MIN-MAC protocol, a different sending packet queue is allocated for each user to enable the users' priorities and channel quality based packet scheduling. The algorithm is applied for each user queue as follows.

- When a TCP data packet arrives at the queue, it compares the sequence numbers between the new data packet and existing data packets in the queue. To improve efficiency, the comparison starts from the tail of the queue.
- If a duplicate packet is found, it replaces the existing packet with the new packet. Because a new ACK number is carried on the new packet which contains the most recent information.
- If no duplicate packet is found, it finds the packet with the highest sequence number smaller than the sequence number of the new packet and insert the new packet after it.

Scenarios	basic TCP Version	queuing option
MIN-TCP A	NewReno	default
MIN-TCP B	NewReno	fast queuing
MIN-TCP C	Reno	fast queuing

Table 4.2: MIN-TCP parameters

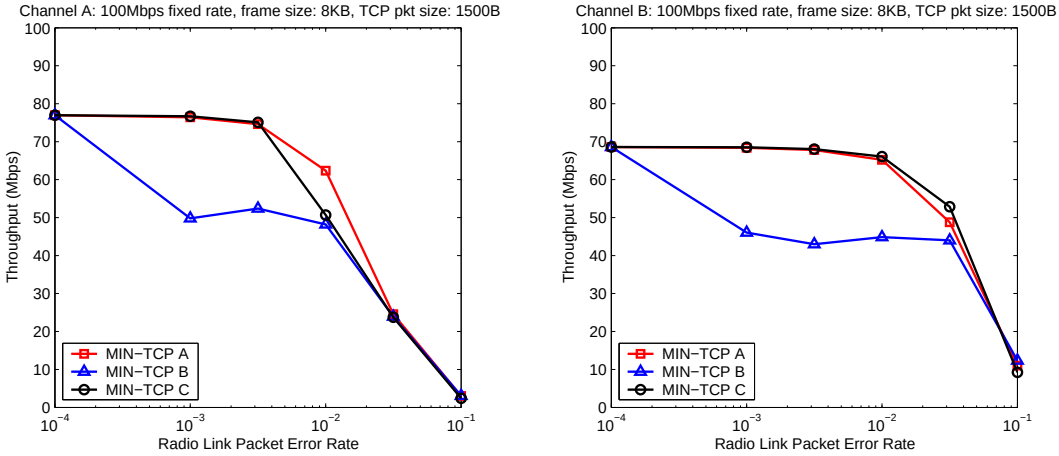

Figure 4.3: Throughput comparison for different MIN-TCP options

- If all packets in the queue have larger sequence number than the new packet, it inserts the new packet at the front of the queue.

A packet sorting algorithm is also used as part of the wireless TCP solution in [40] for different purpose, where a new layer is constructed between the TCP layer and MAC layer to hide the out of order delivery of the TCP packets. As we discuss later, the packet sorting has some side effects for TCP-NewReno.

To evaluate the impact of the fast queuing algorithm, we consider both channel error models A and B for three scenarios shown in Table 4.2.

As shown in Figure 4.3, for MIN-TCP C, with fast queuing algorithm, the packet loss is recovered faster than MIN-TCP A when there are no bursty errors (channel error model B). However, for bursty error link (channel error model A), without NewReno's fast recovery algorithm, MIN-TCP

C has lower throughput than MIN-TCP A. It also shows the MAC header protection (channel error model A) increases the protocol overhead and results in lower throughput for links with low packet error rate. However, it increases throughput for links with high packet error rate because of reduced bursty errors.

To understand the MIN-TCP behavior further, Figures 4.6, 4.7 and 4.8 show the packet traces of MIN-TCP A, MIN-TCP B and MIN-TCP C for both channel error model A (bursty error) and channel error model B (random error). For comparison purposes, the packet trace for TCP-Reno and TCP-NewReno are also shown in Figures 4.4 and 4.5. The TCP-NewReno can recover from multiple packet losses with the new fast recovery algorithm, while TCP-Reno experiences a timeout when there are multiple packet losses in one round trip time.

MIN-TCP A

Figure 4.6 shows the MIN-TCP A behavior with TCP packet traces. The upper plot shows the MIN-TCP response to single packet loss. After three duplicate ACKs, a fast retransmit is performed. The receiver keeps sending duplicate ACKs before the retransmitted packet is received. For each duplicate ACK, a new packet is sent out, because there is no window reduction. In Figure 4.6, there is a seemingly violation of window management principle, i.e., the maximum sequence number should not exceed the sum of the largest ACK number and window size. However, we can show that the number of outstanding packets is unchanged, which is still within the congestion window size, because each duplicate ACK implies that one packet has reached the destination. It also shows that the bandwidth is fully utilized for the single packet loss cases.

The lower plot shows the MIN-TCP A response to multiple packet losses. The MIN-TCP A behavior is the same as single packet loss case, except that for each partial ACK, an old packet is

retransmitted.

MIN-TCP B

Figure 4.7 shows the MIN-TCP B behavior. The single packet loss and multiple packet loss cases are shown in the upper and lower plot respectively. For both cases, after three duplicate ACKs, a fast retransmission is performed. A new ACK is received after the retransmission, which is interpreted as a partial ACK and triggers a retransmission of the packet next to the fast retransmit packet in the queue. However, the next packet in the queue has been transmitted and possibly received at the receiver. Therefore, the partial ACK results in an unnecessary duplicate retransmission. Moreover, the duplicate packet results in chain reaction of partial ACK and fast recovery of NewReno and a window of packets are retransmitted unnecessarily. This explains the fast queuing algorithm cannot coexist with NewReno's fast recovery algorithm.

MIN-TCP C

Figure 4.8 shows the MIN-TCP C behavior. The single packet loss and multiple packet loss cases are shown in the upper and lower plot respectively. Without NewReno's fast recovery scheme, the system recovers from the single packet loss faster. However, multiple packet losses result in under-utilized bandwidth. Because for each duplicate ACK, no new packet can be transmitted. This explains why the performance of MIN-TCP C is better than MIN-TCP A for channel error model B, but worse for channel error model A.

4.3 Performance Evaluation for Reliable File Transfer Application

4.3.1 Throughput Performance Comparison for MIN-MACa and MIN-MACb

Figures 4.9 and 4.10 show the throughput comparison between the MIN-MACa and MIN-MACb for single user and multiple users respectively. With adaptive PHY data rates, the MAC parameters are same as parameters in Table 3.5 except that the maximum aggregated data frame size and sub-frame size are 8000 and 1500 Bytes respectively.

We are especially interested in the performance difference between the system A (UDP with MIN-MACa) and the system B (TCP with MIN-MACb). At the low packet error rate region, system B performs better because of the high efficiency of MIN-MACb and low throughput loss of TCP. At the high packet error rate region, the throughput performance of system A is better. The reason is as follows. The ARQ protocol at the MAC layer requires acknowledgment for every MAC frames. The MIN-MACa protocol knows immediately if the retransmission is successful and responds quickly by a retransmission. However, TCP has to wait for a timeout to know the packet loss. The timeout value is often the upper bound of the possible RTT value to avoid unnecessary retransmission. The frequent timeouts result in gaps of the packet flow and decreases the throughput performance. If many users share the channel, when one user is idle during a timeout, another user can still use the channel and reduce the channel idle time. Therefore, the throughput is higher than the single user case. Even with multiple users, when the packet error rate is extremely high, every user experiences timeout most of the time, and the link usage is still very low as shown in Figure 4.10.

4.3.2 Performance of File Transfer Applications

Consider the following scenario, each regular user has 1 MB size files to send and receive, and the superuser has 10MB size files to send and receive. For both downlink and uplink file transfers, the idle time between the file transfers is exponentially distributed with a mean of 2 seconds. The transmission time of each file is evaluated for both super user and regular users. For system A, the results are shown in Figures 4.11 and 4.12. Figure 4.11 shows when super user has high priority data, all file transfer are completed in 2 seconds. Figure 4.12 shows that when super user has medium priority data, all the regular file transmission of 1 MB are completed within 3 seconds and all 10 MB size file transmission for super user are completed within 5 seconds. These results show that the file transfer time can be controlled with different super user priorities, which in turn is decided by the super user threshold.

4.4 Conclusions and Future Work

In this chapter, we proposed a transport layer protocol MIN-TCP, which has been optimized to improve the throughput performance over the MIN-MACb protocol. In our simulations, we observed that when link error rate is low, TCP/MIN-MACb based scheme provides higher throughput with lower protocol complexity. For higher link error rates, with TCP protocol as the loss recovery mechanism together with all the improvements, there is still a big gap between the throughput performance of system A (UDP/MIN-MACa protocol) and system B (TCP/MIN-MACb protocol). The fundamental reason is that TCP has delayed response for the packet loss due to its large timescale compared with the MAC protocol. Therefore, the bandwidth is wasted during the waiting time (timeout) for TCP to figure out the packet losses. Hence the ARQ protocol at the MAC layer outperforms TCP timeout mechanism at the high packet error rate region.

From the implementation complexity perspective, MIN-MACb has many advantages over MIN-MACa. In the multiple user and moderate packet error rate case, the performance of TCP/MIN-MACb is comparable with MIN-MACa. To reduce the performance gap between the MIN-MACa and MIN-MACb over high packet error rate links, we can consider the following cross-layer approaches: 1) for bi-direction data flow, we can attach an ACK field to the data frame to obtain the information about the transmission failure and provide this information to TCP layer to avoid a timeout event; 2) for downlink data flow only, an ACK field is attached at Beacon frame; 3) for uplink data flow only, an ACK field is attached to CE frames. With these approaches, we can obtain packet loss information with minimum overhead. The TCP protocol can then take advantage of these MAC information to perform fast retransmission and recover from the packet losses.

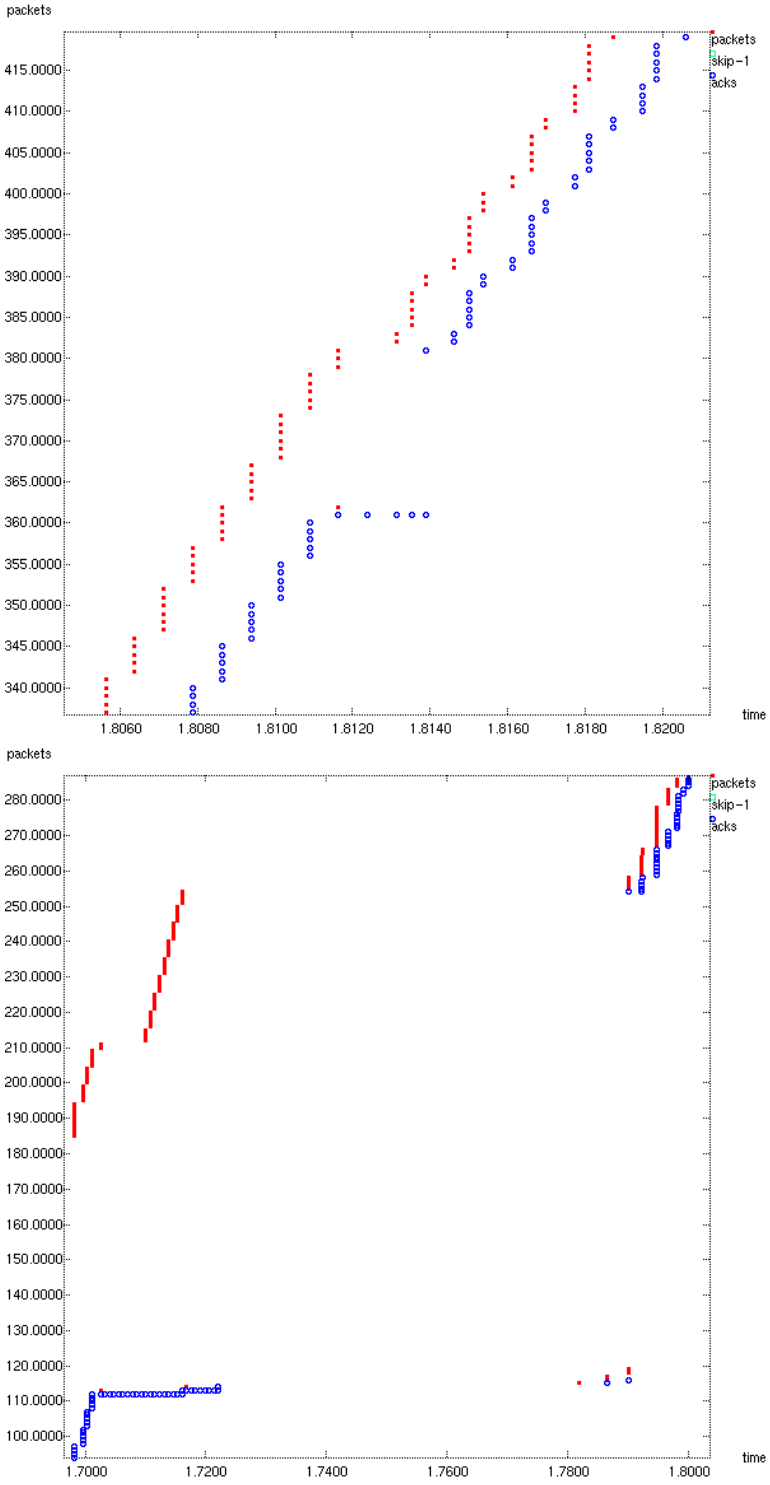

Figure 4.4: Packet trace for TCP-Reno

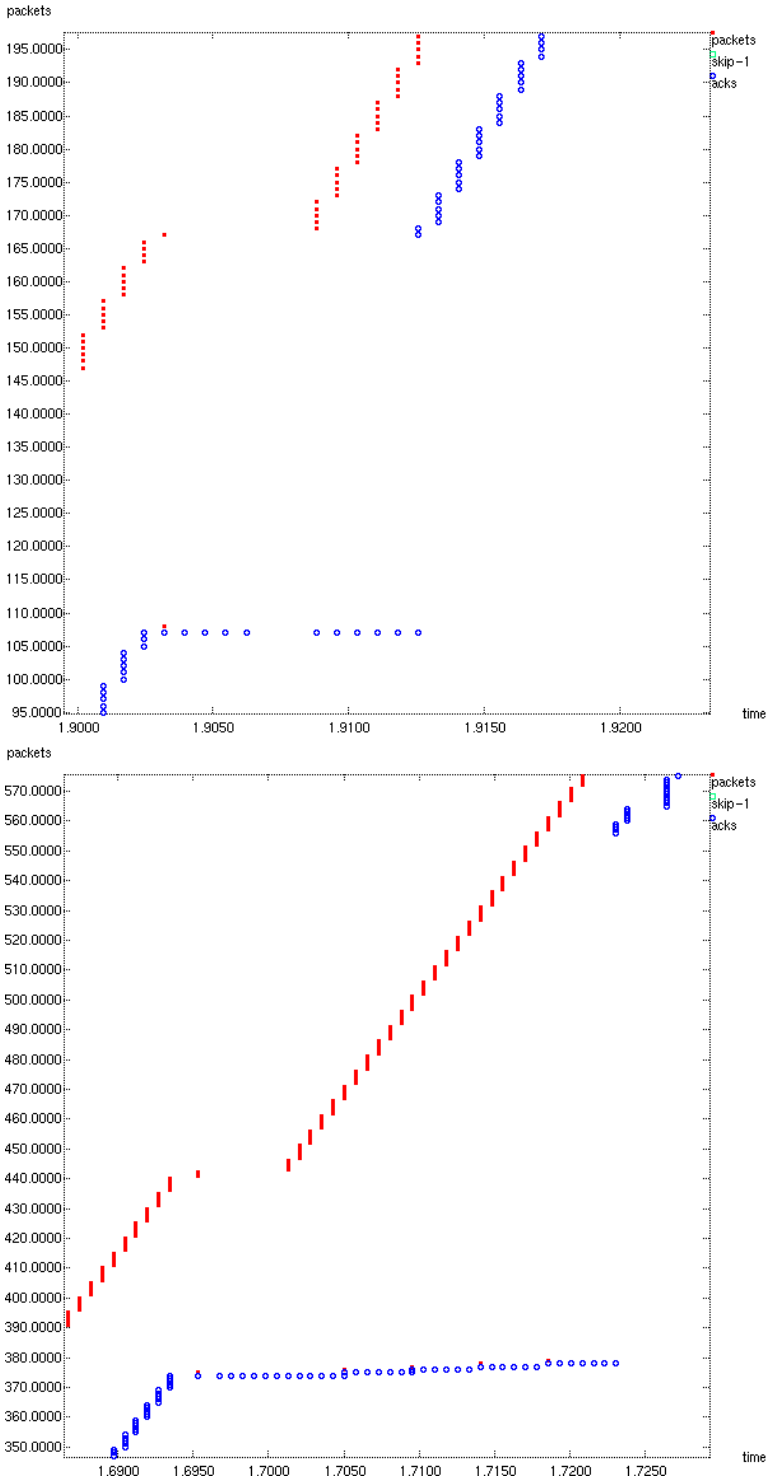

Figure 4.5: Packet trace for TCP-NewReno

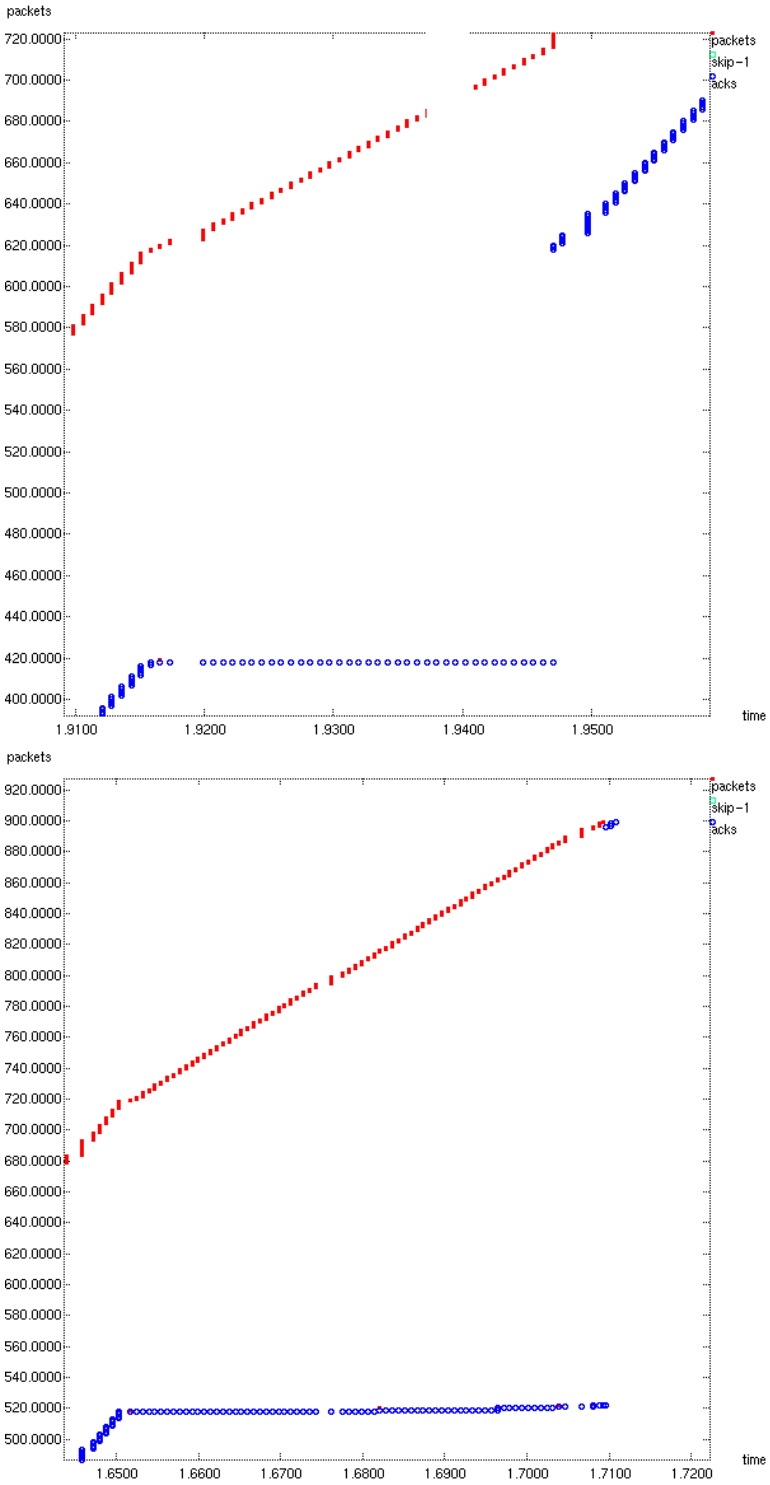

Figure 4.6: Packet trace for MIN-TCP A

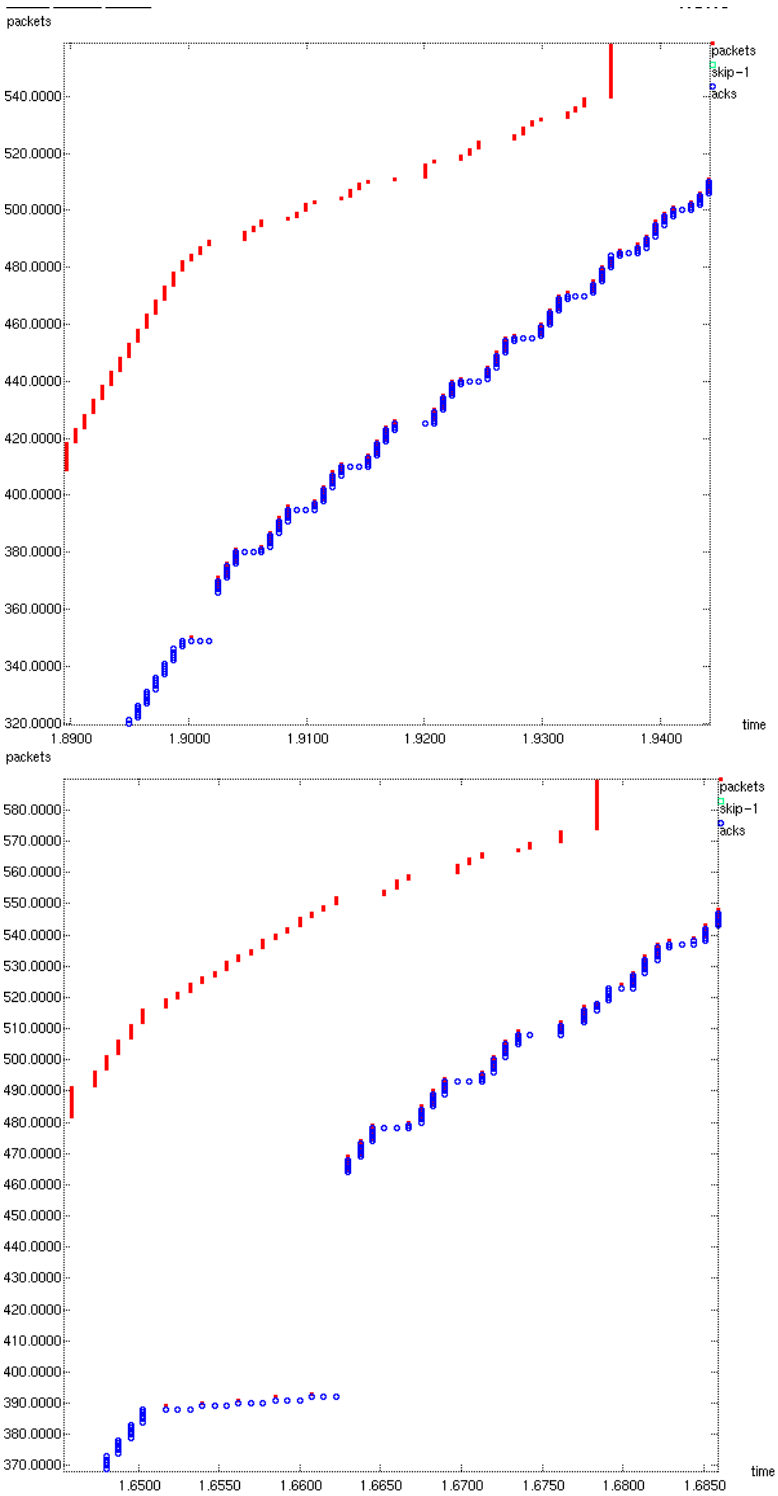

Figure 4.7: Packet trace for MIN-TCP B

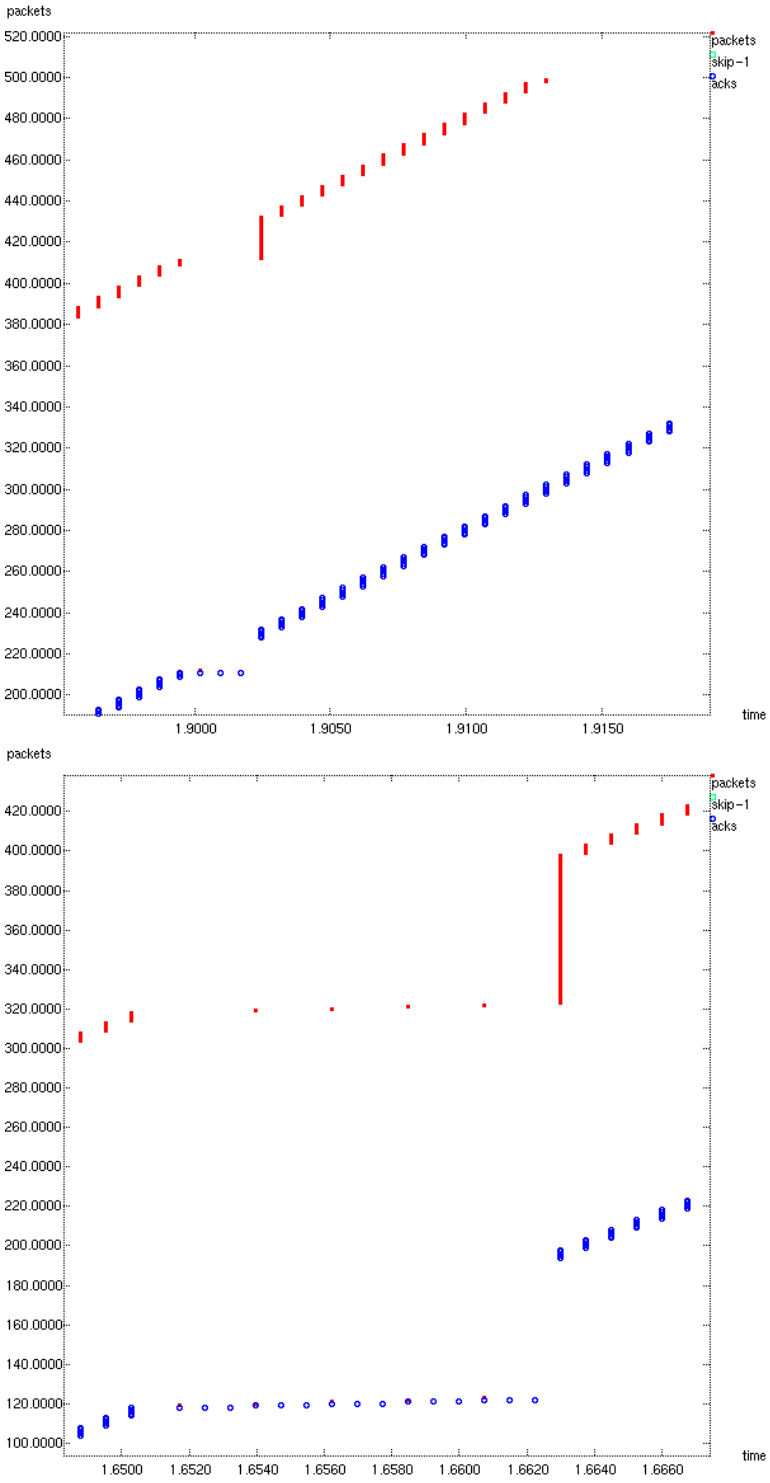

Figure 4.8: Packet trace for MIN-TCP C

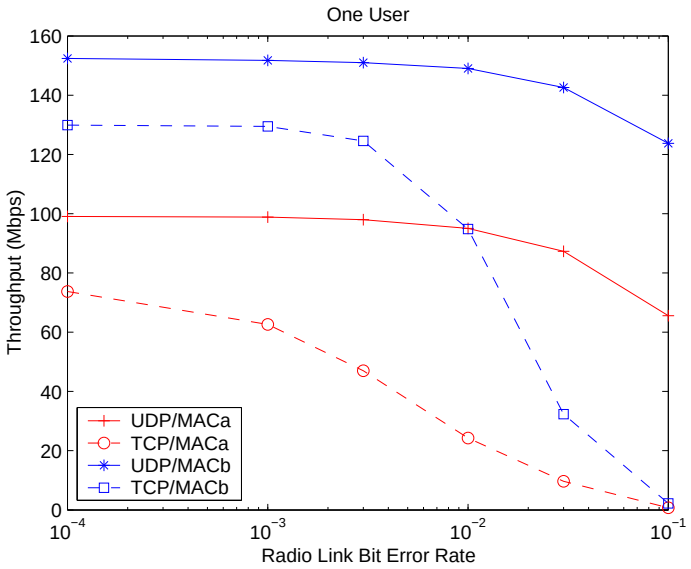

Figure 4.9: Throughput comparison for single user case

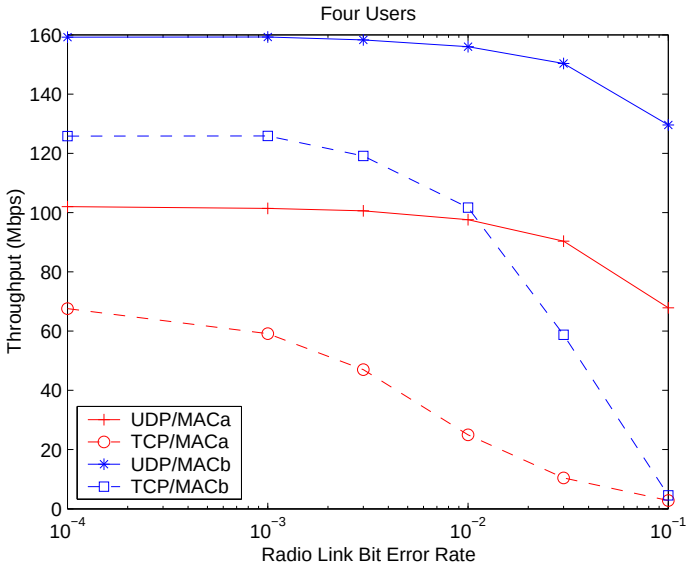

Figure 4.10: Throughput comparison for four-user case

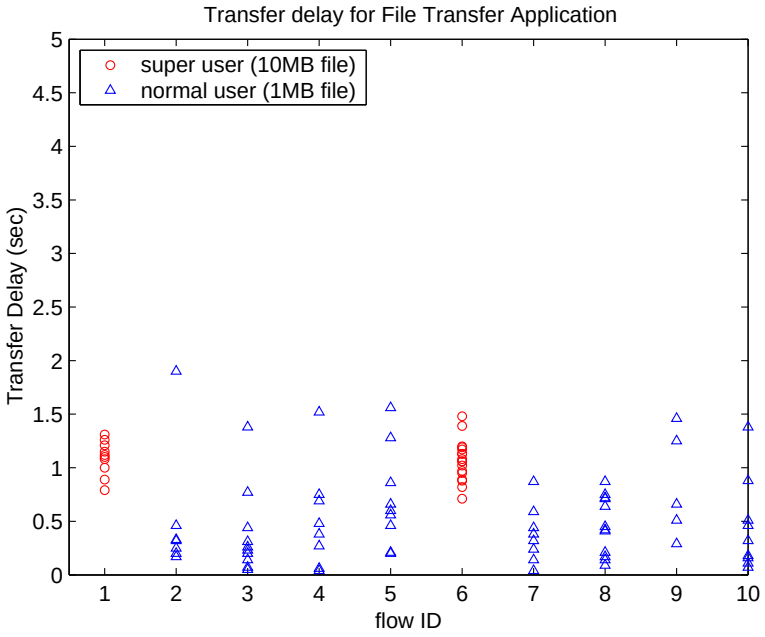

Figure 4.11: File transfer time with high priority super user

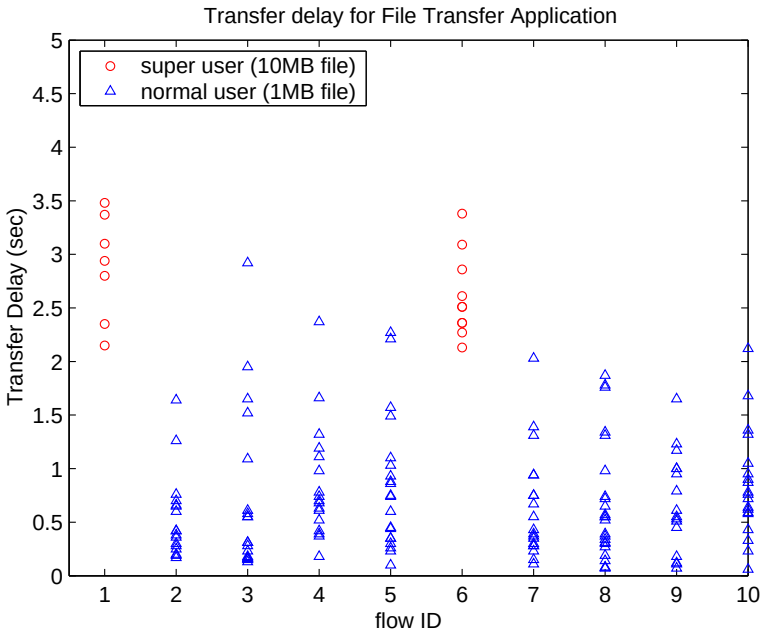

Figure 4.12: File transfer time with medium priority super user

Appendix A

Lower Bound of the Error Probability for Type II Hybrid–ARQ

The lower bound of the error probability for type II Hybrid–ARQ is derived as follows.

Assume a codeword $\mathbf{c} = (c_1, c_2, \cdots, c_l)$ is transmitted in l code blocks and detected as another codeword $\mathbf{e} = (e_1, e_2, \cdots, e_l)$. A decoding error occurs when the different symbols between the two, i.e., $(s_1, s_2, \cdots, s_l)$, is decoded as $(-s_1, -s_2, \cdots, -s_l)$ for the l-th transmission, where s_l is a super symbol composed of all different symbols between c_l and e_l. For an i.i.d. white Gaussian channel, the corresponding received signals $\mathbf{x} = (x_1, x_2, \cdots, x_l)$ have a marginal joint PDF in an l-dimension space as

$$p(\mathbf{x}) = p(x_1) \cdots p(x_l) = \frac{1}{\sigma_1 \sigma_2 \cdots \sigma_n (\sqrt{2\pi})^n} \exp\{-\frac{(x_1 - a_1)^2}{\sigma_1^2} - \frac{(x_2 - a_2)^2}{\sigma_2^2} \cdots - \frac{(x_l - a_l)^2}{\sigma_l^2}\},$$

where $a_i = |s_i|, i = 1, \cdots, l$. The pairwise error probability at the l-th transmission is equal to the probability when $\mathbf{x}$ is within decision region Ω_l, where Ω_l are defined as

$$\begin{aligned} \Omega_1 &= \{\vec{x} : \frac{a_1}{\sigma_1^2} x_1 < 0\} \\ \Omega_2 &= \{\vec{x} : \frac{a_1}{\sigma_1^2} x_1 + \frac{a_2}{\sigma_2^2} x_2 < 0\} \\ &\cdots \\ \Omega_l &= \{\vec{x} : \frac{a_1}{\sigma_1^2} x_1 + \frac{a_2}{\sigma_2^2} x_2 + \cdots + \frac{a_l}{\sigma_l^2} x_l < 0\}. \end{aligned} \tag{A.1}$$

A lower bound of the joint error decision can be derived as follows. For the two-dimension case as

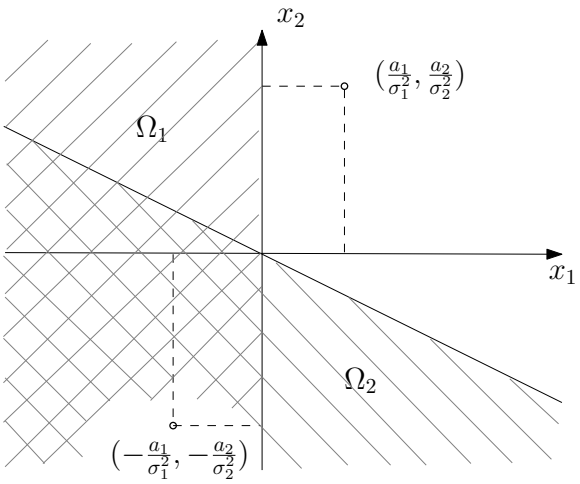

Figure A.1: Decision regions

shown in Figure A.1, the marginal PDF of $p(x_1, x_2)$ is

$$p(x_1, x_2) = \frac{1}{2\pi\sigma_1\sigma_2} \exp\{-\frac{(x_1 - a_1)^2}{\sigma_1^2} - \frac{(x_2 - a_2)^2}{\sigma_2^2})\}.$$

The probability of error events for both the first and second transmission is evaluated as

$$\begin{aligned}
Pr(\mathcal{E}_1, \mathcal{E}_2) &= \int_{\Omega_1 \cap \Omega_2} p(x_1, x_2) dx_1 dx_2 && \text{(A.2a)} \\
&= \int_{-\infty}^{0} \int_{-\infty}^{-\frac{a_1\sigma_2}{a_2\sigma_1}x_1} p(x_1, x_2) dx_2 dx_1 && \text{(A.2b)} \\
&\geq \int_{-\infty}^{0} \int_{-\frac{a_2\sigma_1}{a_1\sigma_2}x_1}^{-\frac{a_1\sigma_2}{a_2\sigma_1}x_1} p(x_1, x_2) dx_2 dx_1 && \text{(A.2c)} \\
&= \frac{1}{2} \int_{\Omega_2} p(x_1, x_2) dx_1 dx_2 \\
&= \frac{1}{2} \int_{\Omega_2} p(y_2) dy_2,
\end{aligned}$$

where $y_2 = \sqrt{\frac{x_1^2}{\sigma_1^2} + \frac{x_2^2}{\sigma_2^2}}$. For the error event of decoding error at third ARQ round, we have

$$Pr(\mathcal{E}_1, \mathcal{E}_2, \mathcal{E}_3) = \int\int\int_{\Omega_1 \cap \Omega_2 \cap \Omega_3} p(x_1, x_2, x_3) dx_1 dx_2 dx_3 \tag{A.3a}$$

$$\geq \frac{1}{2} \int\int_{\Omega_2 \cap \Omega_3} p(x_1, x_2) p(x_3) dy_2 dx_3 \tag{A.3b}$$

$$\geq \frac{1}{4} \int\int_{\Omega_3} p(y_2, x_3) dy_2 dx_3 \tag{A.3c}$$

$$= \frac{1}{4} \int_{\Omega_3} p(y_3) dy_3 \tag{A.3d}$$

$$= \frac{1}{4} \int_{\Omega_3} p(x_1, x_2, x_3) dx_1 dx_2 dx_3 \tag{A.3e}$$

where $y_3 = \sqrt{\frac{x_1^2}{\sigma_1^2} + \frac{x_2^2}{\sigma_2^2} + \frac{x_3^2}{\sigma_3^2}}$. The equation (A.3d) comes from the fact that y_2 is orthogonal to x_3 in a two-dimension space, and therefore, equation (A.2) can be applied.

It follows that

$$Pr(\mathcal{E}_1, \mathcal{E}_2, \cdots, \mathcal{E}_n) = \int_{\bigcap_{k=1}^{n} \Omega_n} p(\mathbf{x}) d\mathbf{x} \geq \frac{1}{2^{n-1}} \int_{\Omega_n} p(\mathbf{x}) d\mathbf{x} = \frac{1}{2^{n-1}} Pr(\mathcal{E}_n). \tag{A.4}$$

References

[1] 3GPP2 C.S002-D V1.0. 3rd generation partnership project 2; physical layer standard for cdma2000 spread spectrum systems, revision d, February 2004.

[2] Mark Allman and Vern Paxson. On estimating end-to-end network path properties. In *Proceedings of ACM SIGCOMM 1999*, pages 263–274, Aug 1999.

[3] Jorgen Bach Andersen. Array gain and capacity for known random channels with multiple element arrays at both ends. *IEEE Journal on Selected Areas in Communications*, 18:2172 – 2178, Nov. 2000.

[4] Ajay Bakre and B. R. Badrinath. I-TCP: Indirect TCP for mobile hosts. In *Proceedings of International Conference on Distributed Computing Systems*, pages 136–143, May 1995.

[5] Hari Balakrishnan, Venkata N. Padmanabhan, Srinivasan Seshan, and Randy H. Katz. A comparison of mechanisms for improving TCP performance over wireless links. *IEEE/ACM Transactions on Networking*, 5(6):756–769, 1997.

[6] Dimitri Bertsekas and Robert Gallager. *Data Networks*. Prentice Hall, Inc., 1992.

[7] Helmut Bolcskei, David Gesbert, and Arogyaswami j. Paulraj. On the capacity of OFDM-based spatial multiplexing systems. *IEEE Transactions on Communications*, 50:225–234, February 2002.

[8] Stephen Boyd and Lieven Vandenberghe. *Convex Optimization*. cambridge university press, 2004.

[9] R. Braden. Requirements for internet hosts - communication layers. Technical Report RFC-1122, IETF, October 1989.

[10] David Chase. Code combining–a maximum-likelihood decoding approach for combining an arbitrary number of noisy packets. *IEEE Transactions on Communications*, 33:385–393, May 1985.

[11] Mung Chiang, Chee W. Tan, Daniel P. Palomar, Daniel O'Neill, and David Julian. Power control by geometric programming. *IEEE Transactions on Wireless Communications*, July 2007.

[12] A. DeSimone, Mooi Choo Chuah, and On-Ching Yue. Throughput performance of transport-layer protocols over wireless LANs. In *Global Telecommunications Conference, 1993*, volume 1, pages 542–549, Dec 1993.

[13] Andreas Kramling Dietmar Petras. MAC protocol with polling and fast collision resolution for ATM air interface. In *IEEE ATM Workshop*, August 1996.

[14] Richard J. Duffin, Elmor L. Peterson, and Clarence Zener. *Geometric Programming - Theory and Application*. John Wiley & Sons, Inc., 1967.

[15] R. Durrett. *Probability: Theory and Examples*. Wadsworth and Brooks/Cole, CA: Pacific Grove, 1991.

[16] Moncef Elaoud and Parameswaran Ramanathan. TCP-SMART: a technique for improving TCP performance in a spotty wide band environment. In *ICC 2000. 2000 IEEE International Conference on Communications*, volume 3, pages 1783–1787, June 2000.

[17] Patrick TH. Eugster, Pascal A. Felber, Rachi Guerraoui, , and Anne-Marie Kermarrec. The many faces of Publish/Subscribe. *ACM Computing Surveys*, 35:114C13, June 2003.

[18] Ludger Fiege, Felix C. Gartner, Oliver Kasten, and Andreas Zeidler. Supporting mobility in content-based publish/subscribe middleware. In *Proceedings of the ACM/IFIP/USENIX International Middleware Conference, 2003.*, pages 103–122, June 2003.

[19] S. Floyd and T. Henderson. The NewReno modification to TCP's fast recovery algorithm. Technical Report RFC-2582, IETF, April 1999.

[20] Pal Frenger, Pal Orten, and Tony Ottosson. Convolutional codes with optimum distance spectrum. *IEEE Communications Letters*, 3:317–319, November 1999.

[21] R.H. Frenkiel and T. Imielinski. Infostations - The joy of "many-time, many-where" communications. Technical Report TR-119, WINLAB, ECE Dept., Rutgers University, April 1996.

[22] Cheng Peng Fu and Soung C. Liew. TCP Veno: TCP enhancement for transmission over wireless access networks. *IEEE (JSAC) Journal of Selected Areas in Communications*, 21:216–228, Feb 2003.

[23] Zhenghua Fu, Petros Zerfos, Haiyun Luo, Songwu Lu, Lixia Zhang, and Mario Gerla. The impact of multihop wireless channel on TCP throughput and loss. In *IEEE Twenty-Second Annual Joint Conference of the IEEE Computer and Communications Societies, INFOCOM 2003*, volume 3, pages 1744–1753, March 2003.

[24] Hesham El Gamal, Giuseppe Caire, and Mohamed Oussama Damen. The MIMO ARQ channel: Diveristy-multiplexing-delay tradeoff. *IEEE Transactions on Information Theory*, 52:3601–3621, August 2006.

[25] Tom Goff, James Moronski, Dhananjay S. Phatak, and Vipul Gupta. Freeze-TCP: A true end-to-end TCP enhancement mechanism for mobile environments. In *Proceedings of IEEE INFOCOM 2000*, pages 1537–1545, March 2000.

[26] David J. Goodman, Narayan B. Mandayam Joan Borras, and Roy D. Yates. INFOSTATIONS: a new system model for data and messaging services. In *IEEE 47th Vehicular Technology Conference, 1997*, volume 2, pages 969–937, May 1997.

[27] Andrei Gurtov and Reiner Ludwig. Responding to spurious timeouts in TCP. In *Proceedings of IEEE INFOCOM 2003*, volume 3, pages 2312 – 2322, March 2003.

[28] J. Hagenaeur. Rate-compatible punctured convolutional codes (RCPC codes) and their applications. *IEEE Transactions on Communications*, 36(4):389–400, April 1988.

[29] Todd E. Hunter and Aria Nosratinia. Diversity through coded cooperation. *IEEE Transactions on Wireless Communications*, 5:283–289, January 2006.

[30] Seung-Hoon Hwang, Bonghoe Kim, and Young-Sam Kim. A Hybrid ARQ scheme with power ramping. In *Proceedings of Vehicular Technology Conference, VTC 2001*, volume 3, pages 1579–1583, October 2001.

[31] IEEE Std 802.11. IEEE standard for local and metropolitan area networks, Part 11: wireless LAN medium access control (MAC) and physical layer (PHY) specifications, 1999.

[32] IEEE Std 802.11. IEEE Standard for local and metropolitan area networks, Part 11: wireless LAN medium access control (MAC) and physical layer (PHY) specifications amendment 8: Medium access control (MAC) quality of service enhancements, November 2005.

[33] Van Jacobson and Michael J. Karels. Congestion avoidance and control. In *Proceedings of ACM SIGCOMM'88*, August 1988.

[34] Gideon Kaplan and Shlomo Shamai (Shitz). Error exponents and outage probabilities for the block-fading gaussian channel. In *IEEE International Symposium on Personal, Indoor and Mobile Radio Communications*, pages 329 – 334, September 1991.

[35] Thomas Keller and Lajos Hanzo. Adaptive modulation techniques for duplex OFDM transmission. *IEEE Transactions on Vehicular Technology*, 49:1893–1906, September 2000.

[36] Jeong Geun Kim and Indra Widjaja. PRMA/DA: A new media access control protocol for wireless ATM. In *IEEE International Conference on Communications, ICC'96*, volume 1, pages 240–244, June 1996.

[37] R. Knopp and P.A. Humblet. Information capacity and power control in single cell multiuser communications. In *IEEE International Conference on Communications, 1995. ICC 95 Seattle*, volume 1, pages 331 – 335, June 1995.

[38] R. Knopp and P.A. Humblet. Maximizing diversity on block-fading channels. In *IEEE International Conference on Communications, 1997. ICC 97 Montreal*, volume 2, pages 647 – 651, June 1997.

[39] Raymond Knopp and Pierre A. Humblet. On coding for block fading channels. *IEEE Transactions on Information Theory*, 46:189–205, January 2000.

[40] S. Kopparty, S. Krishnamurthy, M. Faloutsos, and S. Tripathi. Split-TCP for mobile ad hoc networks. In *IEEE Global Telecommunications Conference, 2002. GLOBECOM '02.*, volume 1, pages 138– 142, Nov 2002.

[41] T. Kostas, T. F. Kostas, G. Rajappan, and M. Dalal. A hierarchical key management system for secure multicast group communications. In *Proc IEEE Military Communications Conference (MILCOM) 2003*, October 2003.

[42] Shu Lin, Daniel J. Costello Jr., and Michael J. Miller. Automatic-repeat-request error control schemes. *IEEE Communications Magazine*, 22(12):5–17, December 1984.

[43] Changwen Liu and A.P. Stephens. An analytic model for infrastructure WLAN capacity with bidirectional frame aggregation. In *IEEE Wireless Communications and Networking Conference, 2005*, volume 1, pages 113–119, March 2005.

[44] Hongbo Liu, Leonid Razoumov, Dipankar Raychaudhuri, Changho Suh, and Seokhyun Yoon. Optimal power allocation for type II H-ARQ under frame error rate constraint. In *Conference on Information Sciences and Systems, 2003*, volume 1, pages 720–725, March 2003.

[45] R. Ludwig and K. Sklower. The Eifel retransmission timer. *ACM SIGCOMM Computer Communication Review 2000*, 30:17 – 27, July 2000.

[46] Reiner Ludwig and Randy H. Katz. The Eifel algorithm: making TCP robust against spurious retransmissions. *ACM SIGCOMM Computer Communication Review 2000*, 30:30 – 36, January 2000.

[47] Luiz Magalhaes and Robin Kravets. Transport level mechanisms for bandwidth aggregation on mobile hosts. In *Ninth International Conference on Network Protocols, 2001.*, pages 165 – 171, Nov 2001.

[48] David M. Mandelbaum. An adaptive-feedback coding scheme using incremental redundancy. *IEEE Transactions on Information Theory*, 20:388–389, May 1974.

[49] Stefan Mangold, Sunghyun Choi, Guido R. Hiertz, Ole Klein, and Bernhard Walke. Analysis of IEEE 802.11e for QoS support in wireless LANs. *IEEE Wireless Communications*, 10:40–50, December 2003.

[50] Hua Mao, Gang Wu, James Evans, and Michael Caggiano. An adaptive radio link protocol for infostations. In *IEEE 49th Vehicular Technology Conference, 1999*, volume 6, pages 1345–1349, May 1999.

[51] Syed Aon Mujtaba. TGn Sync proposal technical specification. TGn Sync Homepage, http://www.tgnsyn.org.

[52] Andrew D. Myers and Stefano Basagni. *Handbook of wireless networks and mobile computing*. John Wiley & Sons, Inc., 2002.

[53] Sanjiv Nanda, Rod Walton, John Ketchum, Mark Wallace, and Steven Howard. A high-performance MIMO-OFDM wireless LAN. *IEEE Communications Magazine*, 43:101–109, February 2005.

[54] Nikos Passas, Sarantis Paskalis, Dimitra Vali, and Lazaros Merakos. Quality-of-service-oriented medium access control for wireless ATM networks. *IEEE Communications Magazine*, 35:43–50, November 1997.

[55] Wasan Pattara-atikom, Prashant Krishnamurthy, and Sujata Banerjee. Distributed mechanisms for quality of service in wireless LANs. *IEEE Wireless Communications*, 10:26 – 34, June 2003.

[56] V. Paxson and M. Allman. Computing TCP's retransmission timer. Technical Report RFC-2988, IETF, November 2000.

[57] G. Rajappan, M. Dalal, and T. Kostas. Reliable multicast with active filtering for distributed simulations. In *Proc IEEE Military Communications Conference (MILCOM) 2003*, volume 1, Oct 2003.

[58] Gowri Rajappan, Joydeep Acharya, Hongbo Liu, Narayan Mandayam, Ivan Seskar Roy Yates, and Robert Ulman. Mobile infostation network technology. In *Proceedings of SPIE 6248, (2006)*, volume 6248, pages 62480M1–62480M9, May 2006.

[59] S.S. Rao. *Optimization theory and applications*. John Wiley & Sons, Inc., 1983.

[60] Dipankar Raychaudhuri and Newman D. Wilson. ATM-based transport architecture for multiservices wireless personal communication networks. *IEEE Journal on Selected Areas in Communications*, 12:1401–1414, October 1994.

[61] Pasi Sarolahti, Markku Kojo, and Kimmo Raatikainen. F-RTO: an enhanced recovery algorithm for TCP retransmission timeouts. *ACM SIGCOMM Computer Communication Review 2003*, 33:51 – 63, April 2003.

[62] C. E. Shannon. A mathematical theory of communication. *Bell Systems Technical Journal*, 27:379–423, 623–656, 1948.

[63] Wu Shiow-yang and Wu Kun-Ta. Dynamic data management for location based services in mobile environments. In *Proceedings of Seventh International Database Engineering and Applications Symposium, 2003*, pages 180 – 189, July 2003.

[64] W. Stevens. TCP slow start, congestion avoidance, fast retransmit, and fast recovery algorithms. Technical Report RFC-2001, IETF, January 1997.

[65] R. Stewart, Q. Xie, K. Morneault, C. Sharp, H. Schwarzbauer, T. Taylor, I. Rytina, M. Kalla, L. Zhang, and V. Paxson. Stream control transmission protocol. Technical Report RFC-2960, IETF, Oct 2000.

[66] Randall Stewart and Chris Metz. SCTP: new transport protocol for TCP/IP. *IEEE Internet Computing*, 5:64–69, Nov 2001.

[67] Z. Sun and X. Jia. Energy efficient Hybrid ARQ scheme under error constraints. *Wireless Personal Communications*, 25:307–320, July 2003.

[68] Vahid Tarokh, Nambi Seshadri, and A. R. Calderbank. Space-time codes for high data rate wireless communication: Performance criterion. *IEEE Transactions on Information Theory*, 44:744–765, March 1998.

[69] G. Wright and W. Stevens. *TCP/IP Illustrated vol.2: The Implementation*. Addison-Wesley, 1995.

[70] Gang Wu, Churng-Wen Chu, Kevin Wine, James Evans, and Richard Frenkiel. WINMAC: a novel transmission protocol for infostations. In *IEEE 49th Vehicular Technology Conference, 1999*, volume 2, pages 1340–1344, May 1999.

[71] Yang Xiao. IEEE 802.11n: enhancements for higher throughput in wireless LANs. *IEEE Wireless Communications*, 12:82–91, December 2005.

[72] Shugong Xu and Tarek Saadawi. Performance evaluation of TCP algorithms in multi-hop wireless packet networks. *Wireless Communications and Mobile Computing*, 2:85–100, Dec 2001.

[73] Andrea Zanella, Gregorio Procissi, Mario Gerla, and M. Y. M̈edyS̈anadidi. TCP Westwood: Analytic model and performance evaluation. In *Proceedings of IEEE Globecom 2001*, volume 3, pages 1703–1707, November 2001.

[74] Lizhong Zheng and D.N.C Tse. Diversity and multiplexing: a fundamental tradeoff in multiple-antenna channels. *IEEE Transactions on Information Theory*, 49:1073 – 1096, May 2003.

Curriculum Vita

Hongbo Liu

1990-1994 B.E. in Electrical Engineering, Huazhong University of Science and Technology, Wuhan, China

1994-1997 M.E. in Electrical and Computer Engineering, Institute of Automation, Chinese Academy of Sciences, Beijing, China

1997-1998 Software Engineer, Engineering Research Center of Integrated Automation, Institute of Automation, Chinese Academy of Sciences, Beijing, China

1998-2001 M.S. in Electrical Engineering, WINLAB, Electrical and Computer Engineering, Rutgers University, New Jersey

1999-2001 Graduate Assistant, DIMACS & WINLAB, Rutgers University, New Jersey

2001-2002 Research Engineer, Computer and Communication Research Lab (CCRL), NEC USA Inc.

2002-2007 Ph.D. in Electrical Engineering, WINLAB, Electrical and Computer Engineering, Rutgers University, New Jersey

2002-2006 Graduate Assistant, WINLAB, Electrical and Computer Engineering, Rutgers University, New Jersey

1999 J. Cowie, H. Liu, J. Liu, D. Nicol, and A. Ogielski. ”Towards Realistic Million-Node Internet Simulations”, *Proceedings of the 1999 International Conference on Parallel and Distributed Processing Techniques and Applications (PDPTA’99)*, June 1999

2002 D. Cavendish, M. Lajolo, and H. Liu, ”On the evaluation of fairness for input queue switches”, *IEEE International Conference on Communications, 2002, ICC2002*, Volume 2, Page(s):996 - 1000, April 2002

2002 D. Cavendish, M. Lajolo, and H. Liu, ”On the support of minimum service rates for input queue switches”, *IEEE International Conference on Communications, 2002, ICC2002*, Volume 2, Page(s):1315 - 1320, April 2002

2003 H. Liu, H. Bhaskaran, D. Raychaudhuri, and S. Verma, ”Capacity analysis of a cellular data system with 3G/WLAN interworking”, *IEEE 58th Vehicular Technology Conference, 2003. VTC 2003-Fall*, Volume 3, Page(s): 1817 - 1821, Oct. 2003.

2004 H. Liu, L. Razoumov, D. Raychaudhuri, C. Suh, and S. Yoon, ”Optimal power allocation for type II H-ARQ under frame error rate constraint”, *Proceedings of the Conference on Information Sciences and Systems, 2004*, volume 1, Page(s): 720-725, March 2004.

2005 H. Liu, L. Razoumov and N. Mandayam, ”Optimal power allocation for type II hybrid-ARQ via geometric programming”, *Proceedings of the Conference on Information Sciences and Systems, 2005*, March 2005.

2006 G. Rajappan, J. Acharya, H. Liu, N. Mandayam, I. Seskar, and R. Yates, ”Mobile infostation network technology”, *Proceedings of SPIE 6248, (2006)*, volume 6248, Page(s): 62480M:1-9, May 2006.